# THE EFFECTS OF END RESTRAINT ON STEEL DECK REINFORCED CONCRETE FLOOR SYSTEMS

by

Craig Steven Young

Thesis submitted to the faculty of the
Virginia Polytechnic Institute and State University
in partial fulfillment of the requirements for the degree of

**MASTER OF SCIENCE**

in

Civil Engineering

APPROVED:

W. Samuel Easterling, Chairman

Richard M. Barker

Siegfried M. Holzer

Thomas M. Murray

December 1990

Blacksburg, Virginia 24061

# THE EFFECTS OF END RESTRAINT ON STEEL DECK REINFORCED CONCRETE FLOOR SYSTEMS

by

Craig Steven Young

Committee Chairman: W. Samuel Easterling
Civil Engineering

**(ABSTRACT)**

Extensive research to determine the strength of steel deck reinforced concrete floor systems has been carried out on single span, single panel width test specimens. Little of this research has considered the benefits that actual field conditions have on overall strength and stiffness. This experimental study investigates typical field details at intermediate supports and end spans. In particular, the influence of adjacent spans and typical pour stop details are considered. Additionally, this study illustrates the applicability of simple analytical models, which can be used to determine the strength and stiffness of steel deck reinforced concrete floor systems.

## ACKNOWLEDGEMENTS

The author would like to thank Dr. W. Samuel Easterling for instigating this research. Without his friendship, patience and understanding this study would not have been successful. He would also like to thank the entire Structures Division faculty for their contribution to his education. In particular, Dr. Siegfried M. Holzer, Richard M. Barker, and Thomas Murray for serving on his committee. Thanks also to his fellow Research Assistants, Ben Anderson, Lee Rayburn, David and Stacy Gibbings, Chuck Sublett, and David McGowan who were all coaxed into placing concrete, moving steel, carrying deck and testing at all hours of the day and night. A special thanks also to Dennis Huffman for welding, placing concrete etc. Additional thanks go to Eric Wishart for his patience during this thesis. Thanks guys! Friends like you are rare.

A very special thanks goes to Lorie Compton. Your help, caring and understanding during the writing of this thesis is greatly appreciated.

A special thanks goes to the Steel Deck Institute and Member Companies for their funding and support for this research (and for the trip to Florida).

This thesis is dedicated to Mr. and Mrs. Clinton B. Young, Mom and Dad.

Dad, you were so proud to see your son start engineering but you didn't get to see me finish. There just isn't words... Mom, your patience and love have been all that has kept me going. God love you both. I couldn't have done it without you.

# CONTENTS

## CONTENTS ... continued

## LIST OF FIGURES

## LIST OF FIGURES ...continued

## LIST OF FIGURES ...continued

## LIST OF TABLES

## LIST OF SYMBOLS

$a$ = depth of concrete compressive block

$A_s$ = cross sectional area of deck

$b$ = width of slab

$b_r$ = effective width of slip block

$B_b$ = width of bottom flange

$B_t$ = width of top flange

$C_s$ = cell spacing

$d_d$ = deck depth

$d$ = distance from extreme compressive fiber to centroid of deck, in.

$D_w$ = width of web

$e_1$ = distance from compressive resultant force to top of deck

$e_3$ = distance from compressive resultant force to bottom of steel deck

$e_2$ = distance from compressive resultant force to mid-height of deck web

$E_c$ = $57{,}000(f'c)^{1/2}$

$f'_c$ = concrete compressive strength, psi.

$f_{yc}$ = corrected yield stress of deck

$f_y$ = measured yield stress of deck

$h$ = out to out depth of slab

$H_{rib}$ = rib resistance force per unit length without clamping force

## LIST OF SYMBOLS ...continued

$I$ = Uncracked / Average moment of inertia

$k_2$ = mechanical bond factor

$k_3$ = slab width factor

$K$ = Bond force transfer property

$l'$ = shear span

$L$ = clear span length, ft.

$m$, $k$ = slope and ordinate intercept of regression line developed from laboratory test program.

$M$ = applied moment

$M_{conc}$ = dead weight moment of concrete slab

$M_{et}$ = Moment based on first yield of extreme fibers, k-in / cell

$M_t$ = Modified bending moment

$M_n$ = nominal moment strength

$n$ = modular ratio

$S$ = spacing of shear transferring devices, in.

$t$ = deck thickness

$T$ = resultant tensile force in sheeting

$T_{anch}$ = ultimate strength of end anchorage system

$T_i$ = deck element tensile forces ($i$ = 1 to 3)

## LIST OF SYMBOLS ...continued

$V_u$ = design shear strength

$V_\mu$ = total vertical reaction and end support at ultimate load

w = slab dead load, psf

x = distance to a slab cross-section

$y_{cc}$ = distance from neutral axis of composite section to top of slab

$\Phi$ = capacity reduction factor

$\gamma$ = shoring reaction factor

$\rho$ = reinforcement ratio

$\rho$ = reinforcement ratio

$\mu$ = coefficient of friction between sheeting and concrete

# Chapter 1
# INTRODUCTION

## 1.1 General

Cold-formed steel deck has been a part of floor systems in buildings since the early 1920's. Initially, the deck was used strictly as a stay-in-place, or permanent, form. Not long after the first uses, engineers recognized the potential for utilizing steel deck as tensile reinforcement, thus improving the efficiency of the floor systems.

As the desire to use the deck as reinforcement became greater, so did the need to perform design calculations. Predicted strengths based on ultimate strength reinforced concrete theory did not agree with laboratory tests of the slab elements. Continued attempts to develop analytical methods, which are not dependent on experimental testing, have thus far not been completely successful.

Instead, the current design standard in the United States is based on a testing program that produces data from which statistical coefficients are obtained

(*Specifications* 1984). These coefficients are then used, along with design parameters, to arrive at a design live load capacity. This method resulted from an extensive research program at Iowa State University that was initiated by the American Iron and Steel Institute in 1967 (Porter and Ekberg 1978). The approach developed at ISU, in similar form, is used in the European and Canadian design standards.

The experimental test specimen in the U.S. standard is a single span, single panel width specimen. This arrangement, while convenient for the testing agency, has several details, which do not accurately reflect field conditions. One is the lack of proper representation of end span and adjacent span details. Due to the lack of end restraint, which would typically be present in constructed floor systems, the predominant limit state is shear bond. This limit state is characterized by a breakdown of the bond between the steel deck and concrete within the shear span. The concrete is then essentially free to slip relative to the deck. Pour-stop, or closure angle details, and adjacent spans have a significant influence on inhibiting or preventing the shear bond limit state. The effect of adjacent panels on the overall performance of a floor system is not considered in the standard test configuration. Single panels tend to exhibit edge curl when they are loaded, thus reducing the effectiveness of the connectivity at the deck and concrete interface. Figure 1.1 illustrates the edge curling. Adjacent panels prevent such curl from developing.

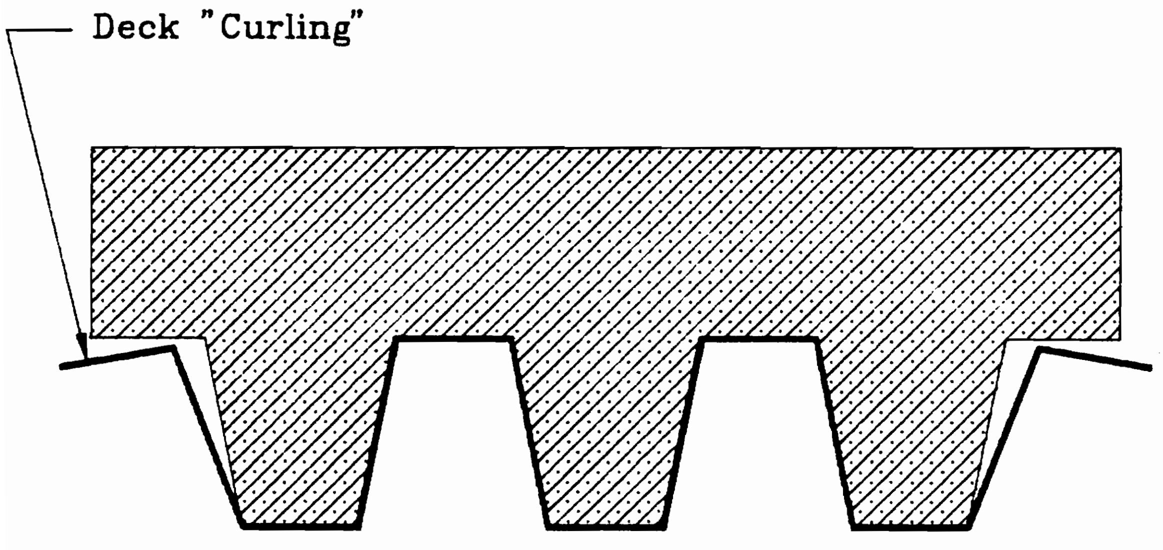


Figure 1.1 Deck Curling

## 1.2 Objective and Scope of Research

The primary objective of this study is to determine the influence of typical field details on the strength and stiffness of composite floor systems. An additional objective is to evaluate the applicability of using traditional reinforced concrete models to predict the strength and stiffness. To achieve this objective, a series of full-scale tests have been preformed and evaluated.

Several specimen configurations were evaluated on a three span setup. This setup permitted the testing of either an interior span or an end span. The interior span tests were used to evaluate the influence of adjacent spans. The end span tests were used to evaluate the effectiveness of various edge details.

Chapter 2 provides background information on steel deck reinforced concrete floor systems including the origin and current research topics. Chapter 3 describes each individual test performed and provides the reader with a descriptive illustration of the testing process. Chapter 4 explains the theoretical formulae used for comparison with the actual data obtained in the testing program. Chapter 5 explains some of the phenomena witnessed during the tests. Chapter 6 suggests some load carrying mechanisms at ultimate. Chapter 7 summarizes, concludes and lists some recommendations.

Two appendices are also included, Appendix A is a summary of each test setup and Appendix B provides sample calculations for the formula given in Chapter 4.

# Chapter 2
# BACKGROUND INFORMATION

At the turn of the century, engineers began to ask the question, "Why should the dead weight of a floor system be so much more than the live load they are designed to carry?" (Dallaine 1971). The challenge was to design a lightweight, easy to produce, easy to install floor system. The solution came on February 23, 1926 when James F. Loucks and Harry Gillett (Holorib Incorporated), received a patent for "Holorib Deck" (United States Patent Office #1,574,586). The company changed hands twice before the product received the name "keystone beam" (Figure 2.1). The first occurred between 1926 and 1931, when Detroit Steel Products Company bought out Holorib. The second was when Fenestra (a division of Detroit Steel Products Company) went out of business in 1967. At this time, the H.H Robertson Company, which up until that point produced metal roof deck, bought Fenestra's deck and panel equipment and began marketing the keystone beam. (Landis 1990).

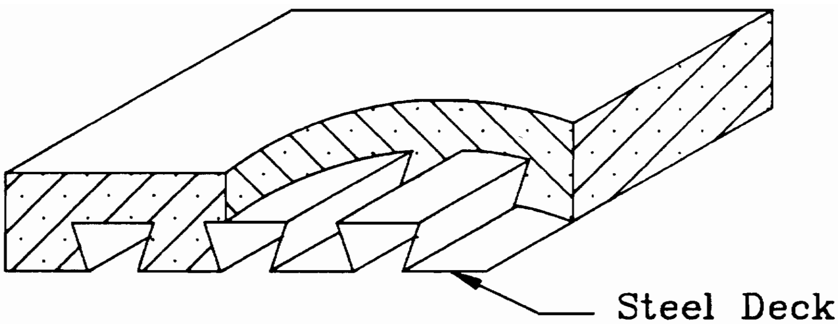


**Figure 2.1 Keystone Beam**

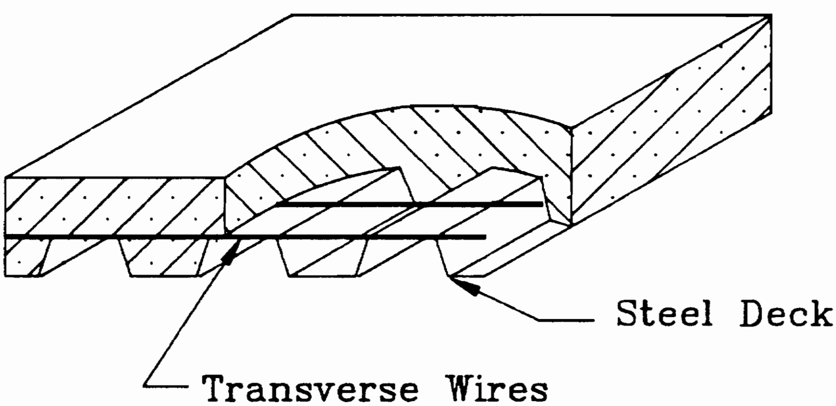


**Figure 2.2 Cofar**

In the early 1930's the first documented keystone, "Holorib", beam floor system was placed at the Baltimore and Ohio Railroad Company warehouse in Pittsburgh[1] (Dallaine 1971). The keystone beam was a non-composite cellular floor system used in industrial buildings. In this first cellular floor system, the steel deck was the only structural element, "concrete fill was added on top of the deck to obtain the needed fire rating and provide a level surface for the carpet, etc." (Dallaine 1971). Additional fire proofing was in the form of fireproof ceilings and fire stops. Although the patent received by Loucks and Gillett mentions "where cement is used for covering or coating. The shape of the ribs ... insures a most efficient bond between the same and sheet ...", if we look at this in context it seems to be discussing waterproofing and/or attaching the "walking surface" to the deck. It does not appear to be a suggestion of composite design.

This type of floor system provides many benefits which include, a channel to run electrical and telephone wires, the deck remains in place and thus does not require the labor intensive work of installation and removal of formwork, and the voids provided by the cells produce a lighter floor system.

---

1 *A note here is, in a Fenestra Composite Beam document there is pictured a project dated in 1924. There is no accompanying documentation to explain the project but pictures do not lie. Thus it is possible that the first keystone floor was placed in 1924.*

By 1950, engineers wanted to use the deck as positive moment tensile reinforcement. The problem was how to attach the deck to the concrete. The solution was provided by the Granco Steel Products company of St. Louis, which welded wire mesh to the top of the deck and allowed transfer of the horizontal shear between concrete and deck and thus provided composite action. Due to the brittle high strength steel in the deck and wire, the ductility of the floor system was a concern. Even with this as a potential drawback, the product, which became known as "Cofar" (Figure 2.2), gained acceptance and significantly reduced the cost and weight of concrete floor systems. This product was marketed by several manufactures until the late 1980's and does not appear to be marketed today in the United States. (Landis 1990).

In 1961 the Inland-Ryerson Company replaced the wire mesh with Hi-Bond lugs or embossments to lock the concrete and steel together. The product was named "Hi-Bond Floor Deck." By this time, cellular floors had reduced overall building weight by as much as 30 percent while reducing construction time by 25 percent and thus producing a reduction in construction and material costs (Dallaine 1971).

An ever increasing labor cost, invention of a spray on fireproof coating and expansionism of the 1960's produced an increased demand for the new composite floor system. To meet this charge, several manufacturers introduced their version of steel deck. No design standards existed, therefore individual manufacturers had to verify that their designs were adequate. This was often done by performing numerous laboratory tests. Bryl (1967) made three critical observations as a result of manufacturer tests: (1) if no shear transfer devices are used a sudden failure occurs, (2) if shear transfer devices are present large deformations occurred and the load carrying capacity increased dramatically, and (3) the slab could be analyzed as uncracked with respect to bending, bond stresses, and permissible load on shear devices.

One of the first documented test results of a cellular floor system was presented by John F. McDermott in 1967. The testing program tried to answer the following significant questions about pan type cellular deck, (Figure 2.3), (McDermott 1967):

(1) Is the bond and the mechanical interlocking between the perforated webs of the steel pans and the concrete sufficient to cause complete composite action in the floor unit?

(2) Does shear lag cause the stresses to vary across the bottom face of the steel pan and thereby reduce the effectiveness of the steel pan carrying bending stresses?

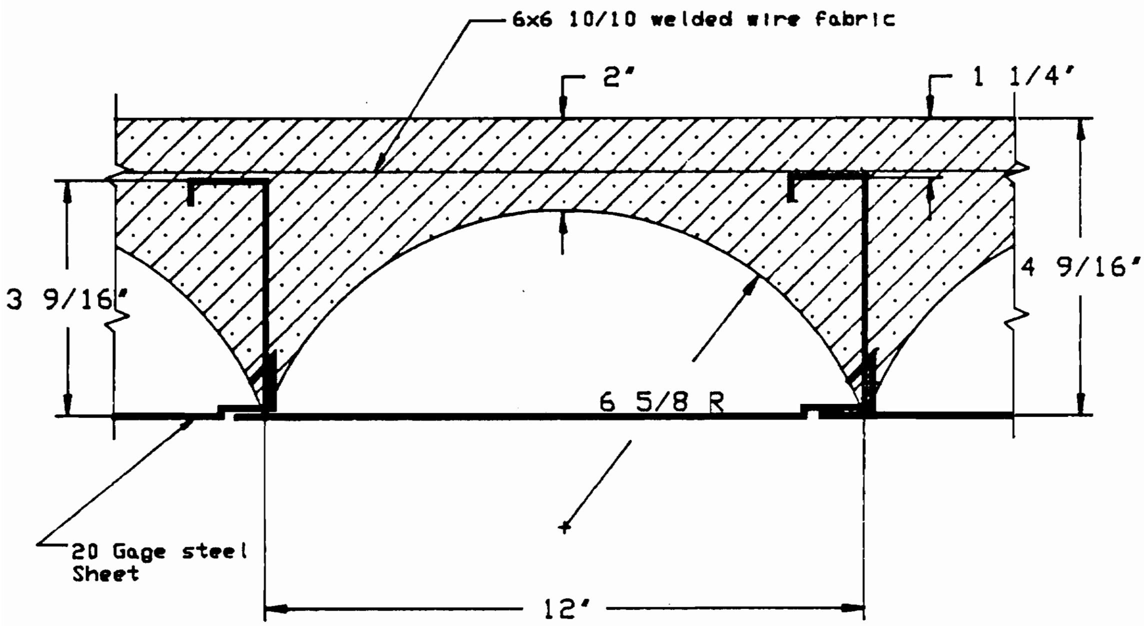


Figure 2.3 McDermott Deck

(3) Does a significant vertical distortion (referred to as curling), of the cross section of the pan occur and reduce the bending strength and stiffness of the unit?

(4) How does a floor of the proposed units behave when adjacent units are unequally loaded? Although the units are designed for one-way bending, lateral (transverse) bending will occur under these conditions and tend to separate adjacent units.

(5) Can the floor unit resist the tendency for concentrated loads to punch through the concrete slab?

(6) Are the units sufficiently rugged to withstand abuse during field pouring of the concrete?

The reported findings and answers to some of the above were (McDermott 1967):

(1) Experimental stress and theoretical stresses based on full composite action were reasonably close.

(2) The measured end slip was negligible for even great loads.

(3) The experimental deflections agreed reasonably well with theoretical deflections based on full composite action.

(4) The specimen was able to reach its theoretical yield moment without large deflections, even though the sheet edges were unrestrained.

(5) The relative flat part of the load-deflection curve demonstrated the ability of the specimen to sustain significant plastic deformation without collapse.

These test results were limited to the particular pan type of deck under consideration, thus the questions still remained to be resolved for the most popular types of cellular decks.

To answer the above questions for other deck types and to gain a better understanding of the behavior of composite floor systems, the American Iron and Steel Institute initiated, in 1967, an extensive research project at Iowa State University (ISU). The purpose of this study was to analyze the behavioral characteristics and develop a design standard for composite steel deck reinforced concrete (SDRC) floor systems. At approximately the same time independent studies with similar objectives began at West Virginia University (Prasannan and Luttrell 1984). A discussion of the significant findings of these two studies follows.

The outcome of the ISU project is documented in several theses, reports and papers (see References by Ekberg, Schuster, and Porter). Several hundred single panel tests were conducted on what has now become the standard test setup (Figure 2.4). One result from the study is the classification and description of limit states. These are

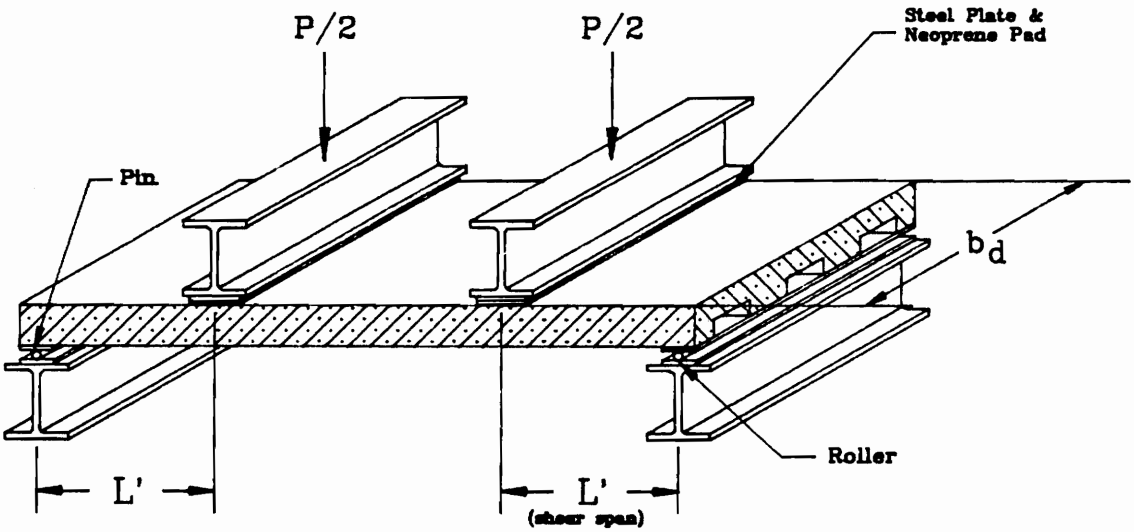


Figure 2.4 Current ASCE Standard Test Setup

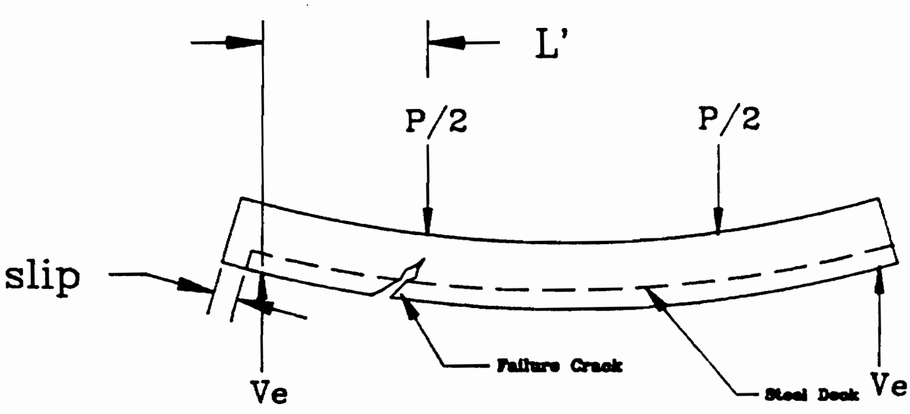


Figure 2.5 Shear Bond Diagram

shear bond, which is the breakdown of adhesion bond between deck and concrete when first cracking occurs, under-reinforced flexure, which occurs when the steel deck and concrete have adequate bonding and yielding of the steel deck occurs, and over-reinforced flexure, which occurs when the bond is adequate and the concrete crushes before full yielding of the deck. Porter and Ekberg (1978) reported that, of the three modes, by far the most common mode of failure was shear bond. This failure generally starts with the formation of a crack under the applied load point, followed closely by the loss of bond between the load point and support reaction as illustrated in Figure 2.5. Porter and Ekberg presented the final form of an empirical equation for shear bond failure, which was initially developed by Schuster (1970).

The equation is given by:

$$V_u = \phi\left[\frac{12d}{S}\left(\frac{m\rho d}{l'} + k\sqrt{f'_c}\right) + \frac{\gamma w_1 L}{2}\right]$$

where,

$V_u$ = design shear strength

$\Phi$ = capacity reduction factor

S = spacing of shear transferring devices, in.

d = distance from extreme compressive fiber to centroid of deck, in.

m, k = slope and ordinate intercept of regression line developed from laboratory test program.

$\gamma$ = shoring reaction factor

l' = shear length (distance from load to support),ft.

L = clear span length, ft.

$w_1$ = slab dead load, psf

$\rho$ = reinforcement ratio

f'c = concrete compressive strength, psi.

The application of this empirical method relies on a laboratory test program from which the regression line coefficients m and k are determined (Figure 2.6). The ISU method, with the appropriate factor of safety, is the basis for the U.S. design standard (*Specifications* 1984).

Similar testing occurred at WVU and from the research performed, Prasannan and Luttrell (1984) developed an approach for the strength determination of composite slabs. This approach is based on a statistical evaluation of previously obtained test data. Regression analyses were performed with various slab and deck properties being the independent variables, and the theoretical moment capacity being the dependent variable.

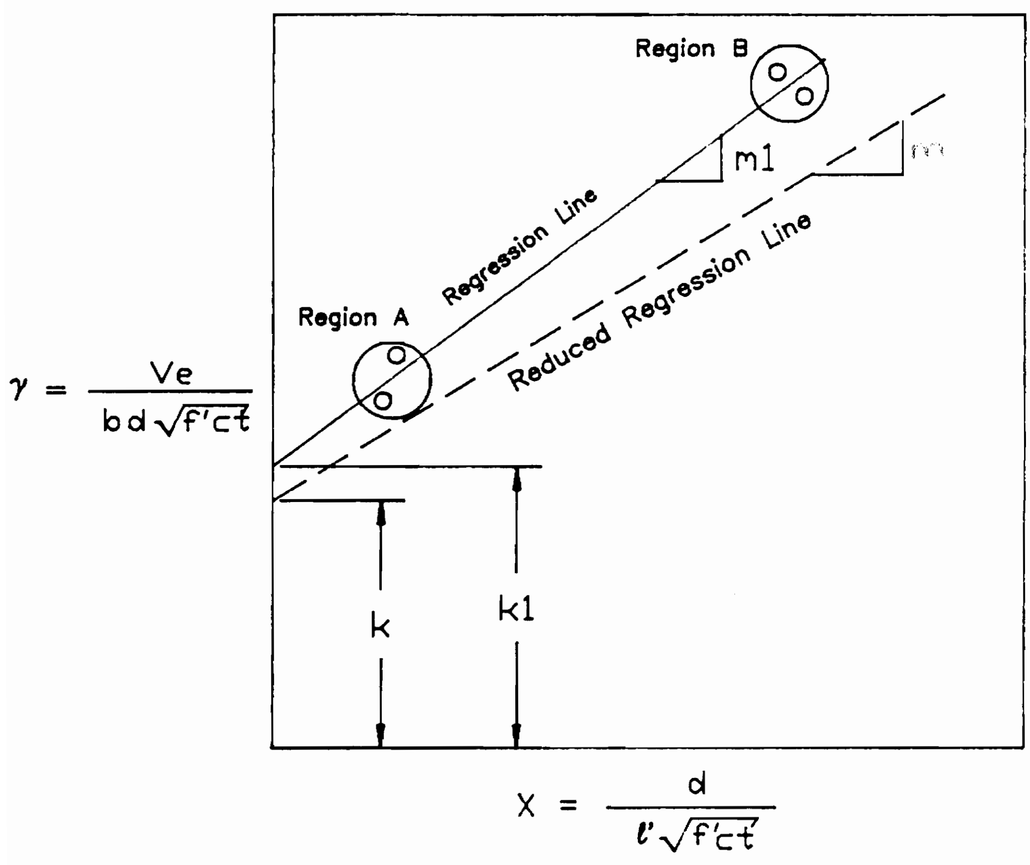


**Figure 2.6 Shear Bond Plot ASCE Standard**

The method is attractive to steel deck manufacturers because it gives them a way to predict the performance of a potential new deck profile and embossment pattern, without having to go to the expense of fabricating new rolling stands to roll the profile and perform numerous tests in advance. With the results of this analysis the "test program can then be used for verification rather than to use it both to predict and verify." (Prasannan and Luttrell 1984). This method is fundamentally based on the test setup that is used in the ASCE Standard, since the data used in the statistical analyses was obtained from tests performed using the setup.

The predictive equation is given by,

$$M_t = K M_f' - k_4 S'$$

where,

$M_t$ = Modified bending moment

$$K = \frac{k_3}{k_1 + k_2} \leq 1.0$$

$M_f'$ = Moment based on first yield of extreme fibers, k-in / cell

$k_1$, $k_2$ = design variables to account for deck type variation and slab depth.

$k_3$ = design variable for number of deck flutes

$k_4$ = shear span factor

$S'$ = Conjugate shear span (span/2.0 - shear span)

Prasannan and Luttrell classify the embossment patterns as one of these (Figure 2.7): (1) Type I -embossments angled with respect to horizontal (usually 45°) or (2) Type II -horizontal embossments. Later a third type of pattern was added to this list: Type III or IM where the embossments are a mixture of the above. The design variables, $k_i$, are a function of the embossment pattern. The method provides insight into the complex nature of composite floor slabs and a refined version of the equation will be a part of the next edition of the ASCE Standard.

By the 1970's, composite floor systems were beginning to be used in Europe. In 1978, Jan Stark reemphasized the necessity of an adequate bond between the deck and concrete. He also points out that "the shape of the burls [indentations or embossments] has a considerable influence on the ultimate shear capacity." (Stark 1978). In the paper, "Design of Composite Floors with Profiled Steel Sheet," Stark presents an elastic method for the calculation of the capacity of steel deck. The method consists of calculating the shear force per burl (embossment) by:

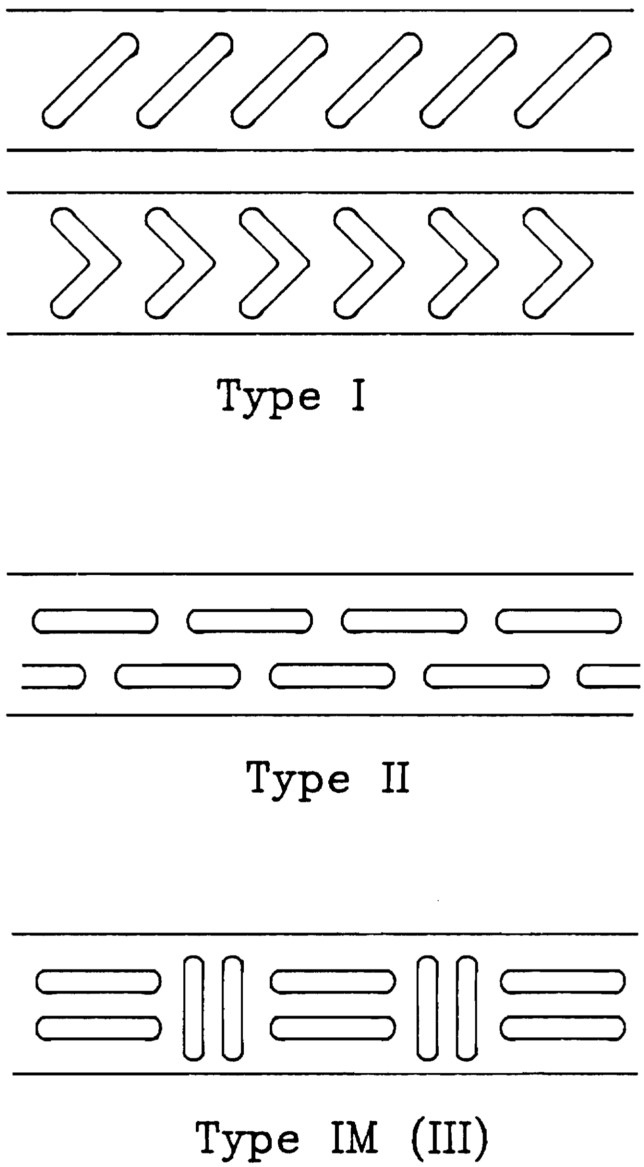


**Figure 2.7 Embossment Classification**

$$S_u = \frac{A\ \sigma_y}{n}$$

where,

$S_u$ = force per burl (embossment or indentation)

A = cross-sectional area of sheet

$\sigma_y$ = yield stress of deck

n = number of burls in shear span

He states that for the deck tested, the ultimate capacity of not less that 0.7 A $\sigma_y$ per burl is attainable. As in the pervious methods, this approach is limited to a particular type of deck and tests must be performed to verify its adequacy for the deck embossment pattern under consideration.

An experimental study was performed at the University of Washington (Roeder 1981) to investigate the effect of damage to a U.S. Government facility which was constructed. This study involved a series of non-destructive load tests on the damaged floor along with several laboratory specimens designed to meet similitude requirements[2]. In the paper "Point Loads on Composite Deck-Reinforced slabs (Roeder 1981), the author states that a "trussing action" developed after the "theoretical shear bond load" and allowed for a higher than predicted load capacity. This testing program showed that "the continuous metal deck caused an approximate average of 40-50% increase in shear bond capacity." Also, increases of "50-100% were obtained with simple span metal deck and stud restraint, and adjacent span blockage. Continuous decks with stud restraint provided increases of 100-150%." These results demonstrate that "complete shear bond failure could not occur because of the restraint provided by the metal studs and continuous deck and slabs." (Roeder 1981).

By the late 1970's, Steel Deck Reinforced Concrete (SDRC) floor systems were gaining popularity in the United Kingdom. Recent research in the U.K. on SDRC floor systems is decribed by Wright et al. (1987). He observed that "the construction or wet concrete stage often produces the critical loading for composite slab design." Based upon this observation, Wright went on to develop a design procedure for the wet-concrete stage (Wright and Evans 1987). This procedure is beyond the scope of this review and is not presented in detail here. Wright also states that "currently it

---

2 *that is, same metal deck and headed studs as well as a similar sized support beam.*

is not possible to obtain an accurate determination of strength other than by performance testing" (Wright et al. 1987).

At this time, the design method, in the U.K., is the "m and k" method developed by Schuster, Porter and Ekberg, although Wright mentions that the m and k coefficients "have no physical significance." (Wright et al. 1987). The key differences between the current U.S. standard and the U.K. standard are that a minimum of six tests must be performed on each configuration and the requirement of "10,000 load cycles, varying between 0.5 and 1.5 times the design load before the test to failure is commenced. This preliminary cycling ensures that any chemical bond between concrete and steel has been destroyed so that the test to failure gives a true value of embossment capacity." (Wright et al. 1987).

As composite floor systems continued to gain acceptance in Europe, new design methods were proposed. One approach was suggested by Wolfel, where elastic theory is used to predict partial interaction of the deck and concrete (Wolfel 1987).

Wolfel's basic equation is

$$\tau = (1-\beta_D)\frac{V}{eA_2}$$

where,

$\tau$ = horizontal shear at deck/concrete interface

$\beta_D$ = coefficient dependent upon loading/deck type

V = Applied shear

e = distance between center of compression and center of tension

$A_2$ = cross-sectional area

This equation allows the designer to predict the stress at the deck/concrete interface and thus predict the load per embossment or indentation. A problem arises in determining the force that each embossment will carry, thus the testing program is not eliminated, but is modified.

Tabulated within the paper are values for the calculation of $\beta_D$ for specific loading cases. The method appears to yield good results in the post-cracking region for deflection and load but, large deviations appear in the pre-cracking region (where service load predictions would be made).

A major drawback with this method is the lack of consideration for end restraint and that the results were compared for only two types of deck. With some modification, verification of other types of deck, and the inclusion of end restraint/multiple spans, this method could be used for design purposes.

The most extensive European testing and analytical studies to date have been conducted by Daniels, O'Leary, and Crisinel. The results of the studies are documented in several papers (Daniels et al. 1990; O'Leary et al. 1990).

The experimental research program included the testing of multiple spans with field end details, pull out shear bond tests, simple support shear bond tests and a finite element study to better understand the interaction of the deck and concrete.

A few of the key observations of the Daniels et al. study (1990) are, "failure due to horizontal debonding may be expected **only on exterior spans without anchorage.** "Continuous and concentrated connection behavior are separated and defined. Continuous being chemical, friction, embossments etc.; concentrated would include shear studs, shot fired pins, etc. Also the observation was made that "anchorage increases both load carrying capacity and ductility." (Daniels et al. 1990).

As part of the research, Daniels investigated the slab response using Finite Elements (Daniels et al. 1990). Although providing a good agreement with test data the finite element approach would not be practical for general design; although, firms and deck manufacturers with the capability could take advantage of the understanding gained by using a finite element model.

At the present time Australian standards for composite slabs are in the process of being formulated. The literature (Patrick 1990) suggests that the standard that may be adopted is based on a partial composite slab model, which will require confirmatory push off tests to determine the strength of the concrete to deck interface.

The push off tests are referred to as a "slip block test" in which "the conditions during longitudinal slip failure in a full sized slab are simulated using small slab elements", Figure 2.8 (Patrick 1990). This "slip block" allows for the effects of end anchorage, conventional reinforcement, adhesion bond, mechanical interlock and frictional resistance. Patrick states that the tests can distinguish between the last three effects

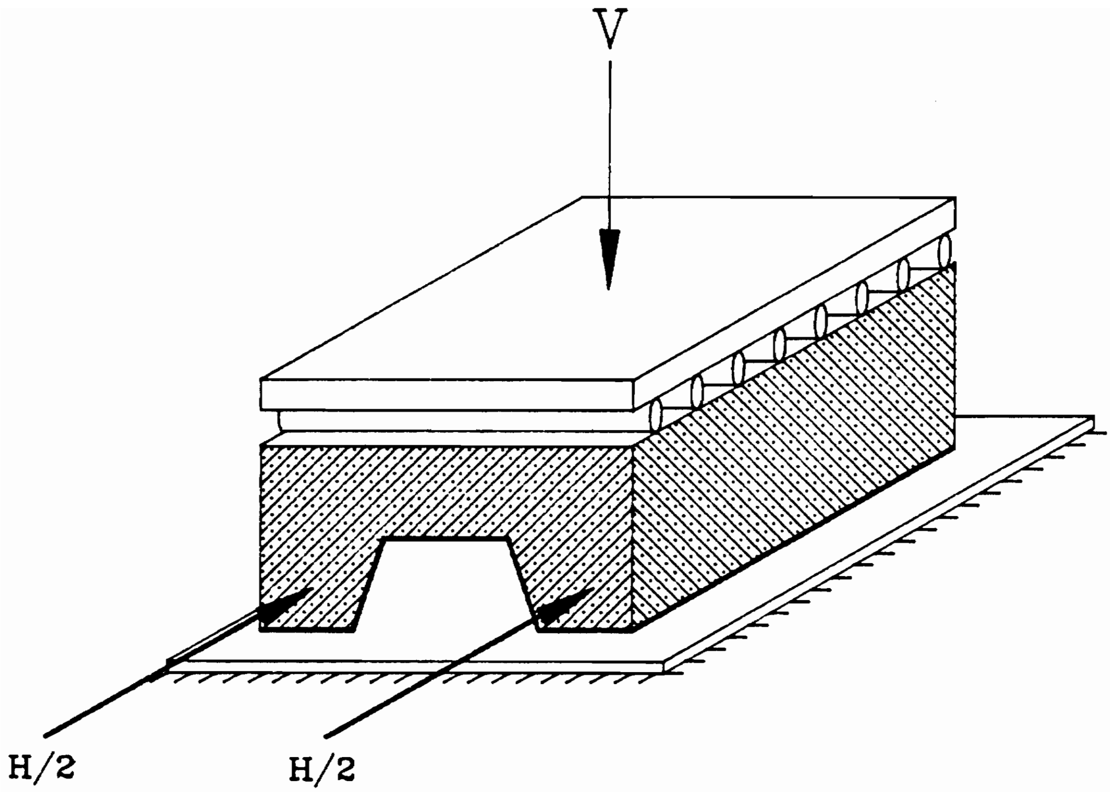


**Figure 2.8 Slip Block**

and thus yield values of the degree of mechanical interlock and the coefficient of friction between the steel deck and concrete.

The final form of the equation after the "slip block test" is:

$$T = x \cdot \frac{H_{rib}}{b_r} + \mu \cdot \frac{V_{\mu}}{b} + T_{anch}$$

where,

$T$ = resultant tensile force in sheeting

$x$ = distance to a slab cross-section

$H_{rib}$ = rib resistance force per unit length without clamping force

$b_r$ = effective width of slip block

$\mu$ = coefficient of friction between sheeting and concrete

$V_{\mu}$ = total vertical reaction and end support at ultimate load

$b$ = width of slab

$T_{anch}$ = ultimate strength of end anchorage system

Research is currently being conducted in the USSR (Airumyan et al. 1990) with confirmatory pull out tests to obtain the strength of different embossment patterns.

Truss shear connectors have recently been investigated in Japan (Asanum et al. 1990), but these results can not be applied to American deck types due to the embedment of the truss within the concrete and thus providing ultimate strength based upon reinforced concrete theory.

Bode et al. (1988) reported on work conducted in Germany on composite slabs. This study uses a program by the name of "NG-Vergund" to predict the strength of concrete slabs. End constraint, embossment parameters and deck type are all accounted for and the results obtained are excellent. The major drawback is that testing is necessary to "tweek" the computer model into agreement with test data. If a method of correcting the model analytically can be developed, this model may provide the best results to date.

Various methods of predicting composite slab deflection have been used. These usually center around the determination of the moment of inertia. The ASCE Standard currently recommends an arithmetic average of the cracked and uncracked moments of inertia. Lamport and Porter (1990) have suggested a modification to Branson's formula used in ACI 318-89 ("Building" 1989). The results are presented in the above paper and provide good agreement but they are based on single panel, single span specimens. None of the methods consider continuous action or end restraint, and thus do not provide an accurate measure of field conditions.

# Chapter 3
# EXPERIMENTAL PROGRAM

This section of the study describes the test set-up, testing procedure and results. The test identification is of the form SDI-*i*-*j*, where *i* indicates the slab number and *j* indicates the test number within the particular slab. For a summary of each test see Appendix A. For theoretical calculations see Chapter 4 and Appendix B.

## 3.1 Test Setup

### 3.1.1 General

In all tests except for a single ASCE standard test (discussed later), a three span set-up was used. For a given slab, either the center span was loaded or the two end spans were loaded. Figure 3.1 is a schematic of the test set-up for a center span test. The length of each span was 8 ft. center to center of supports and the total width was 6 ft. Concrete was placed 5 in. deep, measured from the bottom of the deck to the top of the slab. The steel deck used was a 2 in., 20 gage galvanized trapezoidal section with web embossments. All of the tests except SDI-3-1 used steel deck with a nominal yield stress of 33 ksi. SDI-3-1 used steel deck with a nominal yield stress of 80 ksi. No negative moment reinforcement or shrinkage and temperature steel

Note A: End shown open for clarity.
For actual detail see text

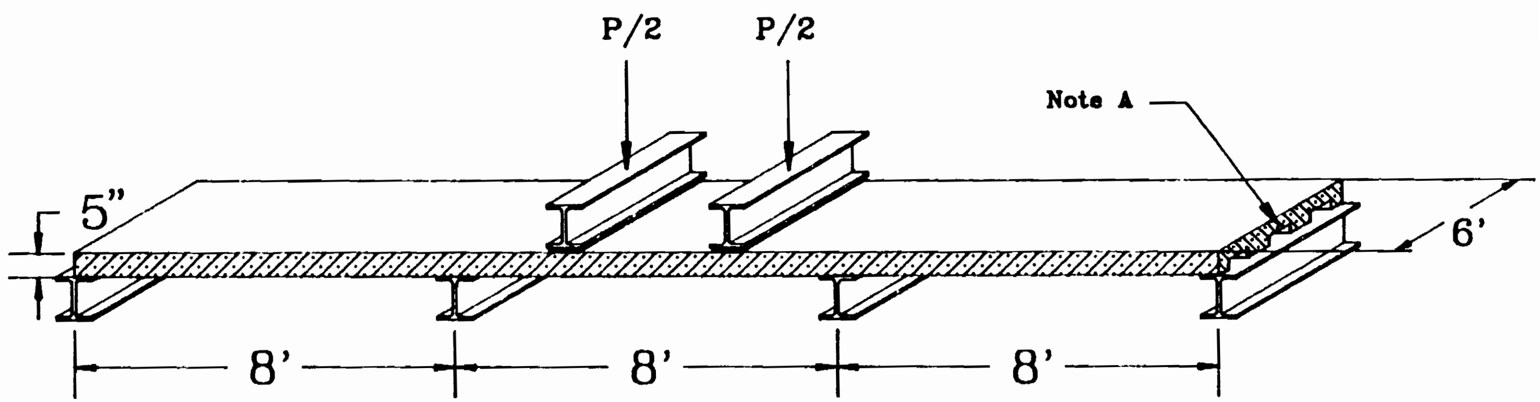


Figure 3.1 Schematic of Multi-Span Test Setup

was provided. The concrete was covered and kept moist for seven days and then allowed to air cure. Form-work along the edges was removed, after seven days, to facilitate observation of the bond between the deck and concrete. Air temperature was not allowed to drop below 65° F for the duration of the cure period.

Strain gages were placed on the bottom side of the deck at the middle of each of the three spans. To measure strain variation on the cross section, gages were placed on the bottom and top flanges. Also, tests SDI-1-1, SDI-2-1, and SDI-2-2 had strain gages at the midpoint of the web. In addition, with the exception of test numbers SDI-1-1, SDI-2-1, SDI-2-2, strain gages were placed on the bottom flange at 1 ft. intervals along the entire tested span. Deflection transducers were placed at midspan and at the quarter points of the span being loaded. Additionally, transducers were placed at midspan of the two spans that were not being loaded. Dial gages were placed at the ends of the specimens to measure slip between the frame and the end of the slab.

All instruments were zeroed prior to the application of the spreader beam system. The first load point consisted of the weight of the spreader beams and associated plates and pads. Subsequent loading was applied with a hydraulic cylinder connected to the test frame. Load was measured by a load cell at this location. The point load of the cylinder was distributed by a spreader beam system which distribute the load to the slab as two line loads transverse to the span. The line loads were located 30 in. from the middle of the supports for the span being loaded.

In the following discussion, the hot rolled angle reference is a L5x5x1/4, the cold-formed angle without a return lip is a L5x5x0.048, and the cold-formed angle with return lip is the same as above except with a 1 in. lip along the top edge, turned into the slab at a 45° angle. All angles were attached to the support members by 1 in. welds placed at 1 ft. intervals along the toe of the attached leg. Intermittent tack welds were placed as needed along the heel of the angles to prevent distortion of the member during the welding process.

### 3.1.2 SDI-1-1, SDI-2-1, SDI-2-2, SDI-4-1, SDI-4-2, SDI-5-1 and SDI-5-2

Specimen configuration for these tests consisted of the general setup with two panels connected, by crimping, at approximately 10 in. intervals to form the 6 ft. width. Steel deck with a measured yield stress of 40 ksi and a tensile strength of 59 ksi was used for these tests. The area of steel was 0.521 square in. per foot width and the moment of inertia of the deck was 0.409 $in^4$ per foot width.

SDI-1-1 was a center span test, with the boundary conditions of adjacent spans on each end. SDI-2-1 was an end span test, with the boundary conditions of an adjacent span on one end and a hot rolled angle on the other end. Figure 3.2 shows the various end span details. SDI-2-2 was an end span test, with the boundary conditions of an adjacent slab on one end and a cold-formed angle without a return lip on the other end. SDI-4-1 was an end span test, with the boundary conditions of an adjacent slab with shear studs on one end and a cold-formed angle with a return lip and shear studs on the other end. SDI-4-2 was an end span test, with the boundary conditions of an adjacent span on one end and a cold-formed angle with a return lip on the other end. SDI-5-1 was an end span test, with the boundary conditions of adjacent span on one end and a cold-formed angle with a return lip on the other. SDI-5-2 was an end span test, with the boundary conditions of adjacent span with a deck joint on one end and a cold-formed angle with a return lip on the other.

### 3.1.3 SDI-3-1

Test SDI-3-1 consisted of three equal triple panel width continuous spans. The steel deck for this test had a measured yield stress of 90 ksi and a tensile strength of 94 ksi. The area of steel was 0.528 square in. per foot width and the moment of inertia of the deck was 0.399 $in^4$ per foot width. SDI-3-1 was a center span test, with the boundary conditions of adjacent spans on each end.

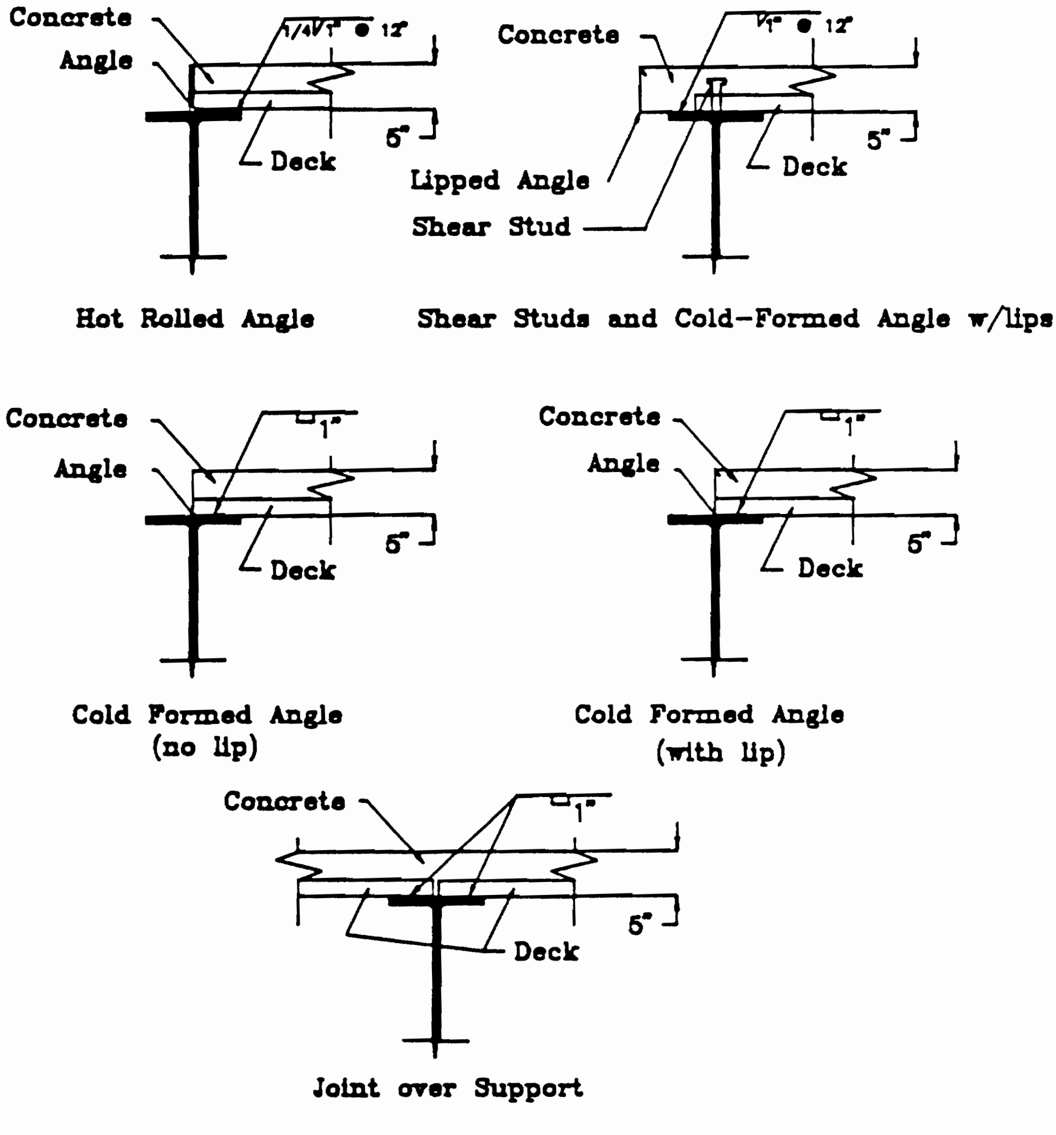


Figure 3.2 Typical End Span Details

### 3.1.4 SDI-6-1 (ASCE Standard Test)

The ASCE Standard Test consisted of an ASCE standard setup with a single panel width simply supported 8 ft. span. The steel deck used was 2 in., 20 gage galvanized trapezoidal section with web embossments with a measured yield stress of 40 ksi and a ultimate strength of 59 ksi. The area of steel was 0.521 square in. per foot width and the moment of inertia of the deck was 0.409 $in^4$ per foot width. Concrete was placed 5 in. deep, measured from the bottom of the deck to the top of the slab. Formwork was placed around the perimeter of the deck and was removed after seven days. The exception to the ASCE standard was that the supports were not rollers, instead the deck was placed directly on the flanges of the two support members without any attachment of the deck.

## 3.2 Test Results and Observations

Strain gages on the extreme fibers of the deck were monitored during the placement of the concrete. Table 3.1 lists average strain due to concrete placement as well as concrete strength on the day of the tests.

Table 3.1

Deck Strain Due to Concrete Placement
and
Concrete Strength on day of Test

| Test | Average Strains ($\mu$) | Concrete Strength (psi) |
|---|---|---|
| SDI-1-1 | 120 | 4330 |
| SDI-2-1 | 300 | 4720 |
| SDI-2-2 | 290 | 4720 |
| SDI-3-1 | 282 | 4400 |
| SDI-4-1 | 260 | 4575 |
| SDI-4-2 | 268 | 4575 |
| SDI-5-1 | 230 | 3300 |
| SDI-5-2 | 380 | 3300 |
| SDI-6-1 | 323 | 3300 |

### 3.2.1 SDI-1-1

*Discussion*

The loading program proceeded by beginning at the first load point as described above. After this, the load was increased in approximately one kip increments until it became necessary to proceed in increments of displacement (at a load of approximately 22.2 kips). Load was then applied in midspan displacement increments of 0.05 in. Loading continued until 2 in. of deflection was recorded. At this point, the test was stopped and unloaded.

*Important Points in Loading Process*

Cracking over the supports was observed at a moment of 58.5 k-in. At a moment of 220.5 k-in., cracking under the spreader beams occurred but no slip at the ends of the slab was measured. Separation of the deck and concrete between the spreader beams was observed at a moment of 315 k-in. The concrete and deck were in contact between the spreader beams and the support members. The maximum applied moment was 400.5 k-in. with no measured end slip occurring.

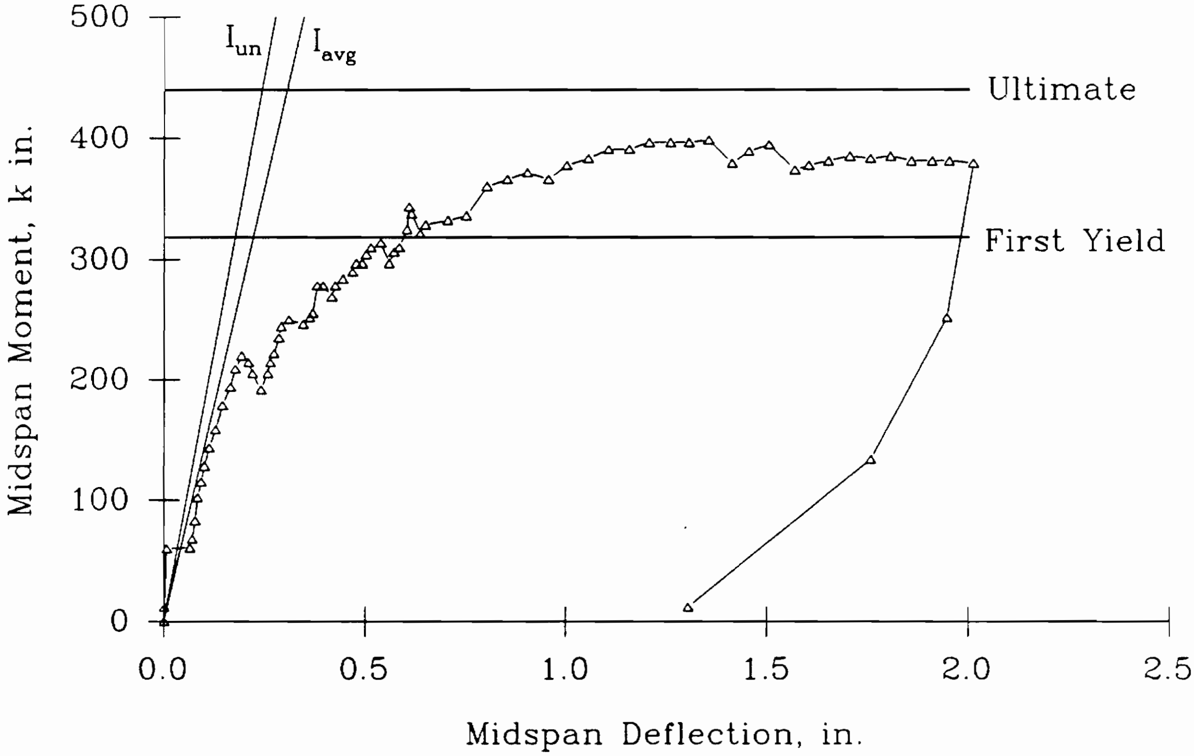


a) Midspan Moment vs. Midspan Deflection

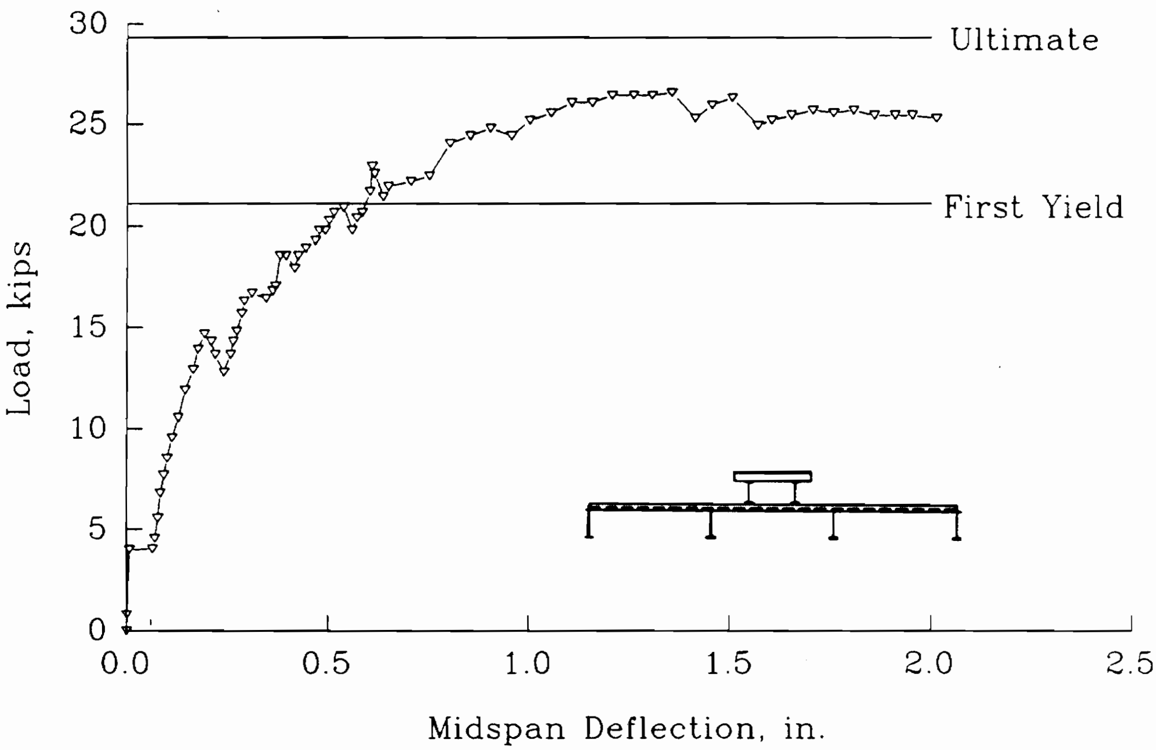


b) Load vs. Midspan Deflection

Figure 3.3 SDI 1-1 Moment (Load) vs. Deflection Plot

*Post-test Discussion*

A plot of the moment verses deflection, shown in Figure 3.3, reveals that there is a gradual change in the slope of the curve and a long plateau of yielding of the steel deck. This phenonomia is verified by the strain measurments taken in the deck (Figure A3).

### 3.2.2 SDI-2-1

*Discussion*

The loading sequence for this test was similar to SDI-1-1 except that the load was increased in three kips increments until a load of 22.3 kips was reached, at which point midspan deflection increments of 0.05 in. were used. Loading was terminated when 2 in. of deflection was recorded. No slip between the deck and concrete occurred until after ultimate load.

*Important Points in Loading Process*

Cracking over the supports was present before the loading process began. At a moment of 184.5 k-in. separation of the concrete and hot rolled angle occurred. At a moment of 195 k-in. cracking under the load points occurred. At a moment of 363 k-in. separation of the deck and concrete between the spreader beams was noticed.

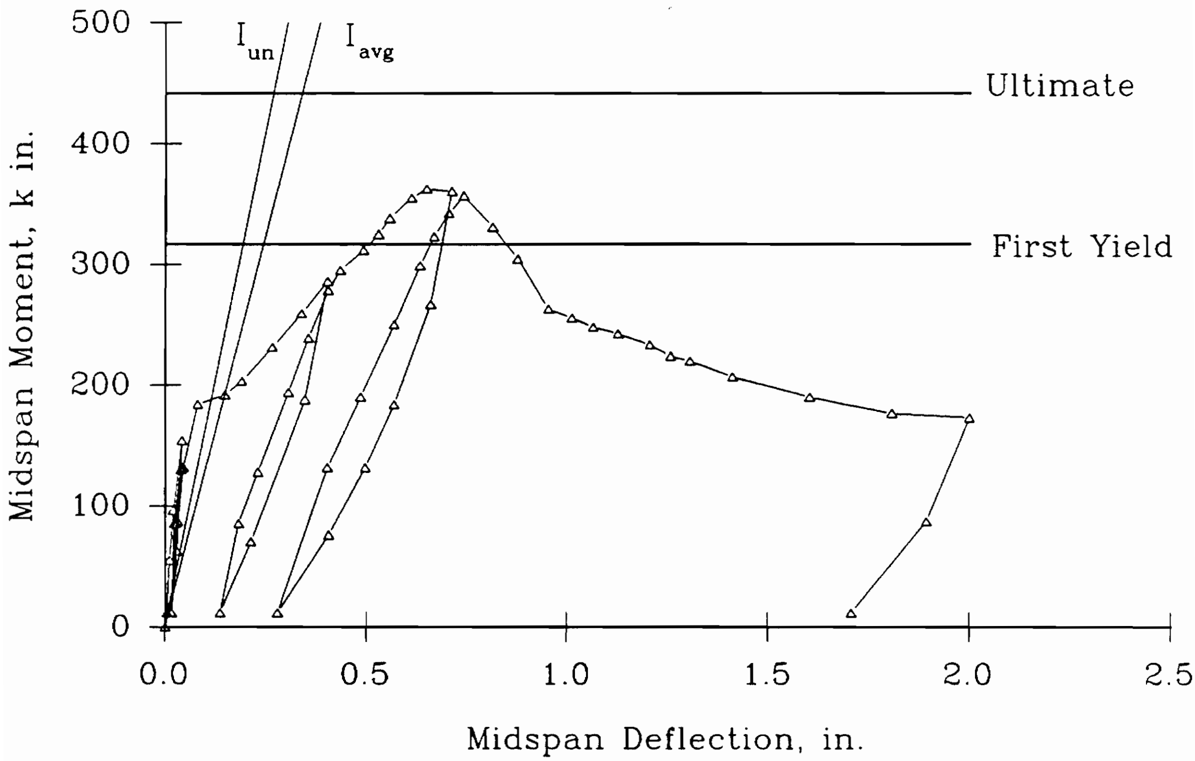


a) Midspan Moment vs. Midspan Deflection

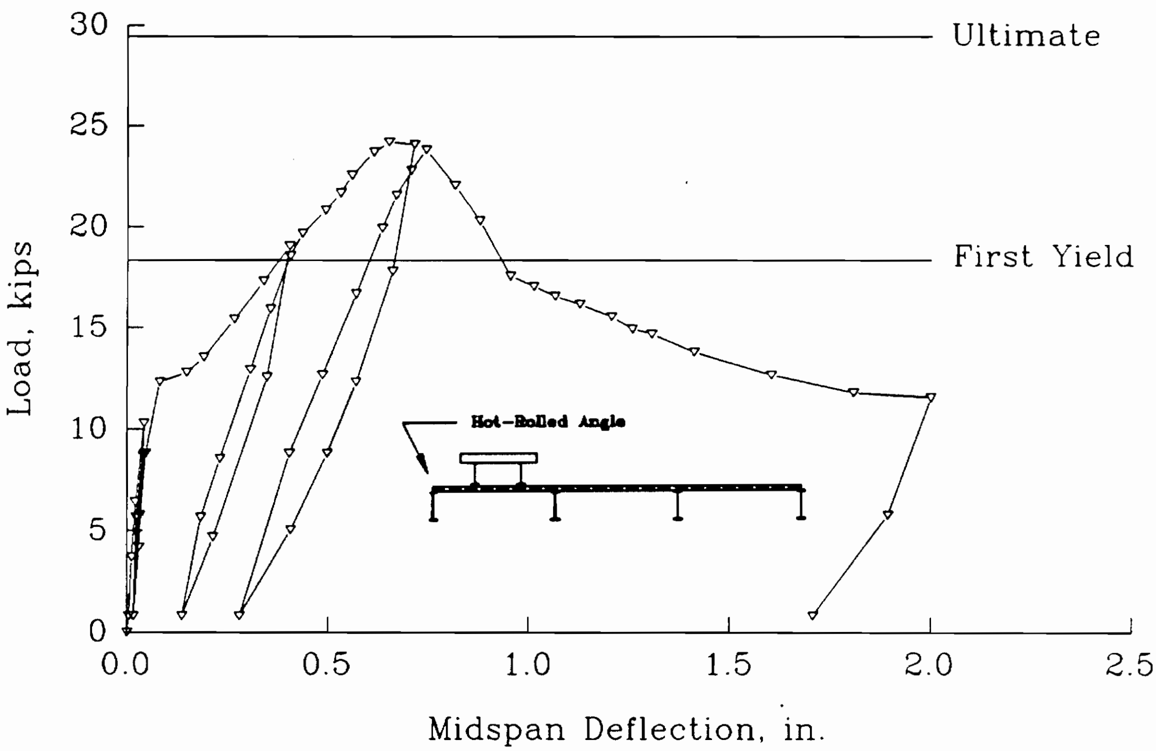


b) Load vs. Midspan Deflection

Figure 3.4 SDI 2-1 Moment (Load) vs. Displacement Plot

At several points during the loading process, the slab was unloaded and then reloaded.

*Post-test Discussion*

The different stiffness values of each unloading can be seen in the plot of moment verses displacement (Figure 3.4a). At the loading point that caused cracking under the loads points, an appreciable change in stiffness can be seen on the plot.

Observation of the end detail during the loading showed that the concrete and deck were rotating about the inside edge of the top flange of the outer support member and thus the end of the concrete was riding up the angle. A comparison of Figures 3 and 4 indicate that the behavior observed in SDI-2-1 is considerably less ductile than that of SDI-1-1. In the post ultimate range for SDI-2-1, the deck tore around the puddle welds at the end of the span and slip between the deck and concrete occurred.

### 3.2.3 SDI-2-2

*Discussion*

The loading sequence was the same as for SDI-2-1 with the exception that no unloading occurred. The transition from load control to displacement control occurred at a load of 24.3 kips. No slip between the deck and concrete occurred until after ultimate load.

### *Important Points in Loading Process*

Cracking over the supports was present before the loading process began. At a moment of 237 k-in. cracking under the spreader beams occurred without a significant drop in load, as can be observed from Figure 3.5. An ultimate moment of 364.5 k-in. was obtained with a corresponding midspan displacement of 0.91 in. After ultimate load, at a moment of 337.5 k-in., separation of the pour-stop and concrete occurred suddenly.

### *Post-test Discussion*

As in SDI-2-1, this test was less ductile than the center span test. Also, as in SDI-2-1, the deck ripped out around the puddle welds and slip between the deck and concrete occurred in the post ultimate range of behavior. The concrete was again rotating about the inside edge of the top flange of the support member thus causing the end of the concrete to ride up and bend the cold-formed angle.

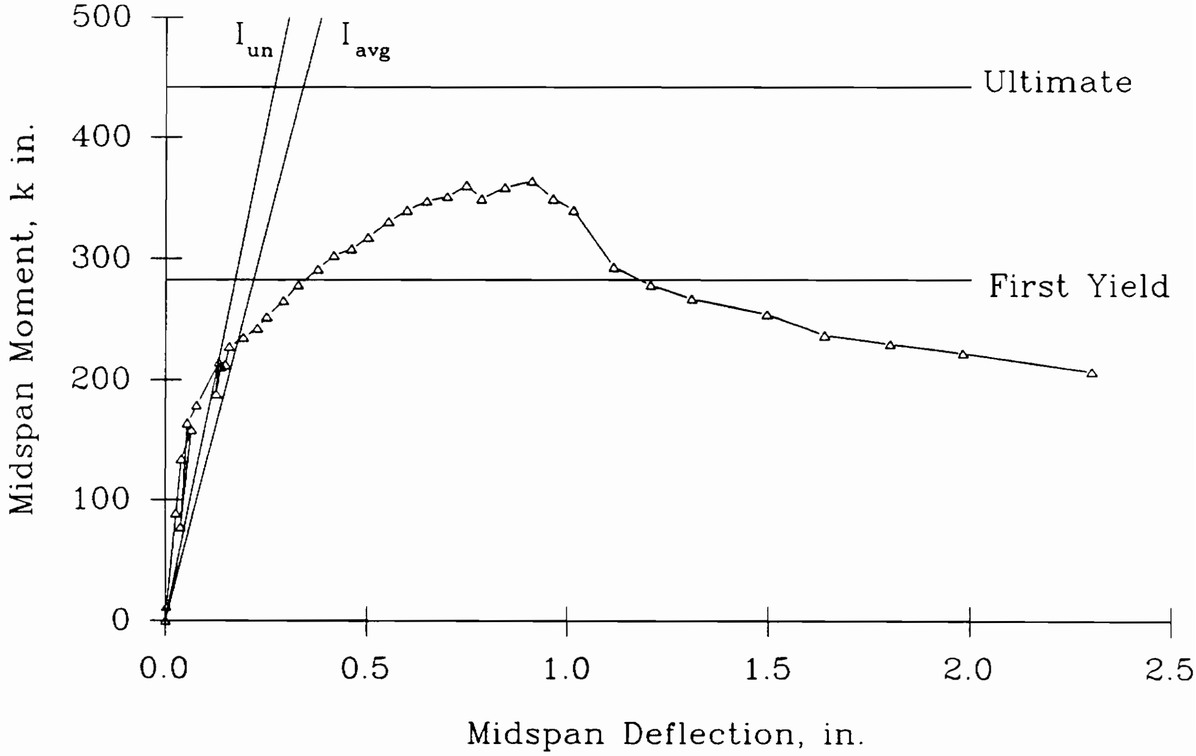


a) Midspan Moment vs. Midspan Deflection

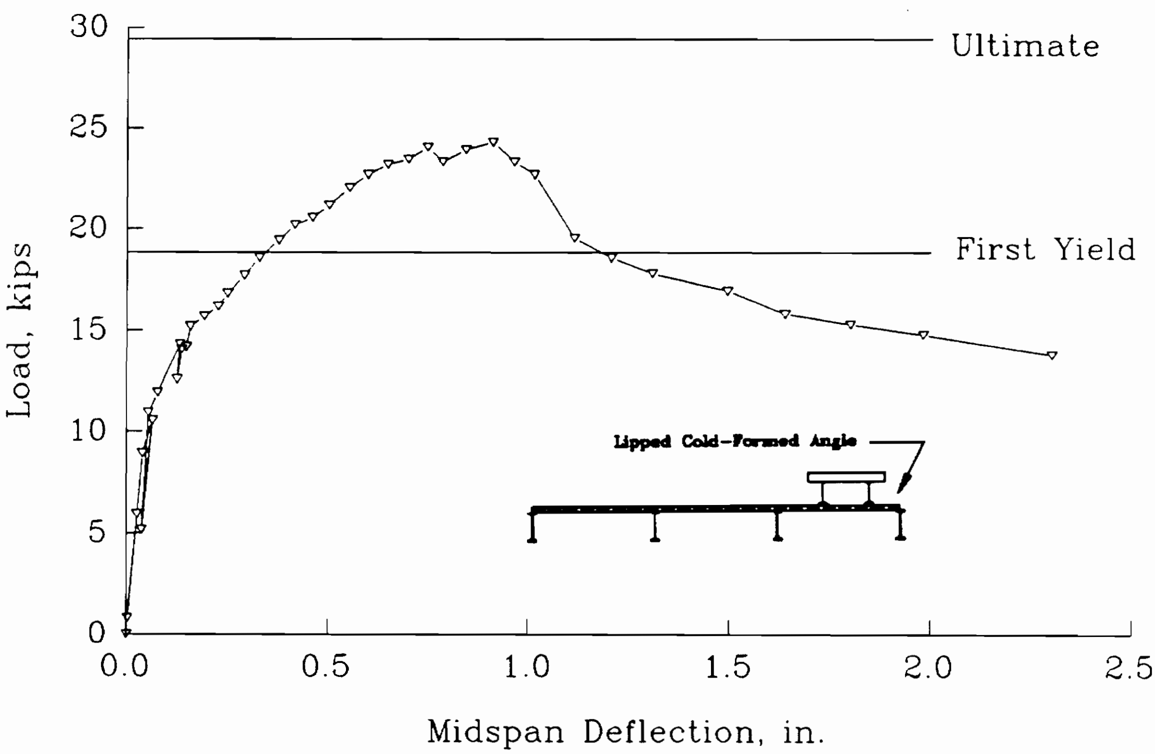


b) Load vs. Midspan Deflection

Figure 3.5 SDI 2-2 Moment (Load) vs. Deflection Plot

### 3.2.4 SDI-3-1

*Discussion*

The loading sequence was similar to that of previous tests. Two unloading cycles were performed at selected points along the loading path, as can be seen in Figure 3.6. Unloading number one occurred at a moment of 148.5 k-in. to obtain an approximate uncracked stiffness and the second unloading occurred at a moment of 270.0 k-in. to obtain a cracked stiffness. No appreciable slip of the deck and concrete occurred after ultimate load had been reached. An ultimate moment of 802.5 k-in. was obtained. The reader is reminded that the deck for this test had a yield strength of 90 ksi and thus the higher moment.

*Important Points in Loading Process*

Cracking over the supports occurred at a moment of 162.0 k-in. At a moment of 260.0 k-in. cracking under the load points occurred. Some cracking between the two loading points occurred at 717.0 k-in. The test was stopped when a midspan deflection of 2 in. was recorded.

*Post-test Discussion*

As with SDI-1-1 there is a long plateau of yielding of the deck. This is confirmed from the strain gage data in Figure A12. It is noted that with a 2 in. deflection on

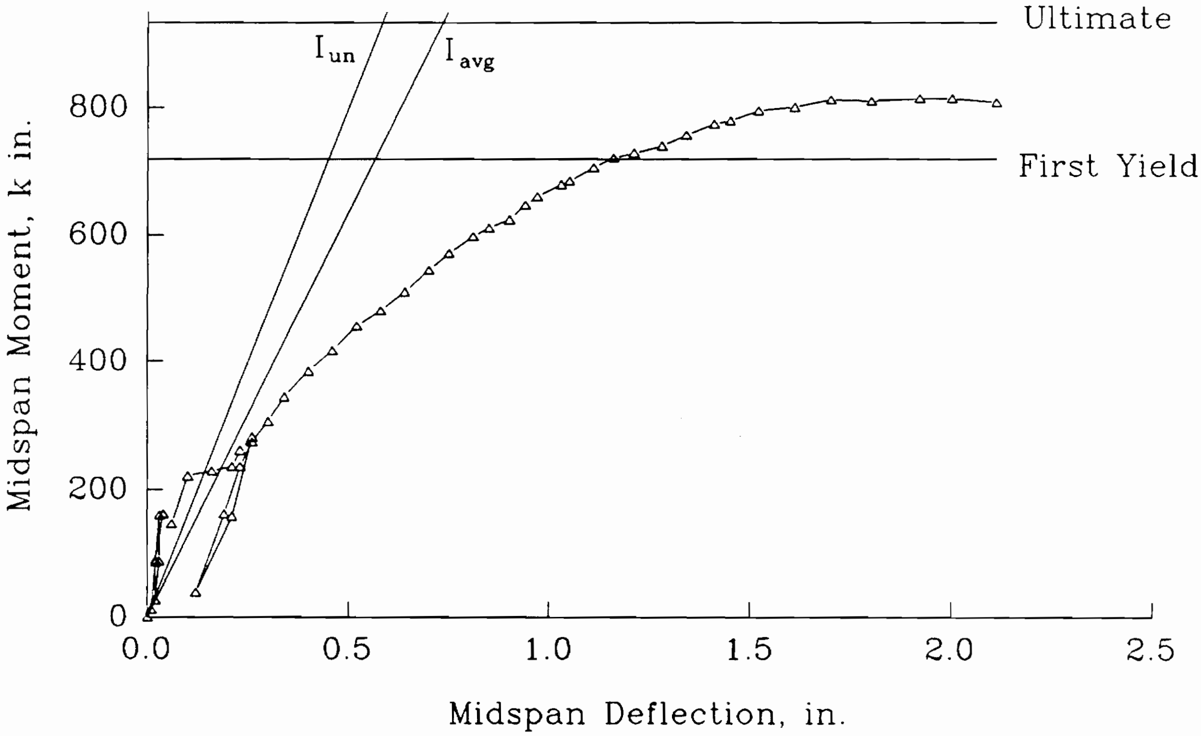


a) Midspan Moment vs. Midspan Deflection

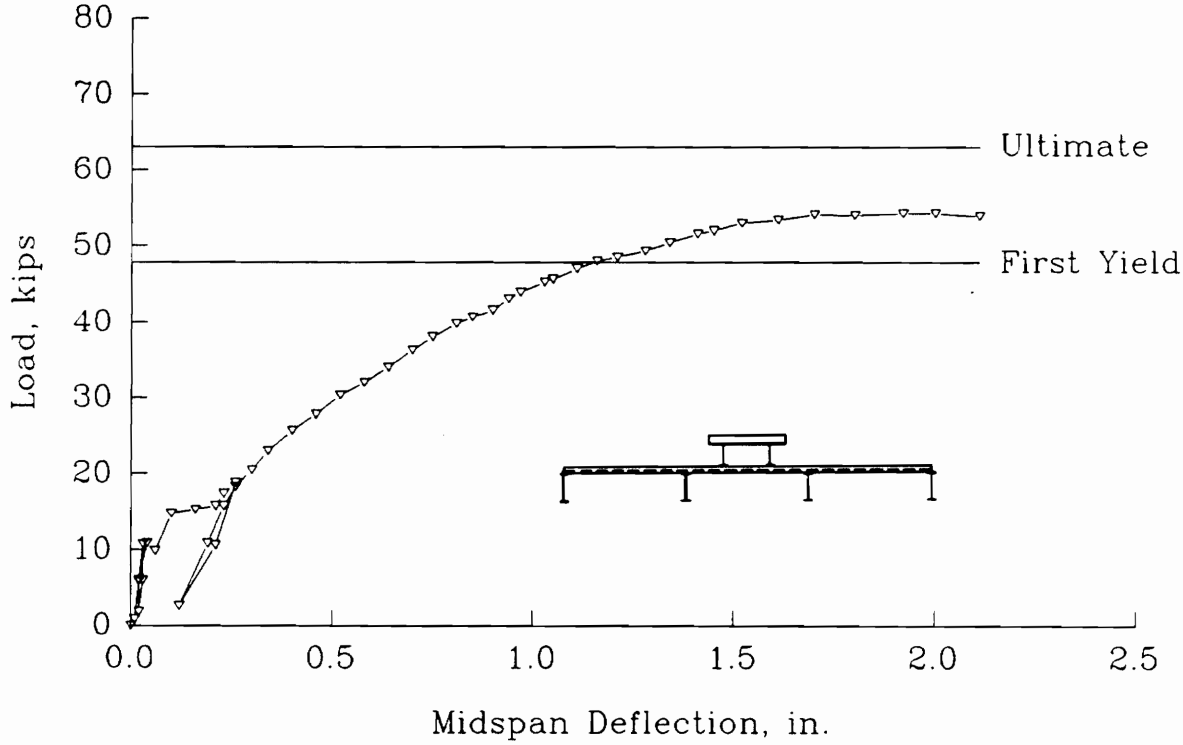


b) Load vs. Midspan Deflection

Figure 3.6 SDI 3-1 Moment (Load) vs. Deflection Plot

an 8 ft. span (L/48) the specimen was holding near ultimate load. Observations at the end of the test indicated that the deck was ripping out around the puddle welds over the supports, suggesting that the welds were preventing the slippage of the deck.

### 3.2.5 SDI-4-1

*Discussion*

The loading sequence for SDI-4-1 was similar to those of previous tests. Four unloading cycles were performed during the course of the test, as can be seen in Figure 3.7. One at a moment of 127.5 k-in. to obtain an approximate uncracked stiffness. The second occurred at a moment of 247.5 k-in. to obtain a cracked stiffness. The third at a moment of 393 k-in. and the fourth after the ultimate load had been surpassed to investigate the overloading characteristics of the slab.

*Important Points in Loading Process*

Cracking over the support occurred at a moment of 58.5 k-in. Cracking occurred under the loading closest to the cold-formed angle detail at a moment of 231 k-in. After ultimate load was reached, cracking over the shear studs occurred and a subsequent drop in load occurred. An ultimate moment of 444 k-in. was obtained.

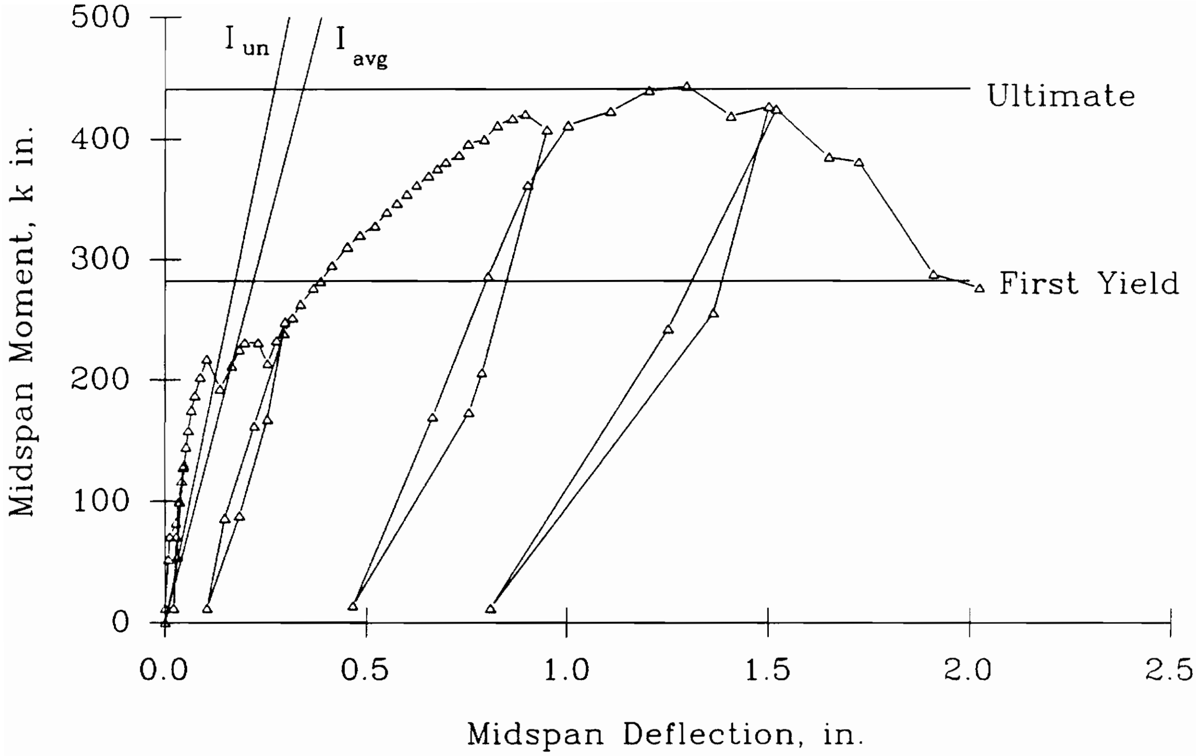


a) Midspan Moment vs. Midspan Deflection

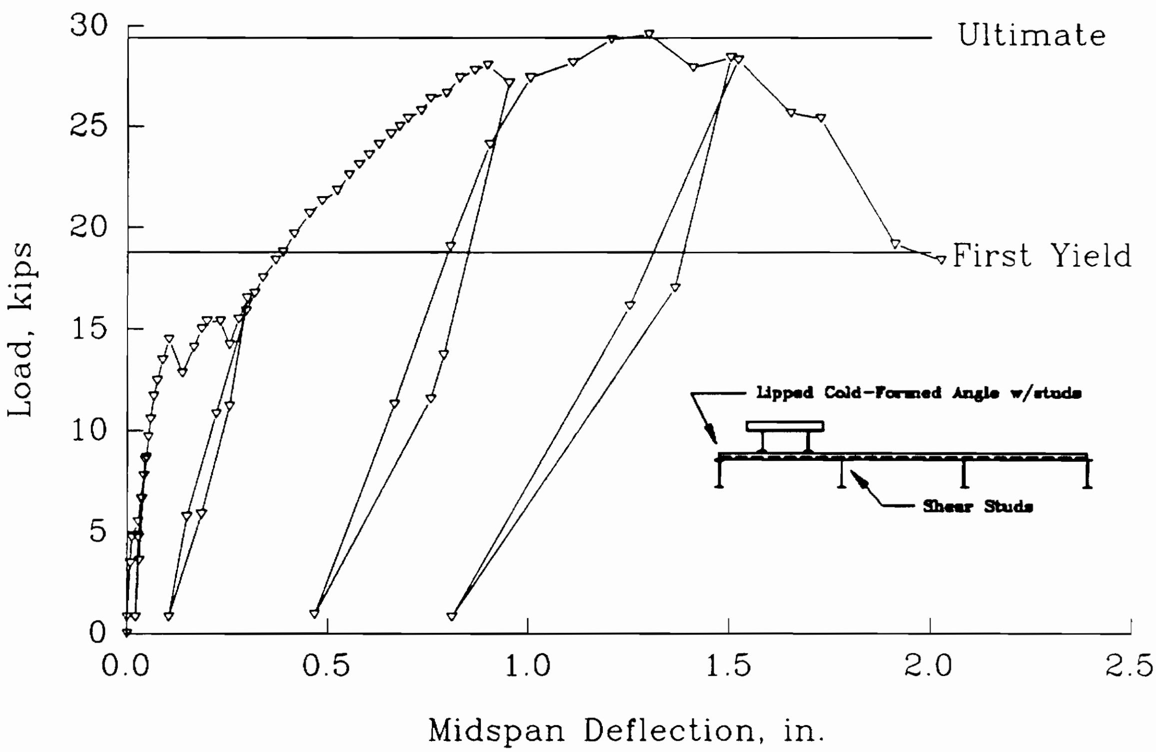


b) Load vs. Midspan Deflection

Figure 3.7 SDI 4-1 Moment (Load) vs. Deflection Plot

*Post Test Discussion*

A post test inspection revealed that in general the shear studs and deck were still attached to the support members. However, the concrete had cracked directly over the studs. It was also observed that the entire deck remained in tension until the last unloading (post ultimate) cycle, this suggests that the studs were adequately preventing slippage of the deck and concrete and thus allowing more of the steel deck to act as positive moment reinforcement.

### 3.2.6 SDI-4-2

*Discussion*

Two unloading cycles were performed during this test, as is seen in Figure 3.8. The first was at a moment of 200 k-in. to obtain a cracked stiffness and the second after a peak moment of 234 k-in.

*Important Points in Loading Process*

Immediately upon loading an end slip was recorded. Cracking over the support occurred at a moment of 178.5 k-in. Note that this cracking occurred at a higher moment than in the previous tests. Cracking under the load points occurred at a moment of 244.5 k-in.

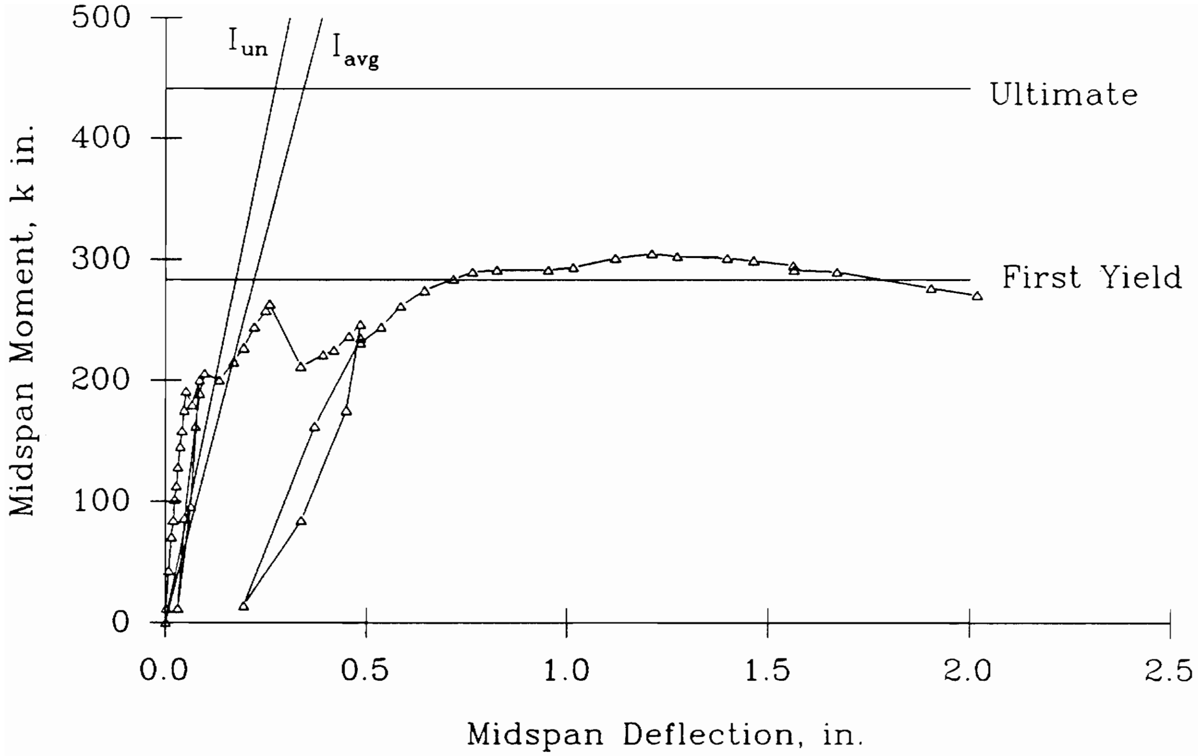


b) Midspan Moment vs. Midspan Deflection

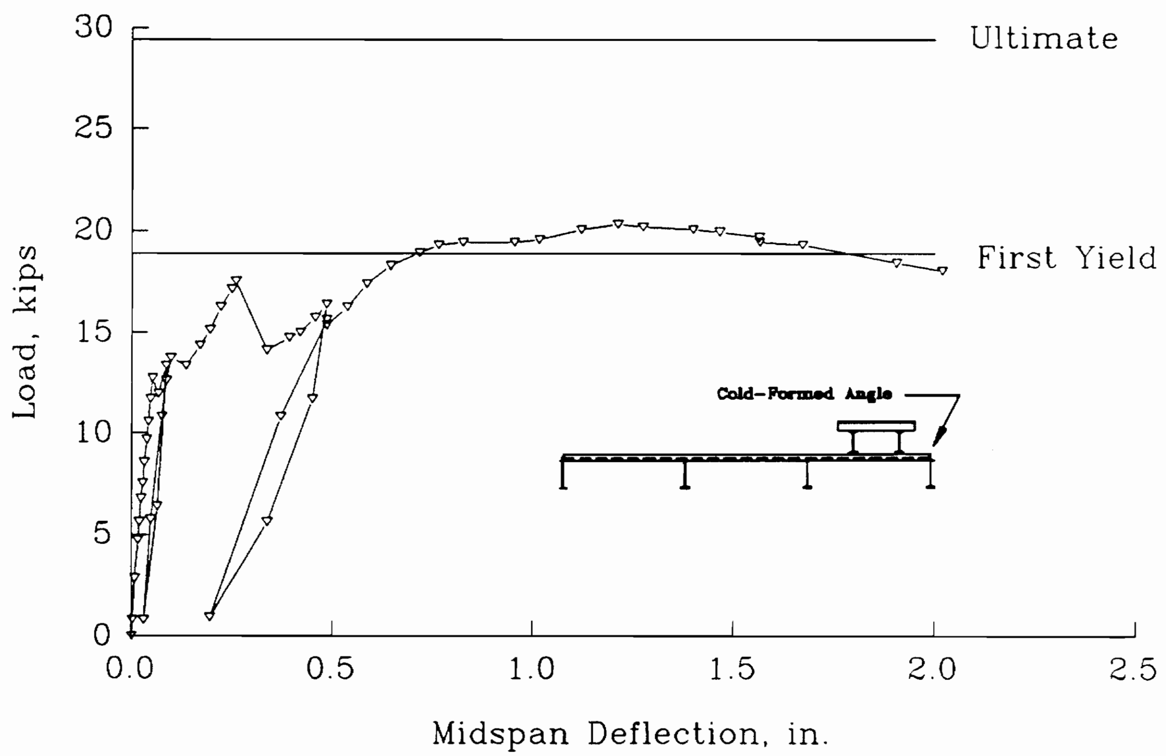


a) Load vs. Midspan Deflection

Figure 3.8 SDI 4-2 Moment (Load) vs. Deflection Plot

*Post-test Discussion*

One should note that the maximum load obtained was less than in previous tests that had similar configuration. After the test the concrete slab, deck, and end details were all closely examined in order to find an explanation for the results. Upon lifting the slab off of the cold-formed angle support end, it was discovered that the welding had been ineffective. Approximately 50% of the puddle welds did not fuse properly with the base metal.

### 3.2.7 SDI-5-1

*Discussion*

Two unloading cycles were performed during the test, as seen in Figure 3.9. The first was at a moment of 159.3 k-in. to obtain a uncracked stiffness and the second was performed at a moment of 246.6 k-in to investigate post ultimate stiffness.

*Important Points in Loading Process*

Cracking over the support occurred at a moment of 121.8 k-in. As in test SDI-4-2 this occurred at a higher value that other tests. Cracking under the load points occurred at a moment of 221.25 k-in. Debonding of the deck and concrete between the load and the support was recorded at ultimate moment of 283.5 k-in.

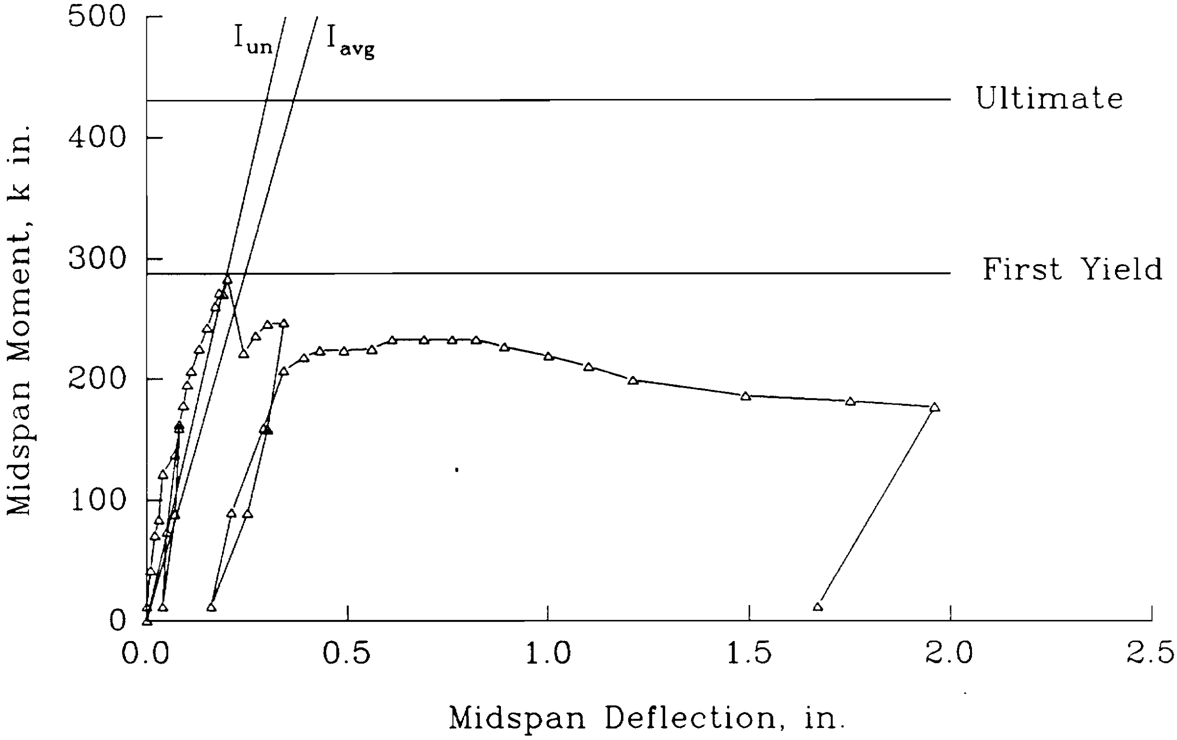


a) Midspan Moment vs. Midspan Deflection

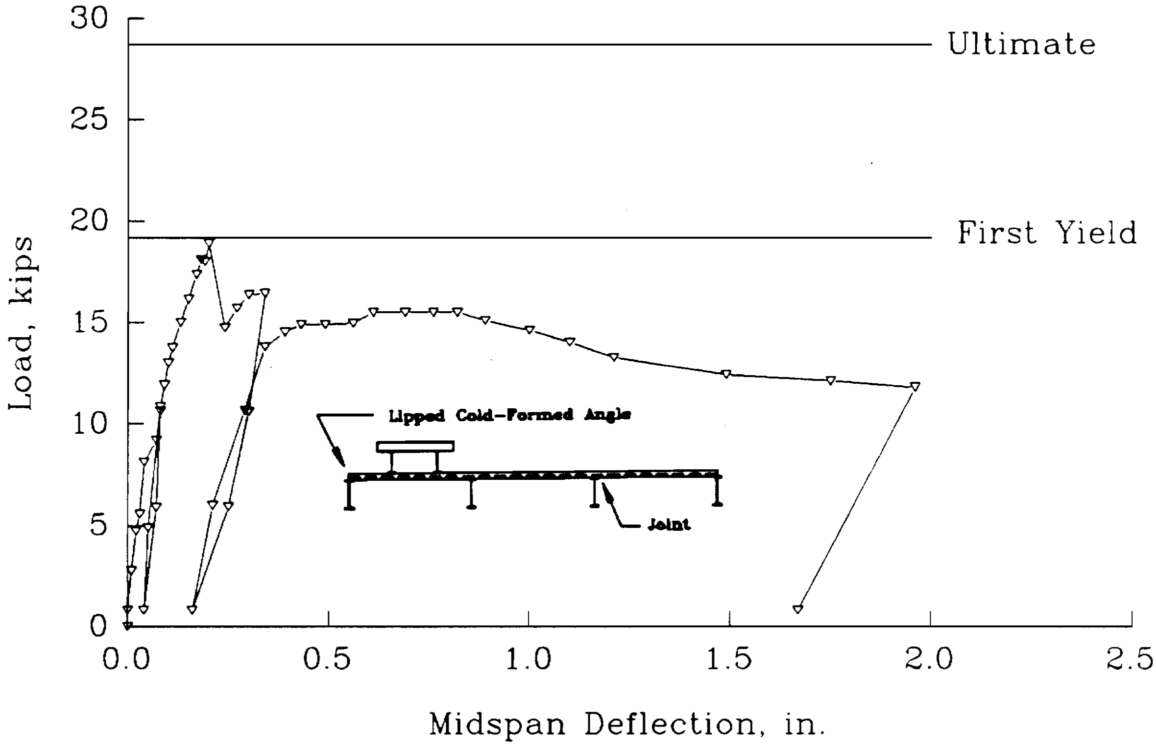


b) Load vs. Midspan Deflection

Figure 3.9 SDI 5-1 Moment (Load) vs. Deflection Plot

*Post-test Discussion*

It was noticed soon after the debonding occurred between the load and support that the deck was pulling out from the puddle welds. A post test inspection revealed that the welding process had not fused to the deck and base metal in approximately 40% of the welds.

### 3.2.8 SDI-5-2

*Discussion*

Two unloading cycles were performed on this test (Figure 3.10). The first at a moment of 95.25 k-in. to obtain an uncracked stiffness. The second at a moment of 246.3 k-in. again provide an approximate uncracked stiffness, as the slab had not showed significant cracking or deviation from linear behavior.

*Important Points in Loading Process*

At a moment of 280.65 cracking over the support occurred. Note that this is extremely high compared with other tests. Cracking under the load points occurred at a moment of 294.0 k-in (ultimate load). It was recorded in the post ultimate region at a moment of 151.5 k-in that the deck buckled under inner load point.

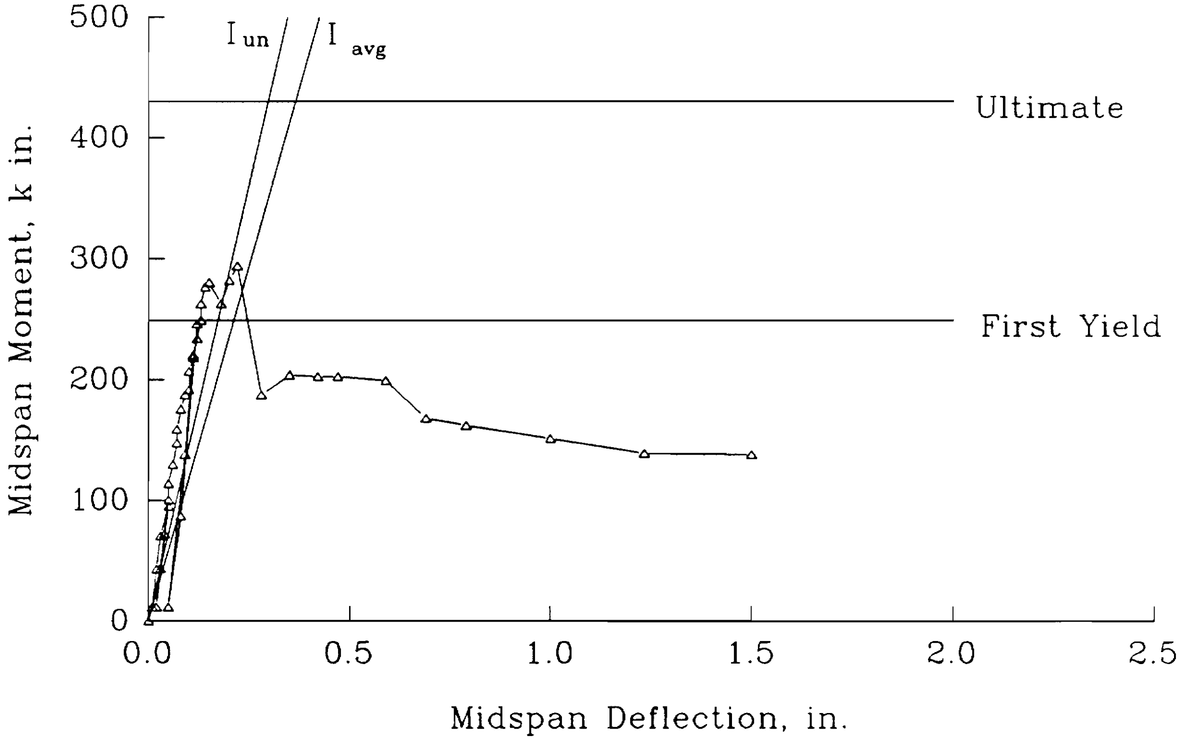


a) Midspan Moment vs. Midspan Deflection

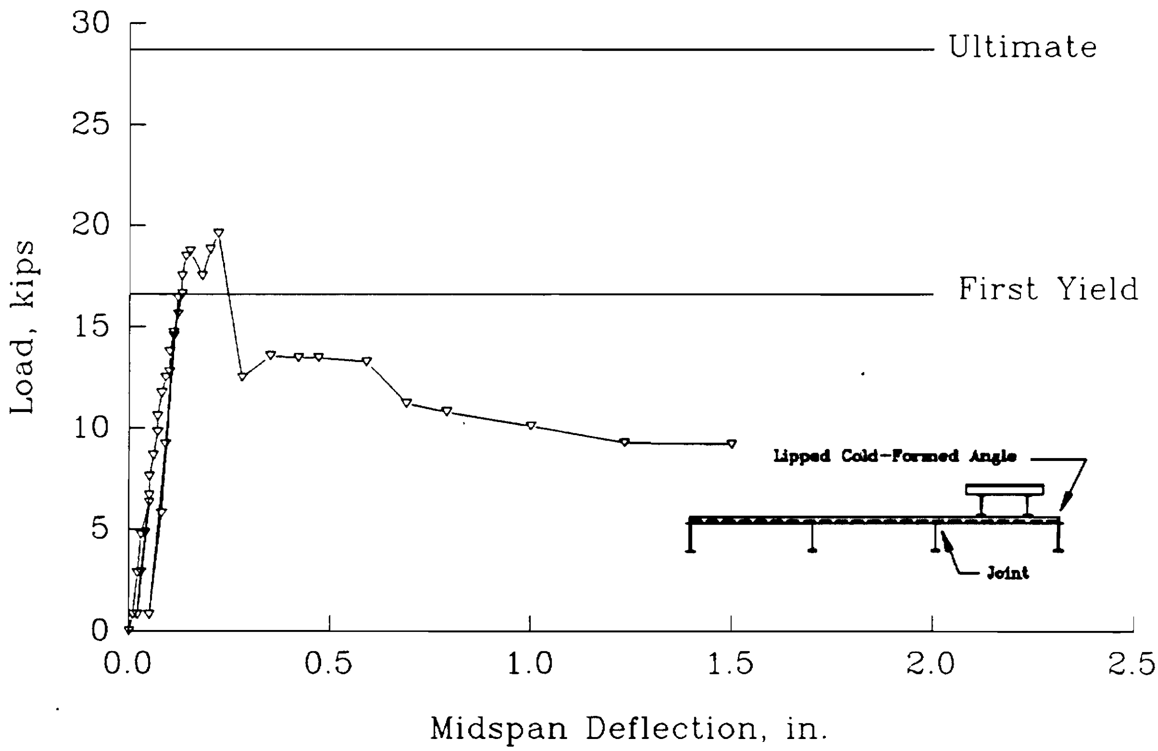


b) Load vs. Midspan Deflection

Figure 3.10 SDI 5-2 Moment (Load) vs. Deflection Plot

*Post-test Discussion*

Post test inspection of the welds connecting the deck with the support member revealed that they appeared to be inadequate at the interior support (near the joint in the deck). This inadequacy is partly due to blowout of the deck and improper bonding to the base material. Upon weld / deck failure it created a near simply supported case for the deck was not continuous over the interior support.

### 3.2.9 SDI-6-1

*Discussion*

This test was performed for comparison purposes between constrained deck and the current standard. A single unloading was performed at a moment of 103.35 to obtain a stiffness value (Figure 3.11).

*Important Points in Loading Process*

Cracking under the load points occurred at a moment of 171.0 k-in with a corresponding loss of bond between the load and support and an appreciable amount of slippage between the deck and concrete.

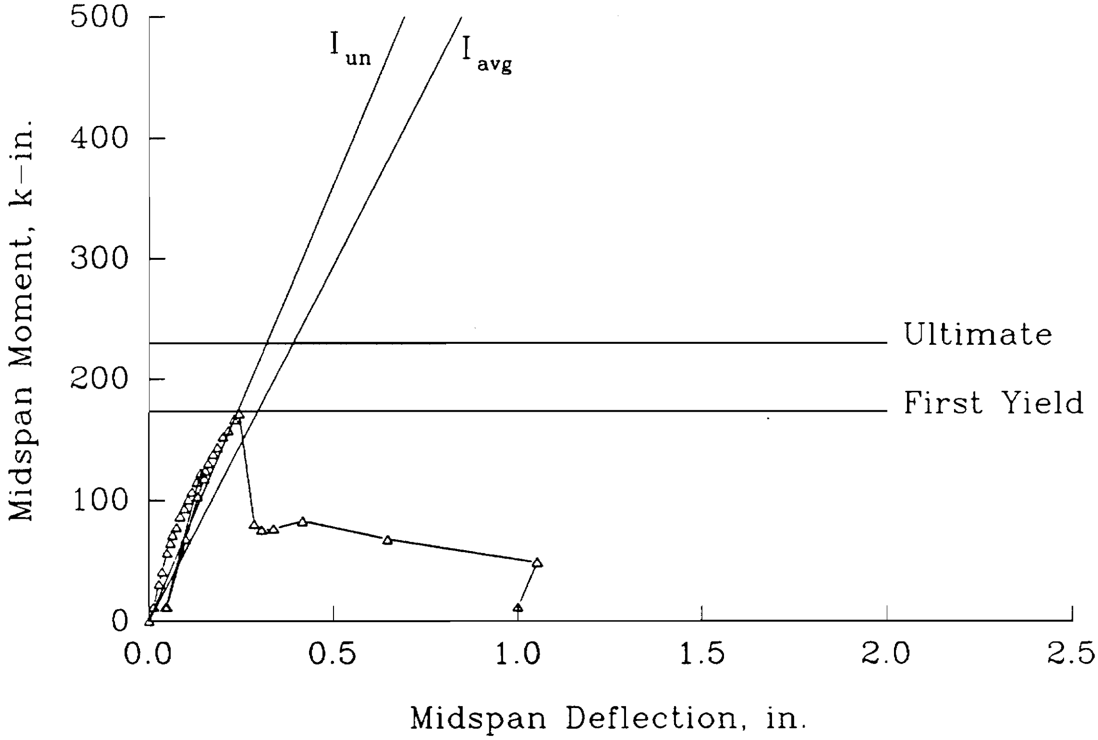


Midspan Moment vs. Midspan Deflection

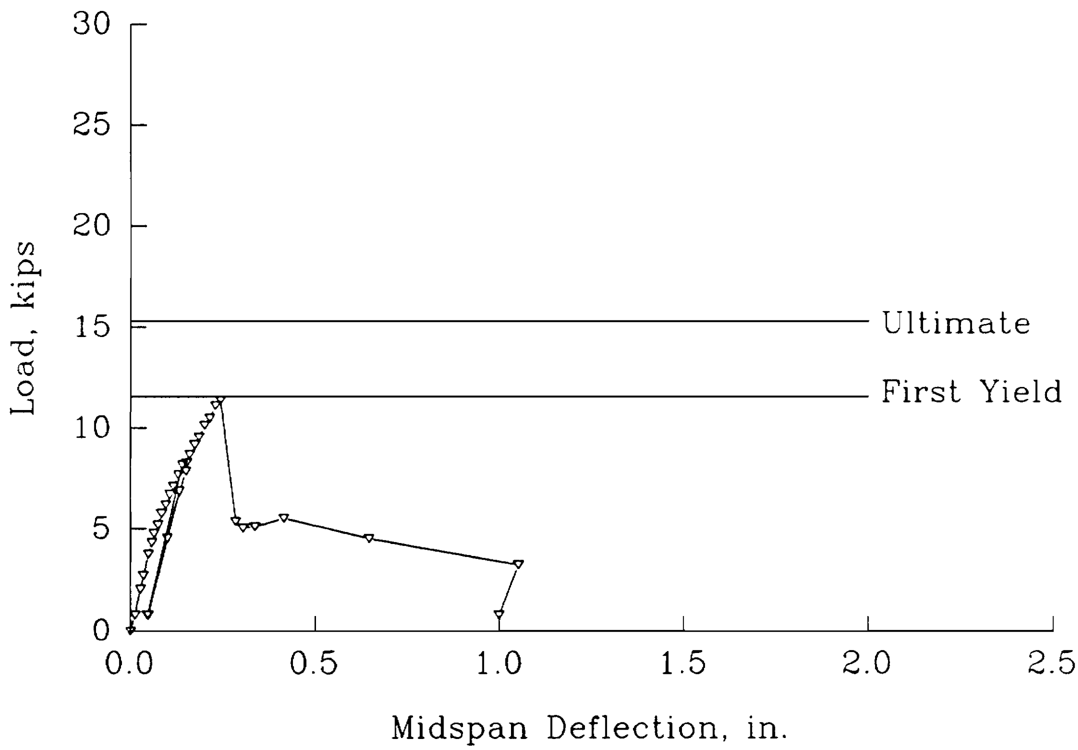


Load vs. Midspan Deflection

Figure 3.11 SDI 6-1 Moment (Load) vs. Deflection Plot

### *Post-test Discussion*

It is noted that a 57% drop in load occurred immediately upon cracking under the load point. The similarity to those tests which possessed inadequate end anchorage is also noted.

# Chapter 4
# STRENGTH AND STIFFNESS FORMULATIONS

Comparisons between the test results and predicted strengths are made. Two limit states are used to predict the strength. These are ultimate strength based on reinforced concrete theory and first yield of the extreme fiber of the deck. For a complete design example see Appendix B. For a summary of the results see Table 4.1.

The ultimate strength line on Figures 3.3 - 3.11 was obtain using reinforced concrete theory with simply supported boundary conditions. The equation used was:

$$M_n = A_s f_y \cdot \left(d - \frac{a}{2}\right) - M_{conc}$$

where,

$M_n$ = nominal moment strength

$A_s$ = cross sectional area of deck

$f_y$ = measured yield stress of deck

d = distance from top of slab to centroid of deck

## TABLE 4.1

## STRENGTH AND STIFFNESS FORMULATIONS SUMMARY

| Test Designation | End Details | Deck Yield Stress (ksi) | Strain Due to Concrete Placement[1] ($\mu$) | Concrete Strength (psi) | Predicted First Yield Moment[2] (k-in) | Predicted Ultimate Moment[2] (k-in) | Moment of Inertia Cracked[3] ($in^4$) | Moment of Inertia Uncracked[3] ($in^4$) |
|---|---|---|---|---|---|---|---|---|
| SDI-1-1 | AS-AS | 40 | 120 | 4330 | 316.5 | 439.4 | 251.30 | 425.07 |
| SDI-2-1 | AS-HR | 40 | 300 | 4720 | 275.1 | 441.8 | 243.96 | 419.70 |
| SDI-2-2 | AS-CA | 40 | 270 | 4720 | 282.6 | 441.8 | 243.96 | 419.70 |
| SDI-3-1 | AS-AS | 90 | 282 | 4400 | 718.7 | 945.0 | 250.02 | 423.42 |
| SDI-4-1 | AS(S)-CA(LS) | 40 | 260 | 4575 | 282.2 | 441.0 | 246.72 | 421.50 |
| SDI-4-2 | AS-CA(L) | 40 | 268 | 4575 | 283.1 | 441.0 | 246.72 | 421.50 |
| SDI-5-1 | AS-CA(L) | 40 | 230 | 3300 | 287.6 | 430.4 | 278.82 | 442.62 |
| SDI-5-2 | AS(J)-CA(L) | 40 | 380 | 3300 | 249.5 | 430.4 | 278.82 | 442.62 |
| SDI-6-1 | None | 40 | 320 | 3300 | 172.5 | 218.0 | 139.41 | 221.31 |

AS - adjacent span
HR - hot rolled angle
CA - cold-formed angle
(S) - with studs
(L) - with lip
(J) - with deck joint

ALL TESTS: (Except SDI-6-1)
- 2 in. deep deck
- 3 in. concrete cover
- 30 in. shear span
- 3-8 ft spans
- 6 ft. wide

Test SDI-6-1
- 2 in. deep deck
- 3 in. concrete cover
- 30 in. shear span
- 1-8 ft. span
- 3 ft. wide

[1] in tested span

[2] see Appendix B for calculations

[3] stiffness line calculated by

$$\Delta = \frac{Pa}{24EI}(3L^2 - 4a^2)$$

See Appendix B for definition of terms.

$$a = \frac{A_s f_y}{f_c' \, b}$$

b = slab width

$M_{conc}$ = dead weight moment of concrete slab

Assumptions made in applying this equation are:

1 - reinforced concrete theory and assumptions apply

2 - simple supports (bending of deck not considered over supports)

3 - single span (continuity of deck/concrete not considered)

In calculating the first yield moment, the strain induced in the bottom fibers of the deck due to the concrete placement was considered by calculating a reduced yield stress and using this value for calculations. The equation used was (see Figure 4.1),

$$M_{et} = (T_1 e_1 + T_2 e_2 + T_3 e_3)$$

where,

$M_{et}$ = Calculated Bending Moment at First Yield

$e_3 = h - (y_{cc} / 3)$

$e_2 = e_3 - (d_d / 2)$

$e_1 = e_3 - d_d$

$T_1 = f_{yc} (B_t \, t)[(h - y_{cc} - d_d) / (h - y_{cc})]$

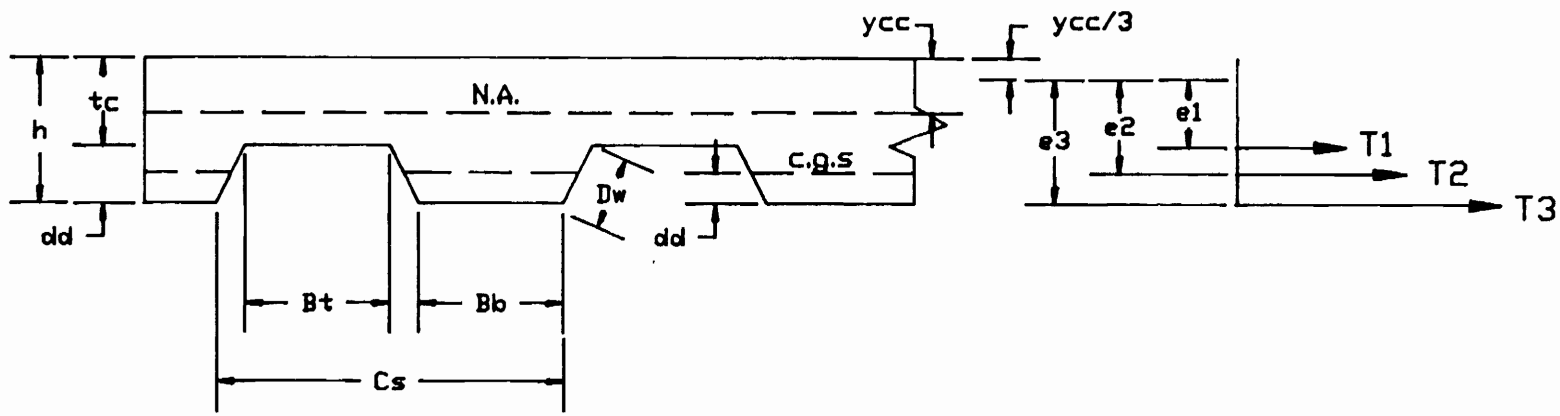


Figure 4.1 Deck Measurments and Force Locations

$T_2 = f_{yc}\,(2D_w\,t)[(h - y_{cc} - d_d/2) / (h-y_{cc})]$

$T_3 = f_{yc}\,(B_b\,t)$

$y_{cc} = d\{[2\rho n + (\rho n)^2]^{0.5} - \rho n\}$

$h$ = out to out depth of slab

$d_d$ = deck depth

$f_{yc}$ = corrected yield stress of deck

$B_t$ = width of top flange

$B_b$ = width of bottom flange

$D_w$ = width of web

$t$ = deck thickness

$\rho$ = reinforcement ratio, $A_s/bd$

$n$ = modular ratio, $E_s/E_c$

Assumptions made in applying this equation:

1 - full composite action

2 - simple supports (bending of deck not considered over supports)

Values for both limit states are shown on the applied moment vs. deflection plots (Figures 3.3 - 3.11).

Stiffness calculations were also made based on simply supported boundary conditions, and with the steel transformed into an equivalent concrete member.

The formula used was,

$$\Delta_{cent} = \frac{M}{24EI} \cdot \left(3L^2 - 4l'^2\right)$$

where,

$\Delta_{cent}$ = deflection at center

M = applied moment

$E_c = 57{,}000(f'_c)^{1/2}$

I = Uncracked / Average moment of inertia

L = span length (8 ft.)

l' = shear span (30 in.)

$f'_c$ = concrete compressive strength (psi)

Two values of the moment of inertia were taken in the calculation of the stiffness. The first is the average of the cracked and uncracked moment of inertia, $I_{avg}$. This is the current ASCE standard recommendation. Also, the uncracked moment of inertia, $I_{un}$, was used and the corresponding stiffness plotted.

# Chapter 5
# KEY OBSERVATIONS

### 5.1 General

This chapter will provide some insight into some of the observed behavior of the test specimens. A complete summary of each test is given in Appendix A and a complete example of the theoretical calculations are given in Appendix B with the assumptions for the theoretical formulas given in Chapter 4.

As can be seen in Table 5.1, in each test the experimental capacity exceeded the predicted load corresponding to first yield (except SDI-5-1 which reached 99% of first yield), but did not reach the predicted ultimate strength (except for SDI-4-1). This behavior is generally indicative of partial composite action.

Interior spans with continuous deck behave in a ductile manner with and ultimate load between first yield and ultimate based on using simply supported boundary conditions (neglecting bending capacity of deck over supports). The details of the end of the deck clearly influence the behavior of a particular specimen. In terms of

## TABLE 5.1

## PROJECT SUMMARY

| Test Designation | End Details | Deck Yield Stress (ksi) | Strain Due to Concrete Placement[1] ($\mu$) | Concrete Strength (psi) | Predicted First Yield Moment[2] (k-in) | Predicted Ultimate Moment[2] (k-in) | Maximum Test Moment (k-in) | $\frac{MTM}{PFYM}$ | $\frac{MTM}{PUM}$ |
|---|---|---|---|---|---|---|---|---|---|
| SDI-1-1 | AS-AS | 40 | 120 | 4330 | 316.5 | 439.4 | 398.3 | 1.26 | 0.91 |
| SDI-2-1 | AS-HR | 40 | 300 | 4720 | 275.1 | 441.8 | 363.0 | 1.32 | 0.82 |
| SDI-2-2 | AS-CA | 40 | 270 | 4720 | 282.6 | 441.8 | 364.5 | 1.29 | 0.83 |
| SDI-3-1 | AS-AS | 90 | 282 | 4400 | 718.7 | 945.0 | 802.5 | 1.12 | 0.85 |
| SDI-4-1 | AS(S)-CA(LS) | 40 | 260 | 4575 | 282.2 | 441.0 | 444.0 | 1.57 | 1.01 |
| SDI-4-2 | AS-CA(L) | 40 | 268 | 4575 | 283.1 | 441.0 | 304.5 | 1.08 | 0.69 |
| SDI-5-1 | AS-CA(L) | 40 | 230 | 3300 | 287.6 | 430.4 | 283.5 | 0.99 | 0.66 |
| SDI-5-2 | AS(J)-CA(L) | 40 | 380 | 3300 | 249.5 | 430.4 | 294.0 | 1.18 | 0.68 |
| SDI-6-1 | None | 40 | 320 | 3300 | 172.5 | 218.0 | 171.15 | 0.99 | 0.78 |

AS - adjacent span
HR - hot rolled angle
CA - cold-formed angle
(S) - with studs
(L) - with lip
(J) - with deck joint

ALL TESTS: (except SDI-6-1)
- 2 in. deep deck
- 3 in. concrete cover
- 30 in. shear span
- 3-8 ft spans
- 6 ft. wide

Test SDI-6-1
- 2 in. deep deck
- 3 in. concrete cover
- 30 in. shear span
- 1-8 ft. span
- 3 ft. wide

[1]in tested span
[2]see Appendix B for calculations

efficiency, the case that exhibits the best behavior is that in which shear studs and a cold-formed angle with return lip are used.

**5.2 Center Spans**

As can be seen in Figures A2 and A11 (plots for SDI-1-1 and SDI-3-1 respectively), spans that have adjacent concrete without a deck joint provide a ductile behavior with no sudden drop in load. The load capacity of a center span without shear studs is approximately the average of the ultimate strength (based upon reinforced concrete theory) and first yield of the bottom fibers of the deck. The two methods used (ie. ultimate and first yield) are based upon a single span simple support condition. This assumption is valid due to the fact that no negative reinforcement was provided over the support and the deck provides negligible stiffness by itself over the supports.

Examining Figure 5.1 (a plot of the variation of strain along the length of the slab) and Figure 5.2 (a plot of individual gages spaced along the length of the slab), one can clearly see the the point of loss of bond. At this point the strains in the deck increase suddenly without the corresponding increase in load. This indicates a shift in the load carrying mechanism from that of a composite slab to one of a partial composite slab, a catenary, an arch or a combination of the above (discussed in

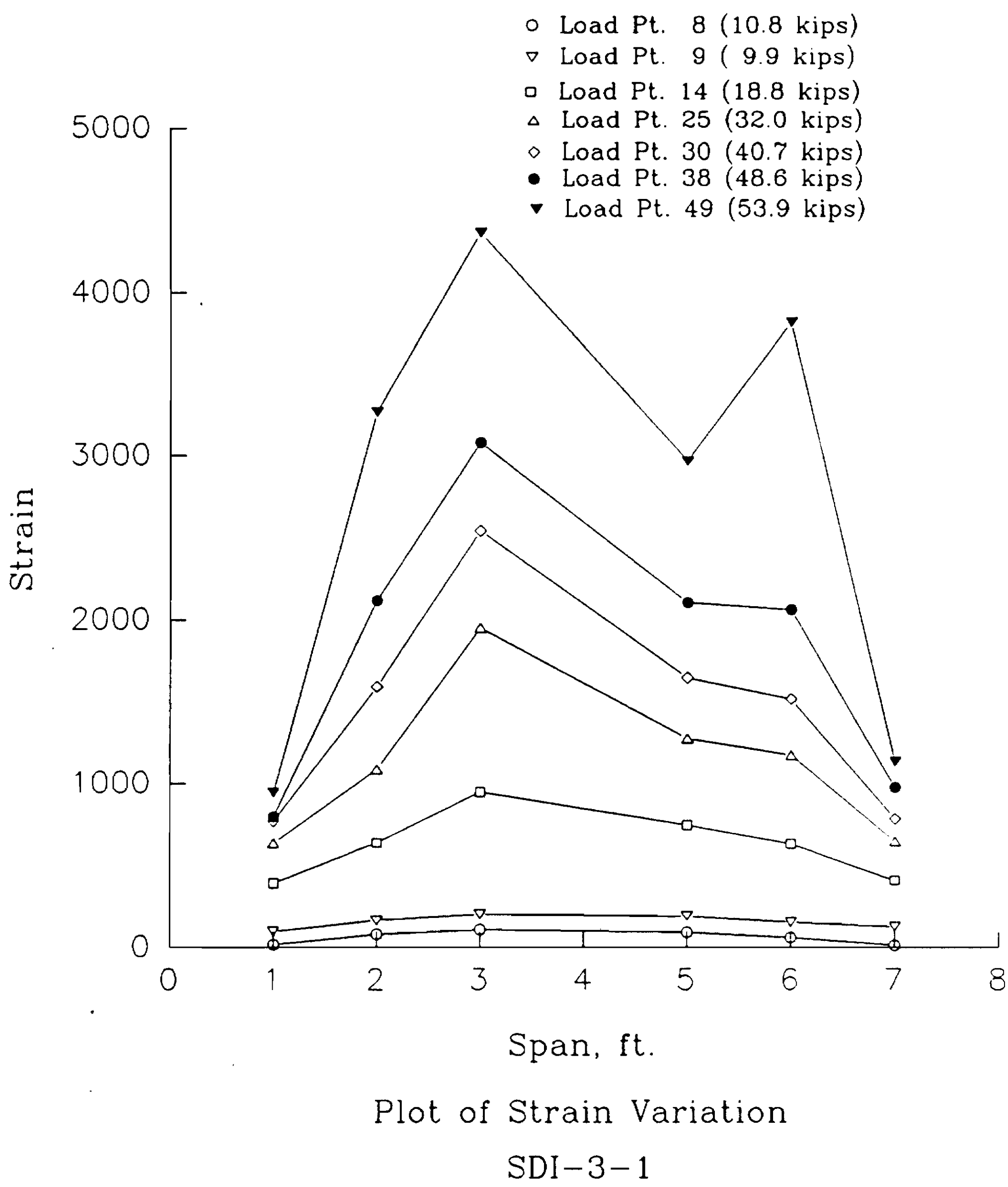


**Figure 5.1 SDI-3-1 Strain Variation**

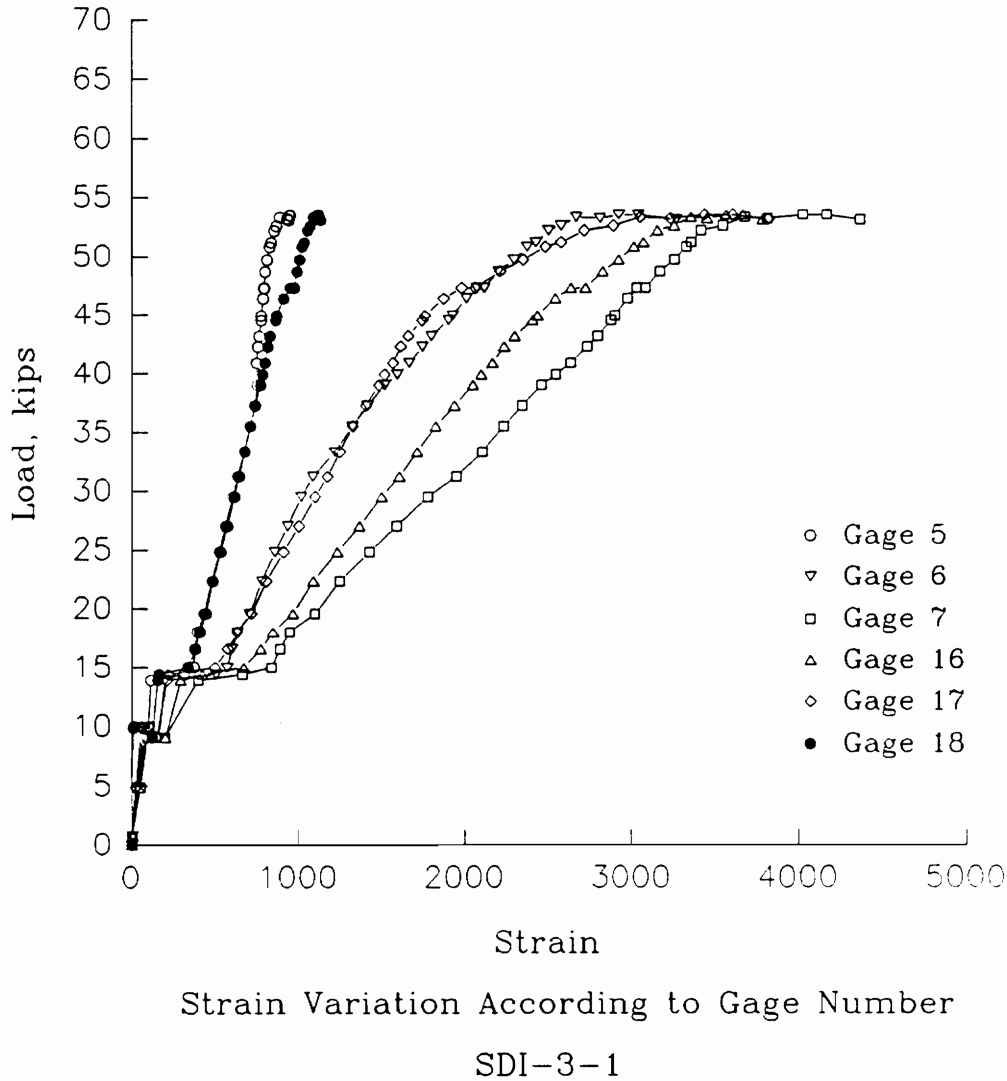


**Figure 5.2 SDI-3-1 Strain Variation according to Gage #**

Chapter 6). It is also observed, in Figure 5.1, the locations of the loss of bond (nearest the load, toward the support). The reader is reminded that SDI-3-1 (Figures 5.1 and 5.2) used 90 ksi steel deck instead of 40 ksi (the remainder of the tests) thus the higher loads.

Looking at the plots in Figures A2 and A11 one can see a noticeable difference in the initial stiffness. An explanation for this is the connection of the deck to the supports. SDI-1-1 (Figure A2) had no connection between the deck and supports and SDI-3-1 (Figure A11) had puddle welds in each flute along each of the support members. It is believed the this welding provided the added stiffness in the deck over the supports and thus SDI-3-1 was stiffer (relative to theoretical lines) than SDI-1-1. If a comparison is made between SDI-3-1 and the remainder of the tests (excluding SDI-1-1), it is seen that the initial stiffness of SDI-3-1 is comparable to the rest of the tests (all of which had anchorage to the support).

**5.3 End Spans**

By examining the plots of end span tests (Figures A5, A8, A17, A20 and A23), excluding test SDI-4-1 (shear studs), it is obvious that the lack of an adjacent span on one end causes a less ductile failure; although, first yield of the bottom fibers was reached on all but one (SDI-5-1 reached 99% of first yield). This behavior can be explained by some observations during the testing procedure. Until ultimate load was reached the end spans exhibited behavior similar to that of center spans. After ultimate load, inadequate welding of the deck to the supports allowed the deck to rip loose from the support members and thus exhibit a less ductile response.

As with center spans discussed above, plots of strain variation along the length of the slab are given in Figures 5.3, 5.4 (SDI-4-1 shear studs) and Figures 5.5, 5.6 (SDI-4-2 cold formed angle) where the horizontal axis is location along the tested span. Examaning Figures 5.3 and 5.5 one can see that the bond is lost between the outside load and the exterior support. One can also see the large differences in the values of strain (Figures 5.4 and 5.6) as you near the exterior support. This indicates that the exterior support is the "weak link" and needs special consideration in design.

Test SDI-4-1 (shear studs) illustrates that with adequate deck attachment an end span will behave in a ductile manner. Observation during the test suggests that the studs provided more of a horizontal shear transfer device than a rotational restraint device. This is supported by observing cracks that develop over the interior support during the test. It is also observed that the measured strain in the top of the deck remained in tension until the last few data points. This suggests that more of a trussing action, with the deck acting as the bottom chord, is present in this test setup

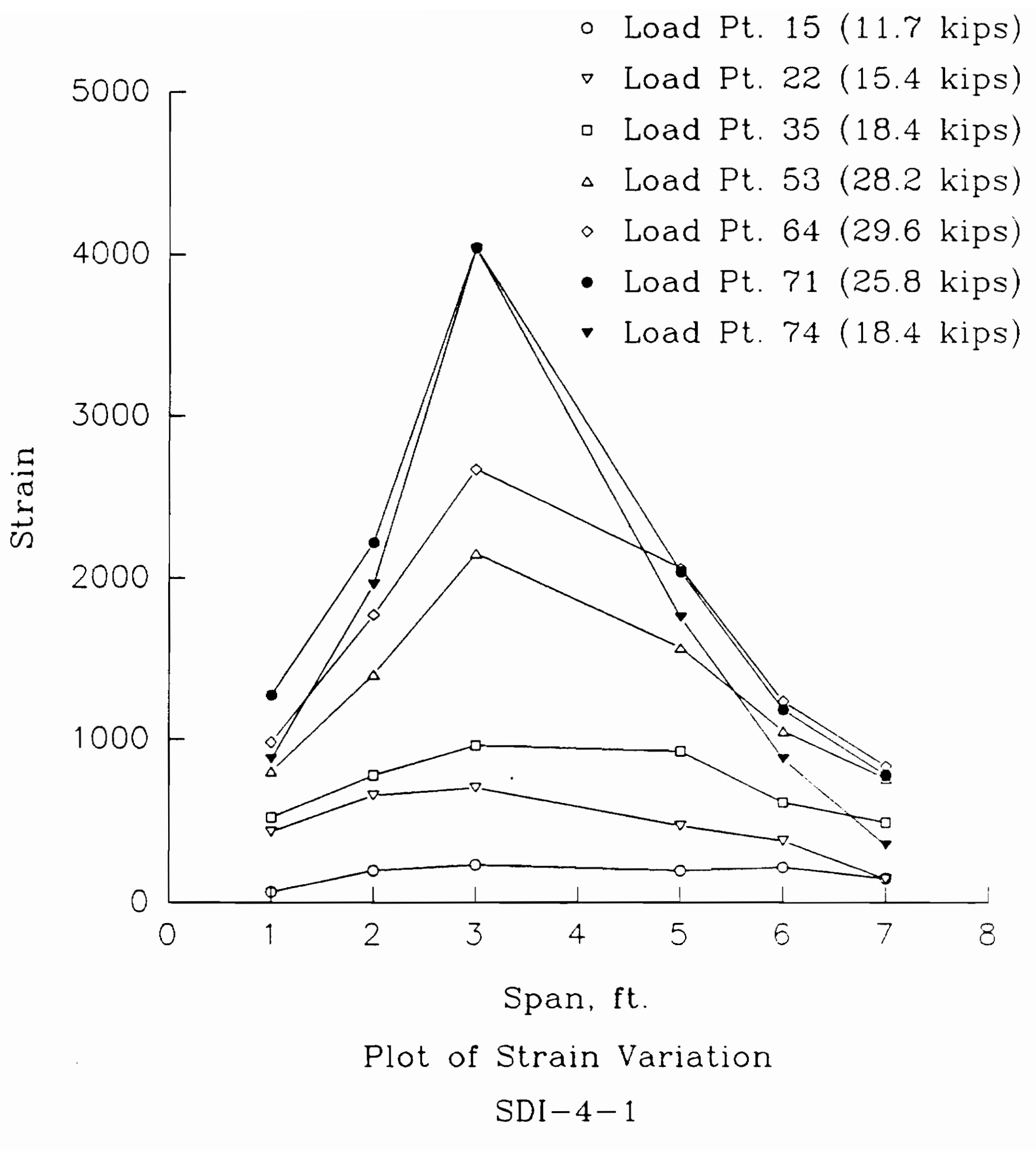


**Figure 5.3 SDI-4-1 Strain Variation**

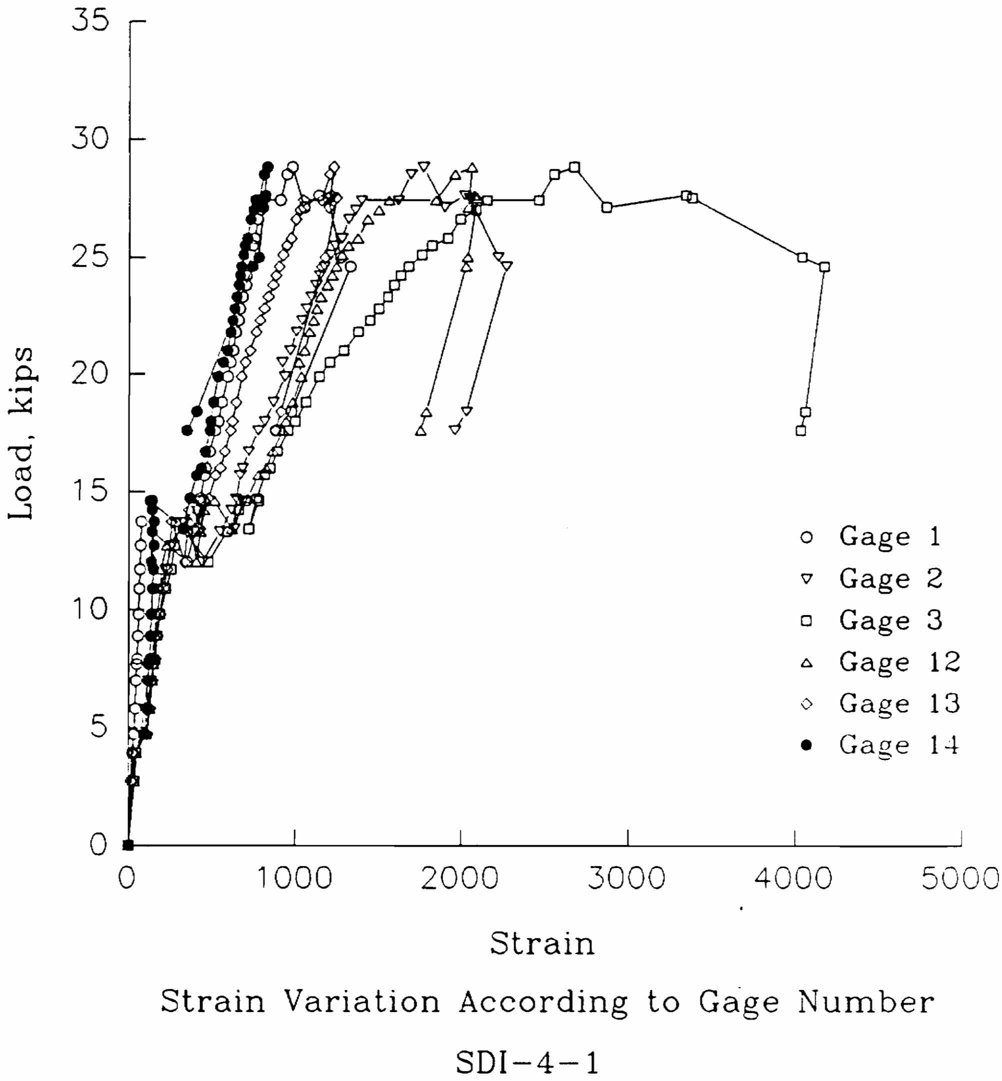


**Figure 5.4 SDI-4-1 Strain Variation according to Gage #**

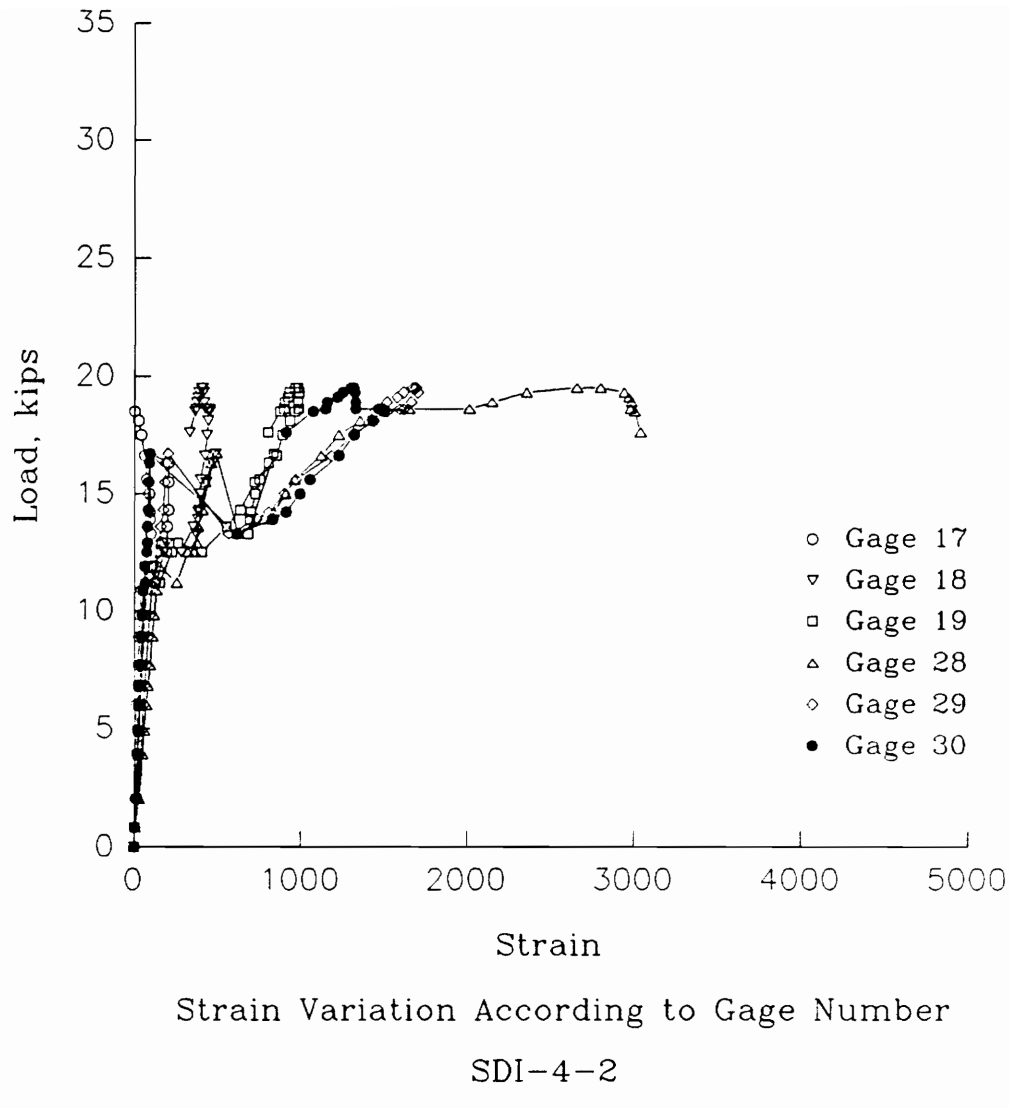


**Figure 5.5 SDI-4-2 Strain Variation**

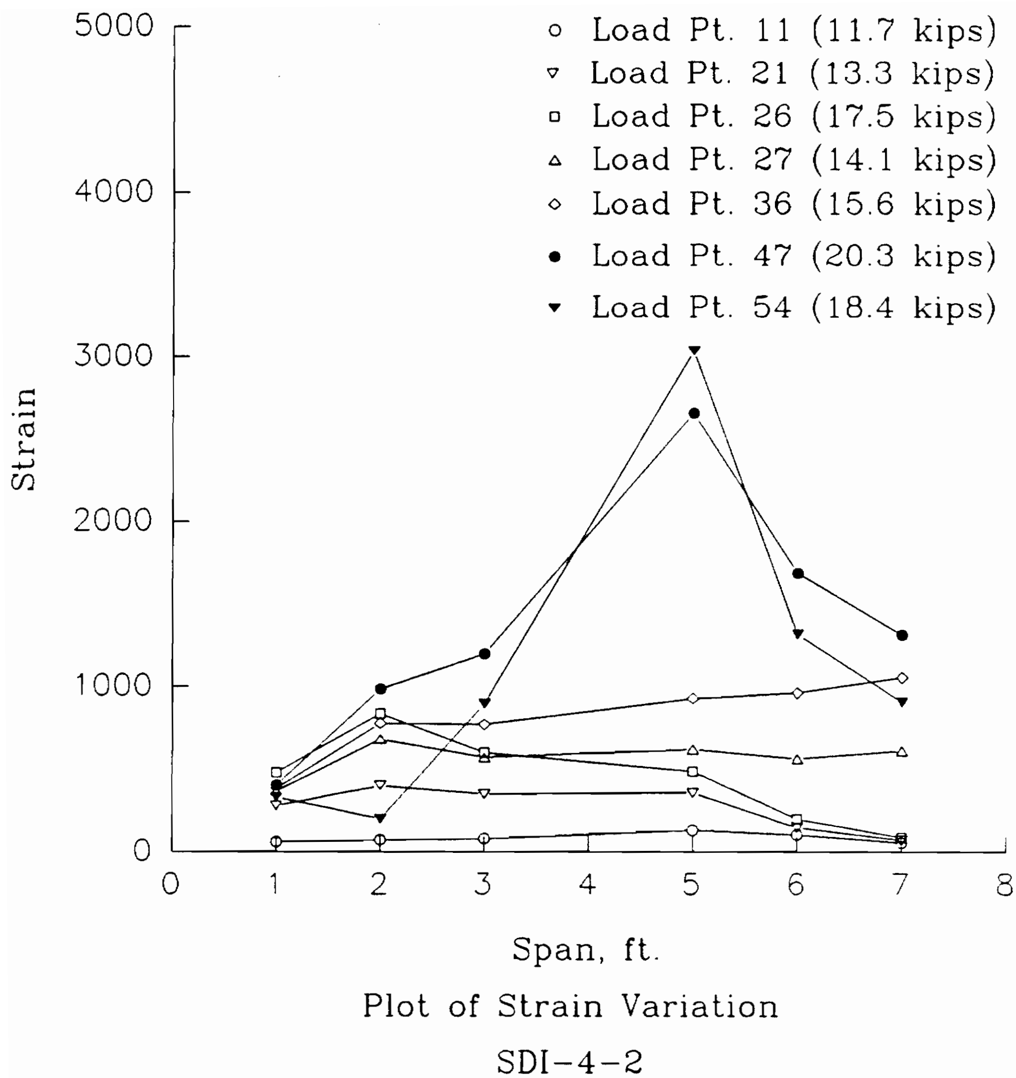


**Figure 5.6 SDI-4-2 Strain Variation according to Gage #**

verses similar test configurations without shear studs. This implies that the shear studs are providing horizontal shear transfer more efficiently than the deck embossments alone and thus allowing for a higher ultimate load.

Comparisons between the test results and the calculated stiffness values (Figures A5, A8, A14, A17, A20 and A23) show, that in the range of loading that extends up to approximately 70% of the yield moment, the slabs are stiffer than would be predicted with the simple model using the ASCE recommended average of the cracked and uncracked moment of inertia. Therefore, serviceability checks can be made with acceptable accuracy using the simple uncracked moment of inertia approach employed herein.

# Chapter 6
# LOAD MECHANISMS

Observation of the specimen at ultimate load suggests that a catenary action of the deck or an arch action of the concrete is the main load carrying mechanism. This chapter will provide some insight into these mechanisms.

### 6.1 Cable Analogy

If one assumes that the deck is carrying the ultimate load by catenary action then the load in the deck may be calculated, by elementary statics. Figure 5.1 shows the model representation.

From the symmetry of the loading,

$$V = P/2$$

Now, assuming 2 in. of vertical deflection along the center segment of the cable (all tests were taken to approximately 2 in. of center line deflection), one can sum moments about the midpoint of the cable,

$$(2in)H - (48in)V + (18in)(P/2) = 0$$

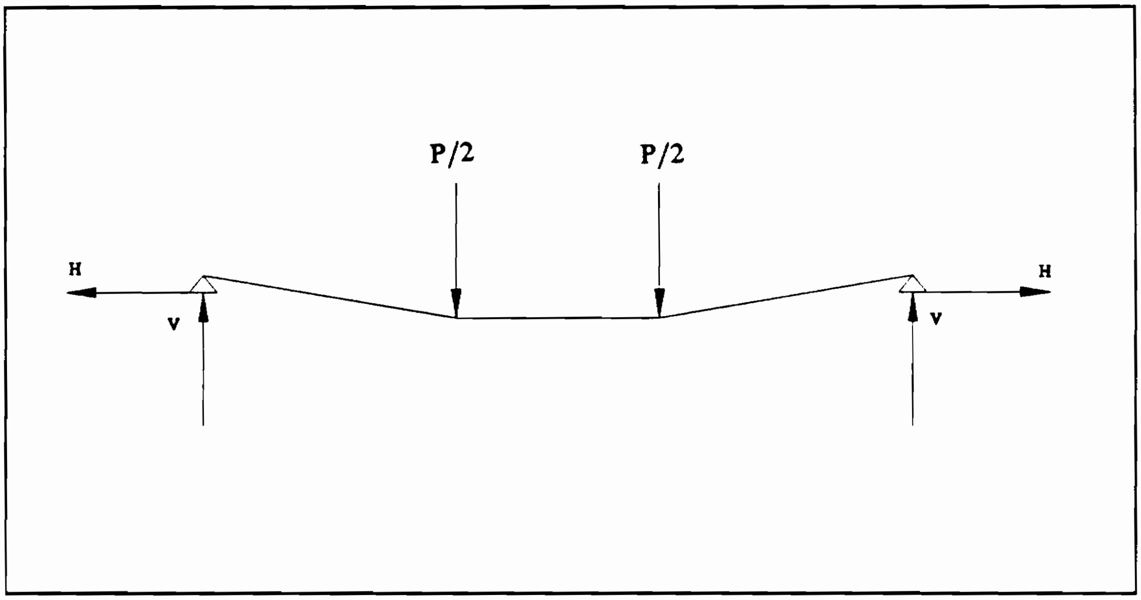


**Figure 6.1** Cable Model

Letting V = (P/2) and solving for H yields

$$H = 15\,(P/2)$$

Thus, the horizontal reaction over the supports is equal to 15 times the load.

The total load in the deck is thus,

$$H^2 + (P/2)^2 = (\text{Deck Load})^2$$

Or,

$$\text{Deck Load} = (15.0333)\,(P/2)$$

Assuming the deck is fully yielded and the area of steel is 3.126 $in^2$, the load in the deck is calculated as

$$(40 \text{ ksi})\ 3.126 \text{ in}^2 \ / \ 15.0333 \ = \ 8.315 \text{ kips}$$

Since the maximum load carried by any of the specimens using 40 ksi deck was approximately 13 kips (26 kips total load), it is obvious that the deck acting as a cable cannot solely carry the load. There must be another method of load transfer or a combination of load mechanisms.

## 6.2 Arch Analogy

A second load carrying mechanism is also possible. This method is an arch action of the concrete. If one assumes a maximum load of 13 kips (26 kips total) and considers the geometry in Figure 6.2, the following equation can be written:

From geometry,

5 in. thick slab - 2 in. of deflection = 3 in. elevation difference

30 in. shear span (from load to support)

$$(3\text{in.}^2 + 30\text{in.}^2)^{1/2} = 30.1496 \text{ in.}$$

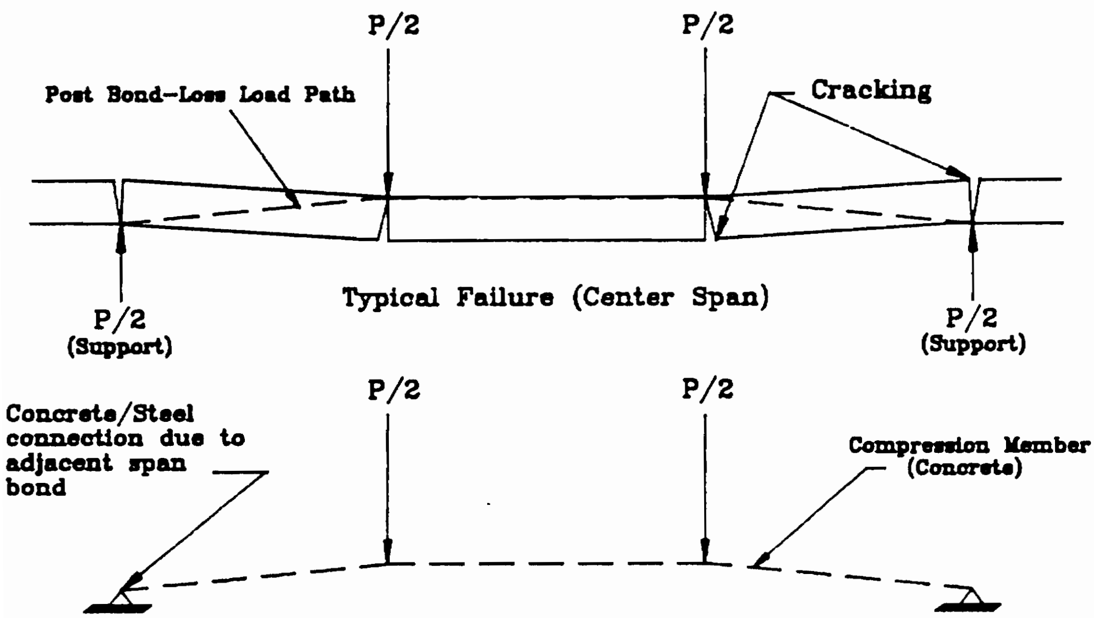


Suggested Arch Representation

Figure 6.2 Truss Anology

From statics, the compression strut force, C, is:

$$\frac{3\ inch}{30.15\ inch}\ C = 13 kips$$

Solving the above yields,

C = 130.65 kips

If one assumes that the concrete surrounding the diagonal portion, that has been assumed to carry the load, provides enough bracing to prevent buckling of this slender column, then the area of concrete needed to carry 130.65 kips is at least,

130.65 kips / 4.33 ksi = 30.17 in$^2$

If the assumption is made that this area is equally distributed over the entire slab width, then the actual width of the "column" of concrete is,

30.17 in$^2$ / (72 in) = 0.42 in wide

A brief check on the load capacity of SDI-3-1, the test that reached the highest load, reveals that the necessary width of concrete is 0.87 in. The concrete provided is more than adequate to carry this load. This method is then a valid load mechanism for the specimens.

The only problem with this method is the horizontal load created by the diagonal. The horizontal load must be transferred into the deck through the adjacent spans or by other means. This brings up the question of how much horizontal shear can the adjacent span handle or mechanical transfer device. An additional question is how much of the concrete is actually effective in load transfer and how much for bracing.

### 6.3 Combination Arch and Cable

Although it is possible, it is not believed that an arch action is the sole load carrying mechanism. Examination of the measured strains during the test suggest that the deck is under bending, with the top in compression (at ultimate) and the bottom in tension (to a higher degree). This suggests a combination of the above two methods (Figure 6.3), possibly coupled with bending of the deck. This is supported by observed buckling of the deck over the supports and under the load point.

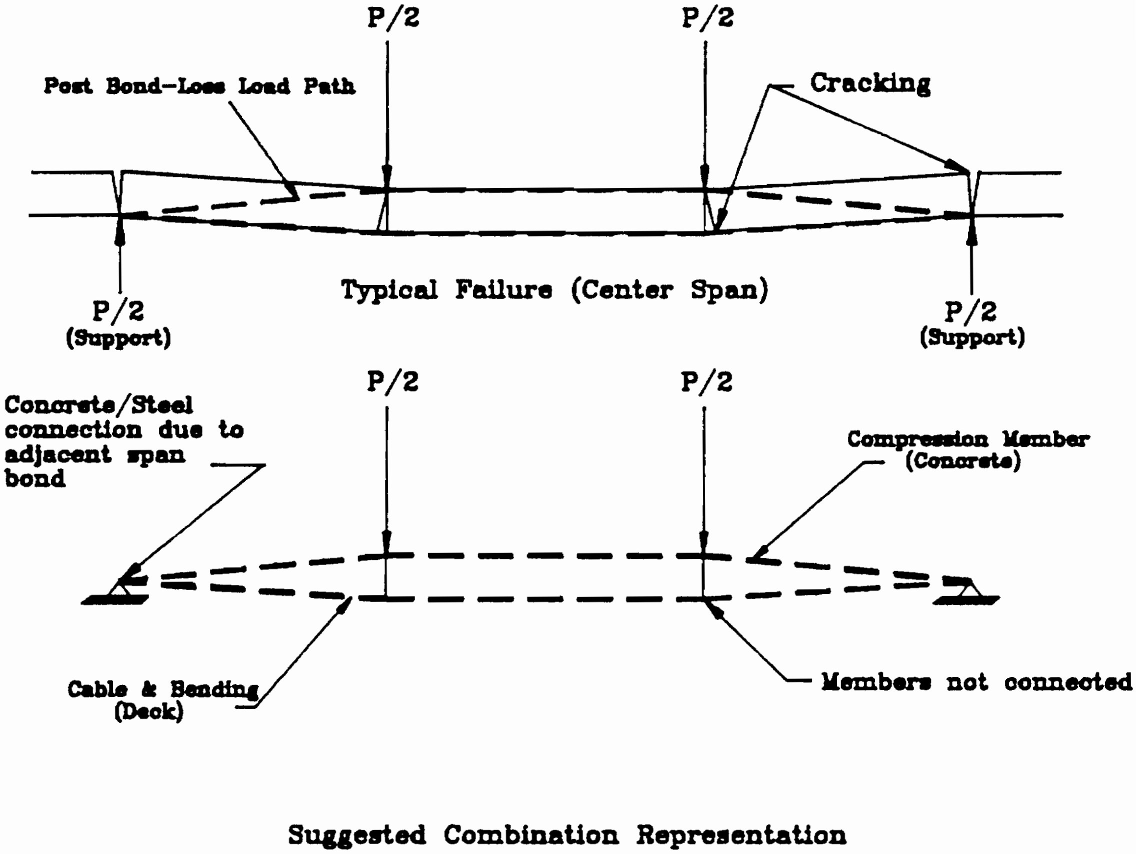


Figure 6.3 Combination Analogy

Based on Sections 6.1 and 6.2 a possible load mechanism is a combination of the above discussed cable action coupled with an arch action of the concrete and possibly bending of the deck. Although the portion of the load carried by each of these three mechanisms is not known, the writer believes these to be valid load carrying mechanisms and should be investigated in future studies.

# Chapter 7
# SUMMARY, CONCLUSIONS AND RECOMMENDATIONS

### 7.1 Summary

This study describes the results of a research program at Virginia Polytechnic Institute and State University under the sponsorship of the Steel Deck Institute. The project is based upon full scale multi-span tests of composite floor systems. A primary objective of the research was to assess the strength of steel deck reinforced concrete floor slabs that are constructed to simulate actual field conditions, with respect to details at the intermediate supports and at end spans. In particular the influence of adjacent spans and typical pour stop details was considered. Another objective was to evaluate the applicability of using traditional reinforced concrete models to predict the strength and stiffness of steel deck reinforced floor systems.

To accomplish these goals, five three span full scale floor systems were constructed, on which eight load tests were performed. The results of these tests are presented.

Based upon the results of these tests, a preliminary design procedure/model (Chapter 5) is presented. This procedure is based on two limit states of reinforced concrete theory for strength predictions and the uncracked moment of inertia for stiffness calculations. The first strength limit state being first yield of the bottom fibers of the deck. This limit state is shown to be applicable to all tested spans. The second limit state is ultimate strength which is applicable when shear studs are used. The tests also confirm the use of the uncracked moment of inertia to predict the deflection in the "elastic range." All of the limit states are based on a model in which the slab is simply supported (neglecting bending of deck over supports) and full composite action is assumed.

This study represents a departure from past work, which has centered around the limit state of shear bond. Results of this study indicate that proper detailing at the slab ends can effectively prevent the end slip associated with shear bond.

### 7.2 Conclusions

By examining the results presented herein, the following conclusions in regards to Steel Deck Reinforced Concrete Floor Systems (SDRCFS) are made:

1- When shear studs were used, the capacity of the SDRCFS was accurately predicted using the ultimate strength approach to reinforced concrete.

2- When the span under consideration had continuous deck and concrete (ie. center span), a lower bound capacity of the SDRCFS was predicted using the limit state of first yield of the extreme fibers of the steel deck.

3 - When the span under consideration was an end span (ie. one end of the deck and concrete continuous, the outer not) and proper consideration is given to the anchorage of the steel deck, a lower bound capacity of the SDRCFS was predicted using the limit state of first yield of the extreme fibers of the steel deck.

4 - Deflection of a SDRCFS can be predicted by transforming the cross section into an equivalent concrete section and using the uncracked moment of inertia.

### 7.3 Recommendations

For the tests considered herein, the range of test variables is not all inclusive. The following recommendations are based on 2 in. 20 gage deck, although similar results should be obtained using other depths and thickness of deck. Research should be conducted to verify the applicability of these findings.

Based upon the results of the eight tests presented in this report and research done by the writer, the following recommendations are made:

1 - if shear studs are used, design based upon ultimate reinforced concrete theory is applicable with the assumptions made in Chapter 4 (although more tests are needed before using this).

2 - if no shear studs are provided but adjacent spans of concrete are present

and deck is adequately attached with welds, design based upon first yield of the bottom fibers of the deck is applicable with the assumptions made in Chapter 4.

3- deflection calculations in the service load range may be made using the uncracked moment of inertia of a single simple span as outlined in Chapter 4.

4 - use of a uniform loading condition would more adequately represent actual loading conditions. This coupled with in-situ testing and using standard end details as in this project will provide results that are representative of actual field conditions.

5 - shear bond is a consideration if the ends are unrestrained and non-continuous

6- design models for the limit states of shear strength and concentrated load strength need to be developed.

In order to use the above design recommendations proper consideration must be given to the end details as shown in SDI 4-2, SDI 5-1 and SDI 5-2. One should recall that all of the calculations are based on a simply supported, single span configuration, which is typical in design when no negative reinforcement is provided. Upon further verification of the results the design recommendations made above should be used independent of laboratory testing.

### 7.4 Future Research

This study does not begin to answer all questions regarding Steel Deck Reinforced Concrete Floor Systems. Additional research is needed in the fields of:

1- Other deck gages.

2- Variable span length configurations.

3- Effect of positive moment reinforcement.

4- If support beam is designed as a composite beam and the floor system is dependent upon the same shear studs then bi-axial loading of the studs needs to be investigated.

5- Effects of screw fasteners on the prevention of shear bond.

6- Effects of more than one span loaded at once, variations on this loading configuration.

7- Loading methods more representative of actual conditions.

8- Analytical study of analysis methods including non-linear, possible generic design formulas.

## References


Airumyan, E., Belyaev, V. and Rumyanceva, I. (1990). "Efficient Embossment for corrugated Steel Sheeting," *International Association of Bridge and Structural Engineers Conference Reports* Vol 60. Zurich, pp 137-142.

Asanuma, M., Yamomoto, A. and Okuda Y. (1990). "Development of Composite Slab with Truss-Type Connector," *International Association of Bridge and Structural Engineers Conference Reports* Vol 60. Zurich, pp 275-276.

"Building code requirement for reinforced concrete." (1989) ACI 318-89, American Concrete Institute, Detroit, Mich.

Bode, H., Kunzel, Roland, K. and Schanzenbach, J. (1988). "Profiled steel sheeting and composite action," *Ninth International Speciality Conference on Cold-Formed Steel Structures*. Department of Civil Engineering, University of Missouri-Rolla. pp. 343-359.

Bryl, Stanislaw, (1967). "The Composite Effect of Profiled Steel Plate and Concrete in Deck Slabs," *23rd International Congress of Steel Informations Centres*.

Dallaine, Eugene E. (1971). "Cellular Steel Floors Mature," *Civil Engineering*, ASCE, July. pp 70-74.

Daniels, B.J., Isler, A. and Crisinel, M. (1990). *Modelling of Composite Slabs with Thin-Walled Cold-Formed Decking*. ICOM Publication No. 235. Ecole Polytechnique Federale De Lausanne.

Ekberg, Carl E. Jr. and Schuster, R.M., (1968). "Floor Systems with Composite Form-Reinforced Concrete Slabs, Final Report," *International Association of Bridge and Structural Engineering Reports,* Zurich, pp 385-394.

Lamport, William B. and Porter, Max L. (1990). "Deflection Predictions for Concrete Slabs Reinforced with Steel Decking." *American Concrete Institute Structural Journal*, September-October. pp. 564-570.

Landis, Donald H. (1990), EPIC Metals Corporation, Rankin, PA, *Personal Communication*, 31 October.

McDermott, John F. (1967). "Structural Tests on a Composite Floor System" *Journal of the Structural Division*, ASCE, February. pp. 255-274.

O'Leary, David; Moum, Chanta and Brekelmans, Jan (1990). "Comparative Study of Composite Slab Tests" *International Association of Bridge and Structural Engineers Conference Reports* Vol 60. Zurich, pp 161-166.

Patrick, Mark, (1990) "A New Partial Shear Connection Strength Model for Composite Slabs", BHP Melbourne Research Laboratories Report Number MLR/PS64/90/016, March.

Porter, Max L. and Ekberg, Carl E. Jr. (1972). "Investigation of Cold-Formed Steel-Deck-Reinforced Slabs," *Proceedings of the First Specialty Conference on Cold-Formed Steel Structures*, Department of Civil Engineering, University of Missouri-Rolla, August. pp 179-185.

Porter, Max L. and Ekberg, Carl E. Jr. (1974) "Design vs. Test Results for Steel Deck Floor slabs" *Proceedings of the 3rd Specialty Conference on Cold-Formed Steel Structures*. Department of Civil Engineering, University of Missouri-Rolla, pp. 793-811.

Porter, M.L., Ekberg, C.E. Jr., Greimann, L.F., Elleby, H. (1976) "Shear-Bond Analysis of Steel-Deck-Reinforced Slabs" *Journal of the Structural Division*, ASCE, December. pp 2255-2268.

Porter, Max L. and Ekberg Carl E. Jr. (1976) "Design Recommendation for Steel Deck Floor Slabs" *Journal of the Structural Division*, ASCE, November. pp 2121-2136.

Porter, Max L. and Ekberg, Carl E. Jr. (1977). "Behavior of Steel-Deck Reinforced Slabs" *Journal of the Structural Division*, ASCE, November. pp 663-677.

Porter, Max L. and Ekberg Carl E. Jr. (1978). *Compendium of ISU Research Conducted on Cold-Formed Steel-Deck Reinforced Slab Systems, Bulletin 200*, College of Engineering Iowa State University, December.

Porter, Max L. (1984). "Shear-Bond Strength of Studded Steel deck Slabs" *Proceedings of the 7th Specialty Conferences on Cold-Formed Steel Structures*. Department of Civil Engineering, University of Missouri-Rolla, pp. 285-304.

Porter, Max L. (1987). "Highlights of New ASCE Standard on Composite Slabs" *Proceedings of an Engineering Foundation Conference on Composite Construction in Steel and Concrete*, ASCE, June. pp 94-106.

Prasannan, Santosh and Luttrell, Larry D. (1984). *Flexural Strength Formulations for Steel-Deck Composite Slabs*, Department of Civil Engineering, West Virginia University, January.

Roeder, Charles W. (1981). "Point Loads on Composite Deck-Reinforced Slabs" *Journal of the Structural Division*, ASCE, December. pp 2421-2429.

Schuster, Reinhold M. (1970). *Strength and Behavior of Cold-Rolled Steel-Deck-Reinforced Concrete Floor Slabs*, PhD Thesis, Iowa State University, Ames, Iowa.

Schuster, Reinhold M., (1972). "Composite Steel-Deck-Reinforced Concrete Systems Failing in Shear-Bond, Preliminary Report," *International Association of Bridge and Structural Engineers Conference Reports*, Zurich, pp.185-191.

Schuster, Reinhold M. (1976). "Composite Steel-Deck Concrete Floor Systems" *Journal of the Structural Division*, ASCE, May. pp 899-917.

*Specifications for the Design and Construction of Composite Slabs and Commentary on Specification for the Design and Construction of Composite Slabs*. ASCE Standard, October 1984.

*Standard for the Structural Design of Composite Slabs*. ASCE Standard, Draft June 1990.

Stark, Jan (1978). "Design of Composite Floors with Profiled Steel Sheet" *Proceedings of the 4th Specialty Conference on Cold-Formed Steel Structures*. Department of Civil Engineering, University of Missouri-Rolla, pp. 893-922.

United States Patent Office, (1926) Patent Number 1,574,586, February 23.

## References ...continued


Wolfel, Eilhard (1987). "Elastic Design of Composite Slabs" *Proceedings of an Engineering Foundation Conference on Composite Construction in Steel and Concrete*, ASCE, June. pp. 680-690.

Wright, H.D; Evans, H.R. and Harding, P.W. (1987). "The use of Profiled Steel Sheeting in Floor Construction" *Journal of Constructional Steel Research*, Vol7, No4. pp. 21-37.

Wright, H.D. and Evans, H.R. (1987). "A Folded Plate Method of Analysis for Profiled Steel Sheeting in Composite Floor Construction" *Thin-Walled Structures*, Vol5, No1. pp. 279-295.

# APPENDIX A
# TEST DATA

Test Number:SDI 1-1
Date:01 November 1989
Test Type:Center Span

---

Measured Dimensions

General

| | |
|---|---|
| Width: | 2 panel, each panel 3'-0", total 6'-0" |
| Span(s): | 8 ft/ 8 ft/ 8ft |
| Shear Span: | 30 in. |
| Midspan Strain: (concrete placement) | 120 micro strain |
| End Details: | Adjacent Slab / Adjacent Slab |
| Deck attachment: | none |

Deck

| | |
|---|---|
| Type: | 20 gage, 2 in. depth |
| Measured Yield Stress: | 40 ksi |
| Measured Ultimate Stress: | 54 ksi |
| Modulus: | 29,500 ksi |
| Type II embossments Depth: 0.050 in. | |

Concrete

| | |
|---|---|
| Type: | A4 |
| Test Strength: | 4330 psi |
| Depth: | 5 in, from bottom of deck, 3 in cover |
| Effective Depth: | 4 in. |

---

Instrumentation

| | |
|---|---|
| Strain Gages: | 36 (shown on diagram) |
| Displacement Transducers | D1-D6 (shown on diagram) |

---

Test Results

| | |
|---|---|
| Maximum Load: | 26.55 kips @1.35 in midspan deflection |
| Maximum Moment: | 398.25 k-in. |
| Maximum Deflection: | 2.020 in. (test stopped) |

Comments

- Cracking over supports at 58.5 k-in.
- Cracking under spreader beams at 220.5 k-in.
- Separation of deck and concrete between spreader beams at 315 k-in.

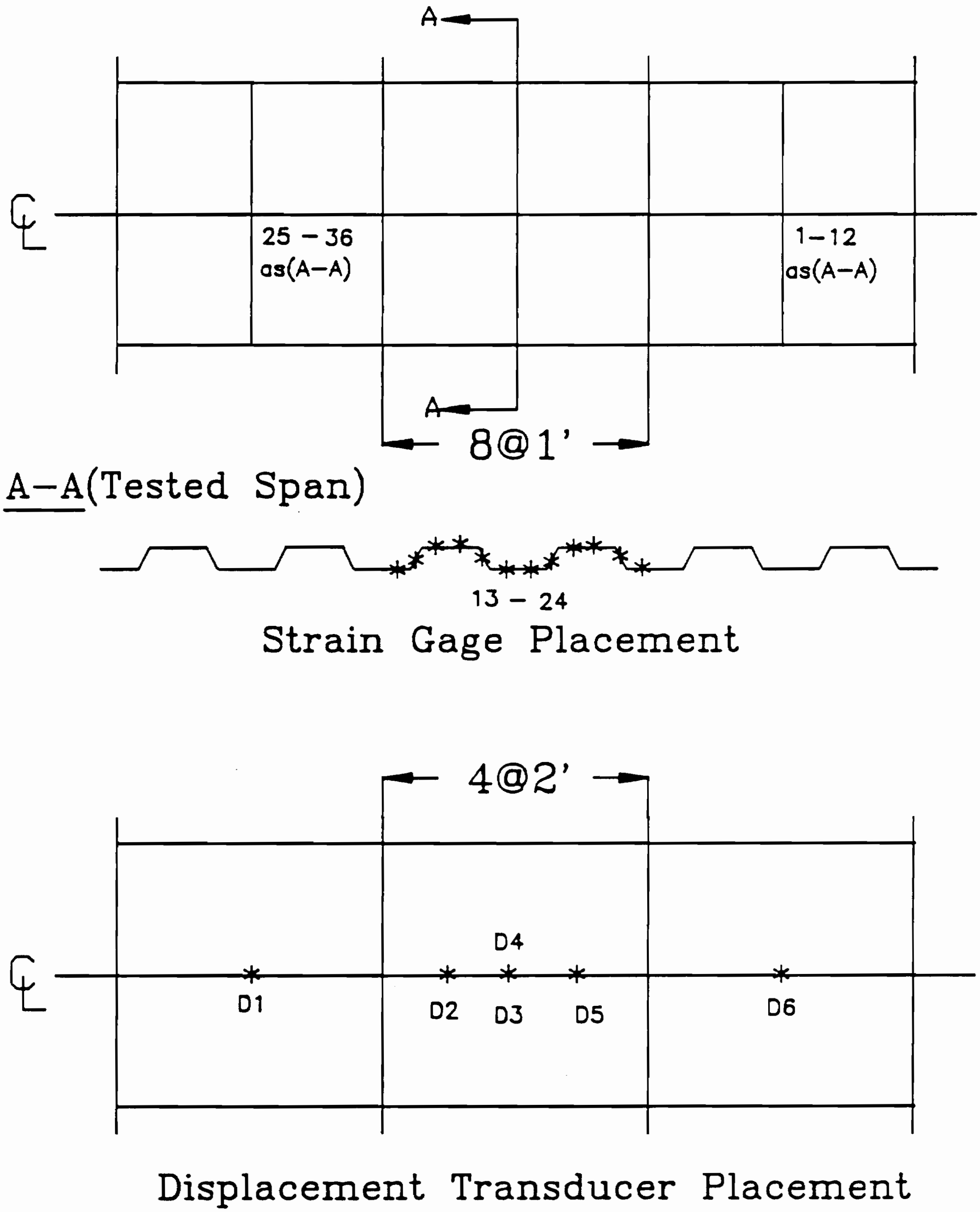


**Figure A1 SDI 1-1 Strain Gage, Displacement Transducer**

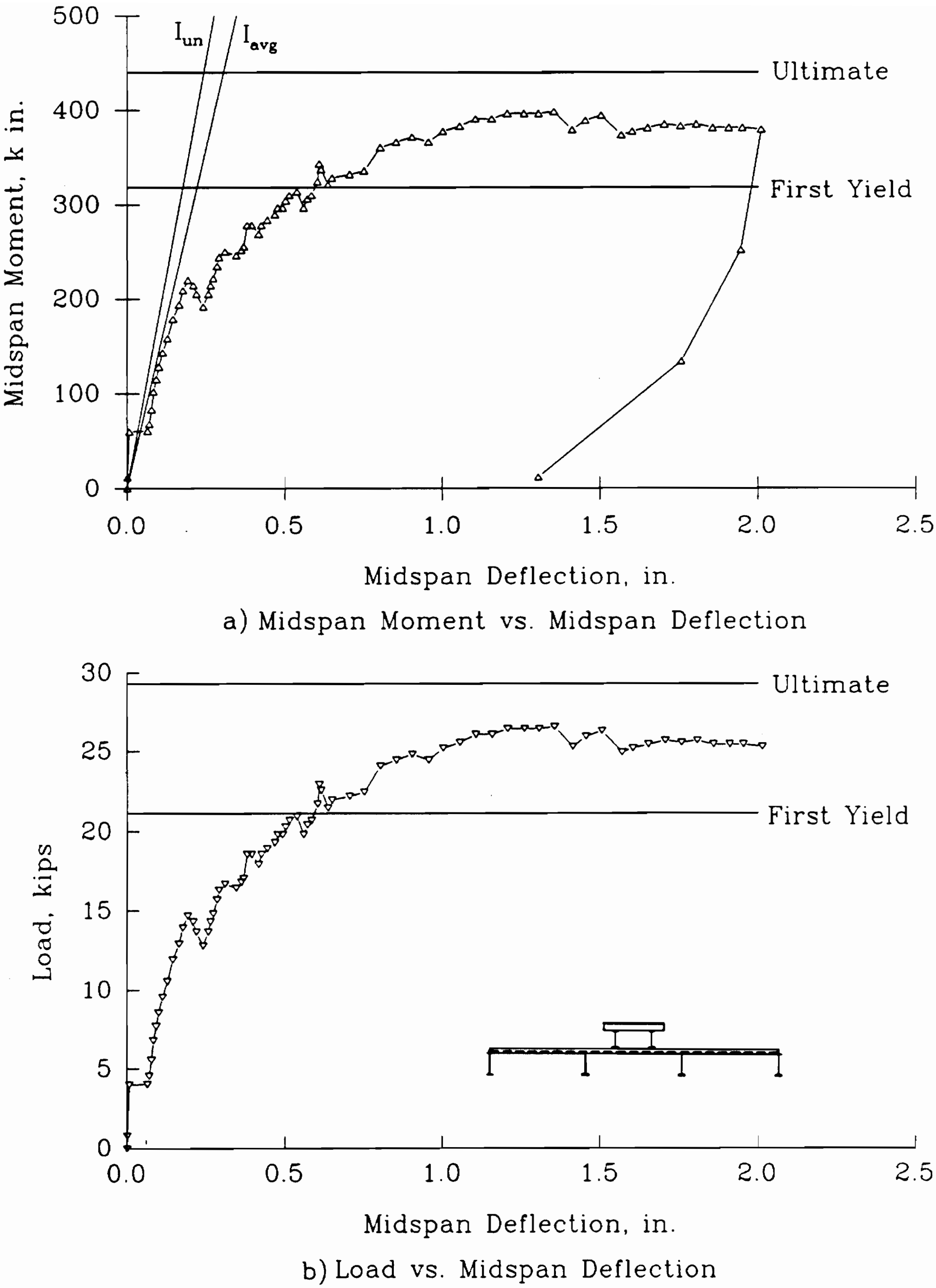


**Figure A2 SDI 1-1 Moment (Load) vs. Deflection Plot**

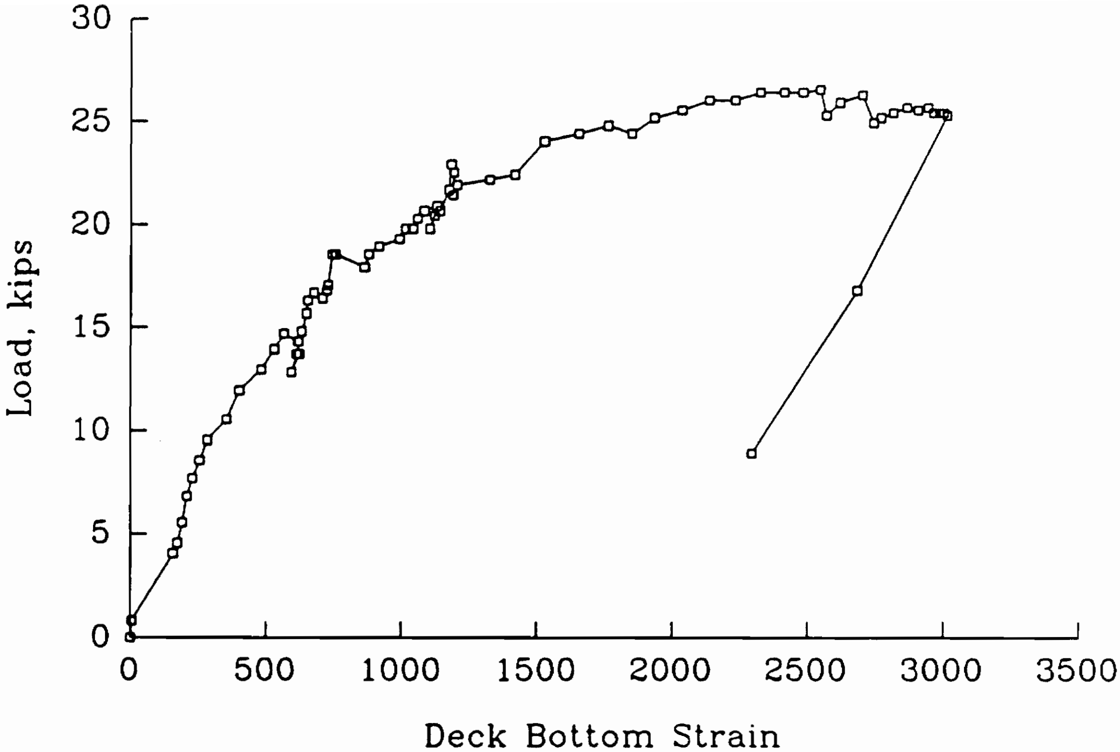


Load vs. Midspan Deck Bottom Strain

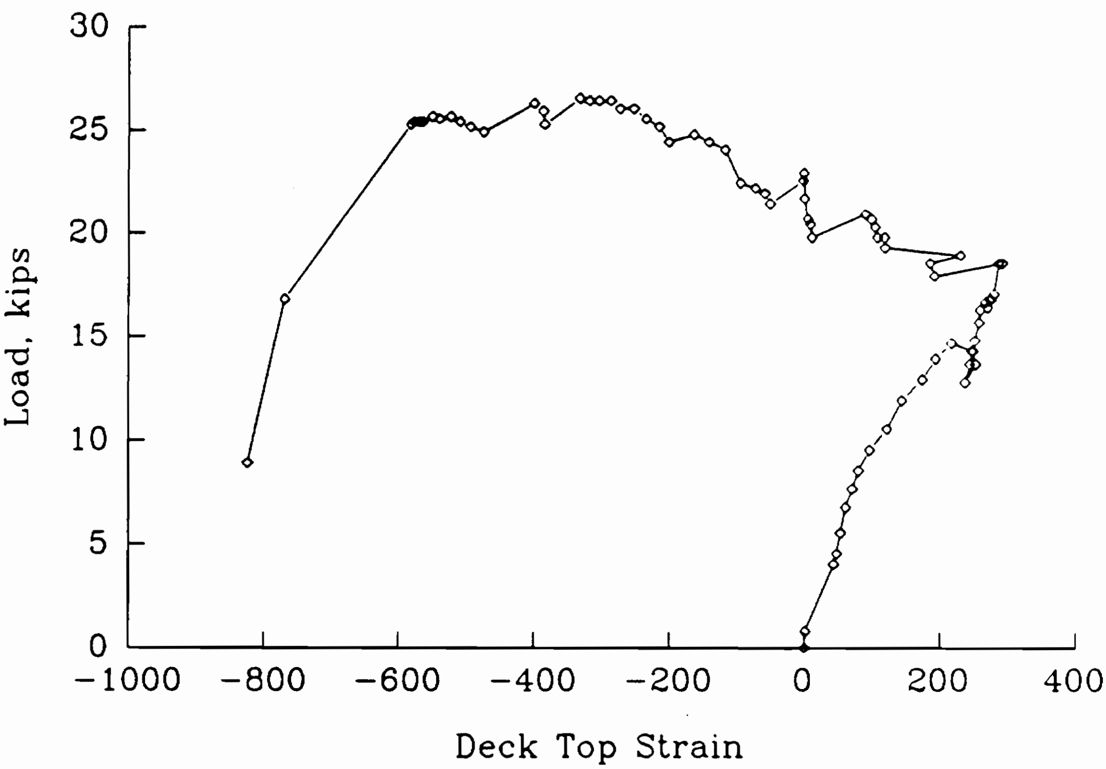


Load vs. Midspan Deck Top Strain

**Figure A3 SDI 1-1 Load vs. Strain Plots**

| | |
|---|---|
| Test Number: | SDI 2-1 |
| Date: | 19 Janurary 1990 |
| Test Type: | End Span, Hot-Rolled Angle |

Measured Dimensions

General

| | |
|---|---|
| Width: | 2 panel, each panel 3'-0", total 6'-0" |
| Span(s): | 8 ft/ 8 ft/ 8ft |
| Shear Span: | 30 in. |
| Midspan Strain: (concrete placement) | 300 micro strain |
| End Details: | Adjacent Slab / Hot-Rolled Angle |
| Deck attachment: | Puddle welds each flute |

Deck

| | |
|---|---|
| Type: | 20 gage, 2 in. depth |
| Measured Yield Stress: | 40 ksi |
| Measured Ultimate Stress: | 54 ksi |
| Modulus: | 29,500 ksi |
| Type II embossments Depth: 0.050 in. | |

Concrete

| | |
|---|---|
| Type: | A4 |
| Test Strength: | 4720 psi |
| Depth: | 5 in, from bottom of deck, 3 in cover |
| Effective Depth: | 4 in. |

Instrumentation

| | |
|---|---|
| Strain Gages: | 36 (shown on diagram) |
| Displacement Transducers | D1-D5 (shown on diagram) |

Test Results

| | |
|---|---|
| Maximum Load: | 24.20 kips @0.65 in midspan deflection |
| Maximum Moment: | 363.0 k-in. |
| Maximum Deflection: | 2.000 in. (test stopped) |

Test Number: SDI 2-1

Comments

- Cracking over supports present before test.
- Separation of hot-rolled angle and concrete occured at 184.5 k-in.
- Cracking under the spreader beams occurred at 195 k-in.
- At 363 k-in. separation of the deck nad concrete between the spreader beams.
- No slip between deck and concrete was recorded until after ultimate load.
- Concrete and deck were rotation about inside edge of the top flange of outer support member.

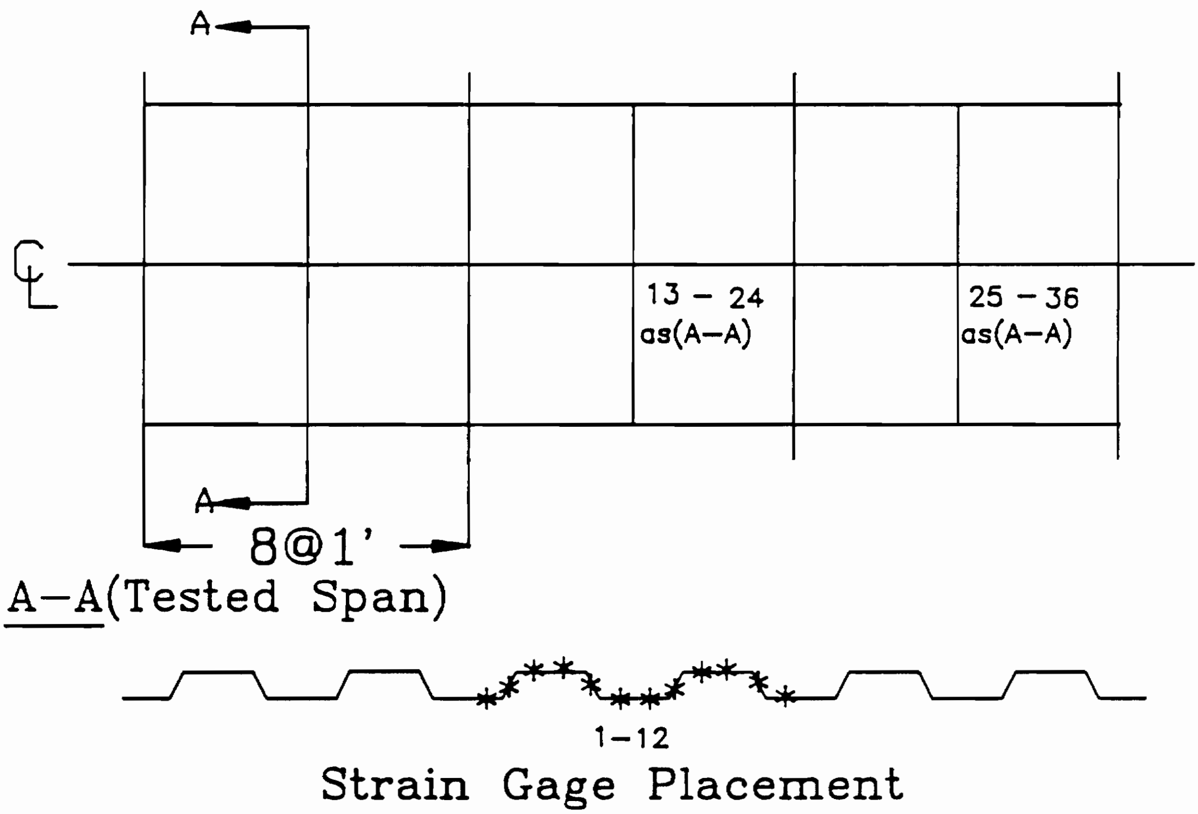


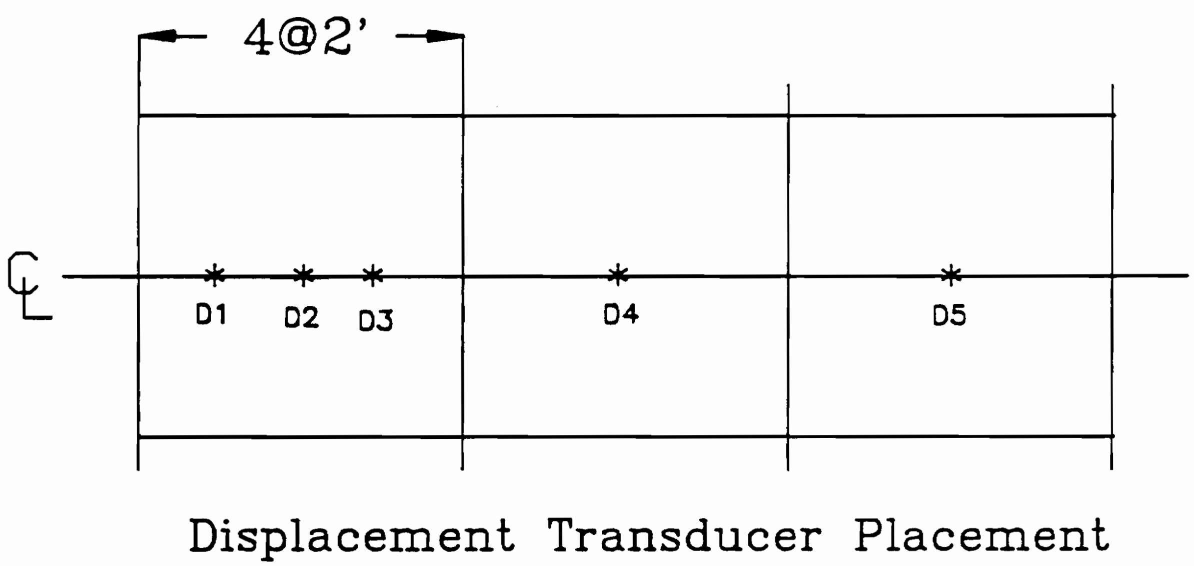


**Figure A4 SDI 2-1 Strain Gage, Displacement Transducer**

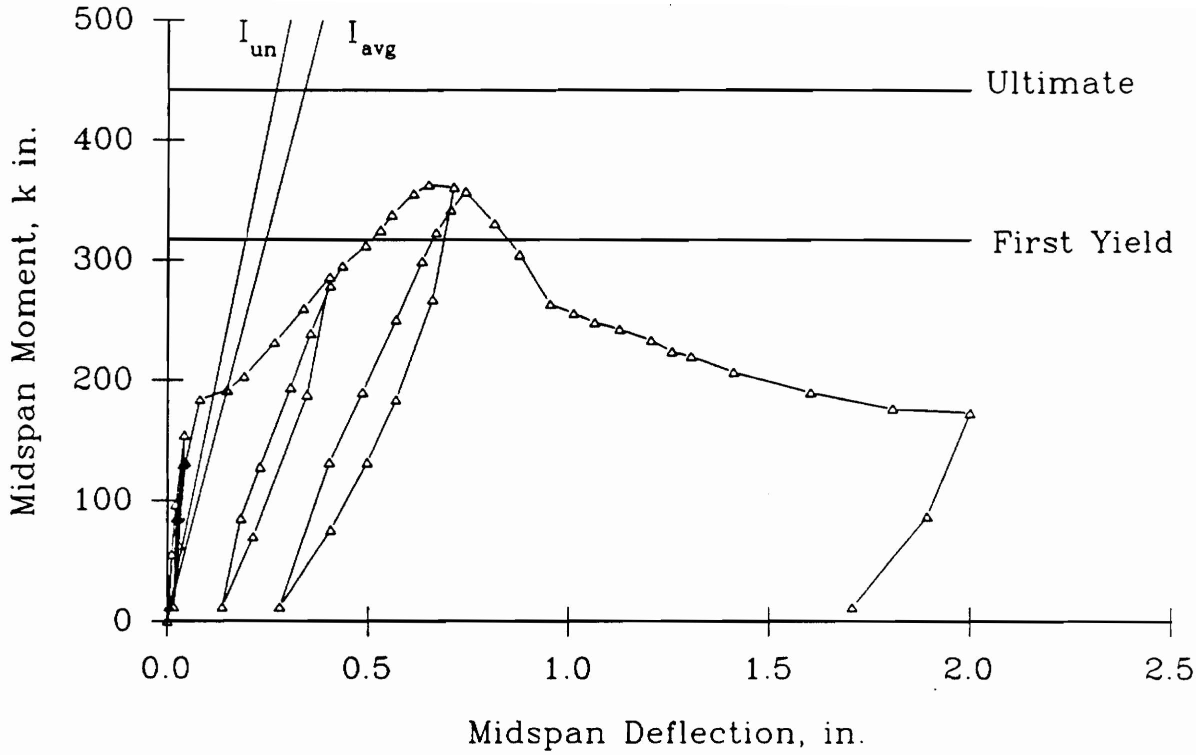


a) Midspan Moment vs. Midspan Deflection

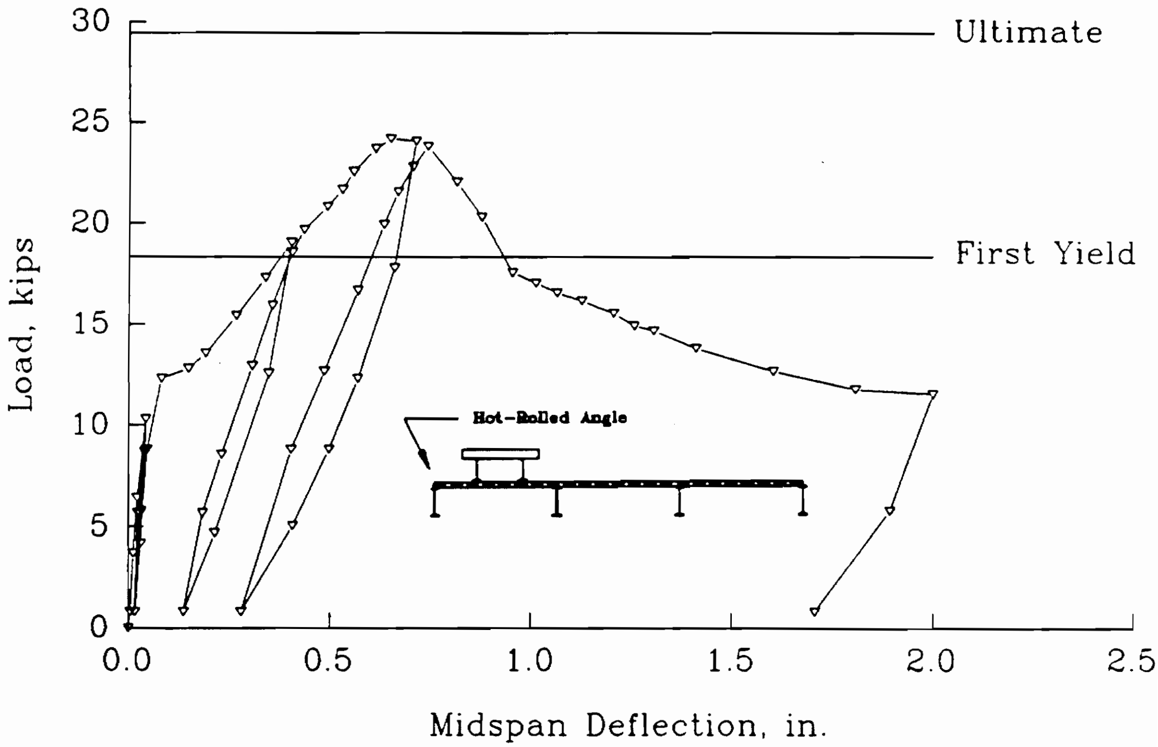


b)Load vs. Midspan Deflection

**Figure A5 SDI 2-1 Moment (Load) vs. Deflection Plot**

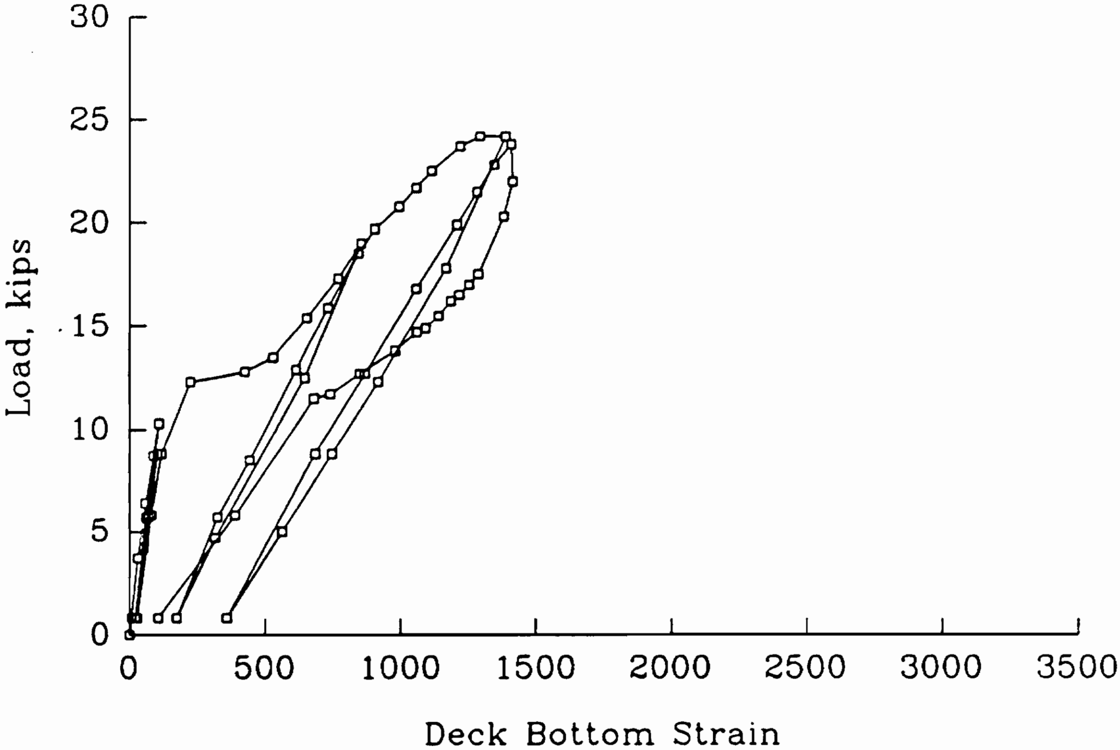


Load vs. Midspan Deck Bottom Strain

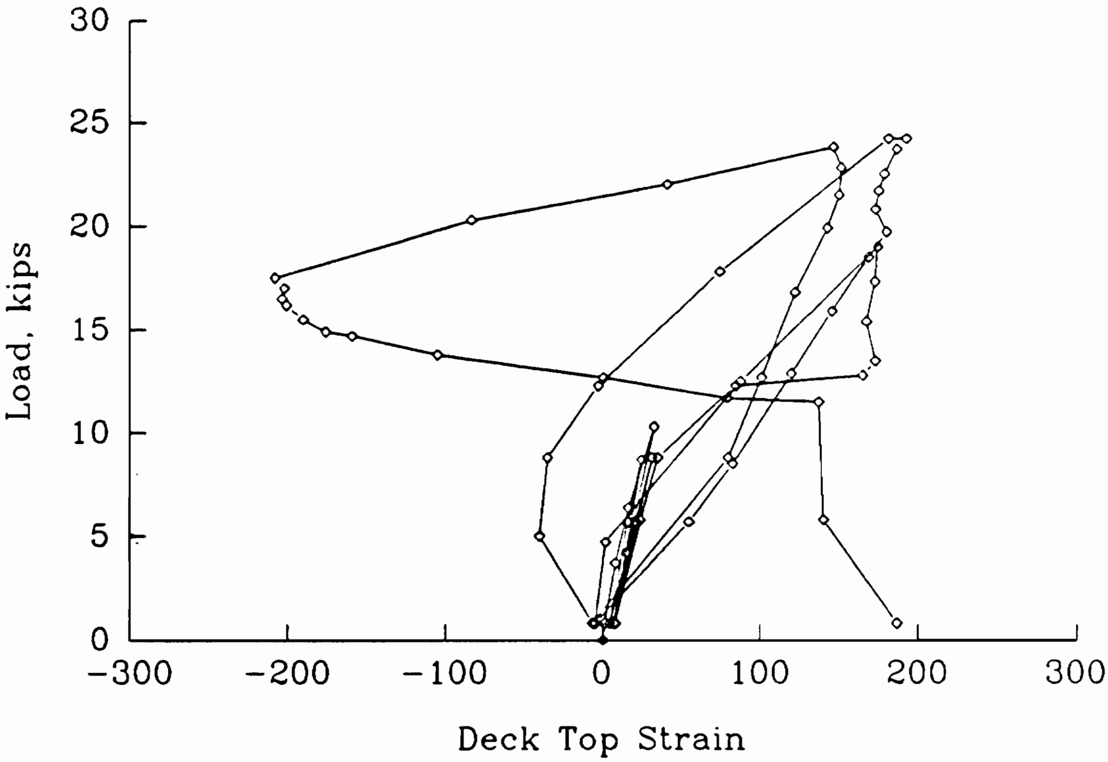


Load vs. Midspan Deck Top Strain

**Figure A6 SDI 2-1 Load vs. Strain Plots**

| | |
|---|---|
| Test Number: | SDI 2-2 |
| Date: | 22 Janurary 1990 |
| Test Type: | End Span, Cold-Formed Angle w/o lips |

Measured Dimensions

General

| | |
|---|---|
| Width: | 2 panel, each panel 3'-0", total 6'-0" |
| Span(s): | 8 ft/ 8 ft/ 8ft |
| Shear Span: | 30 in. |
| Midspan Strain: (concrete placement) | 270 micro strain |
| End Details: | Adjacent Slab / Cold-Formed Angle |
| Deck attachment: | Puddle welds each flute |

Deck

| | |
|---|---|
| Type: | 20 gage, 2 in. depth |
| Measured Yield Stress: | 40 ksi |
| Measured Ultimate Stress: | 54 ksi |
| Modulus: | 29,500 ksi |
| Type II embossments | |
| Depth: 0.050 in. | |

Concrete

| | |
|---|---|
| Type: | A4 |
| Test Strength: | 4720 psi |
| Depth: | 5 in, from bottom of deck, 3 in cover |
| Effective Depth: | 4 in. |

Instrumentation

| | |
|---|---|
| Strain Gages: | 36 (shown on diagram) |
| Displacement Transducers | D1-D5 (shown on diagram) |

Test Results

| | |
|---|---|
| Maximum Load: | 24.30 kips @0.912 in midspan deflection |
| Maximum Moment: | 364.5 k-in. |
| Maximum Deflection: | 2.320 in. (test stopped) |

Test Number: SDI 2-2

Comments

- Cracking over supports was present before test
- At 237 k-in cracking under spreader beams occurred
- After ultimate load, 364.5 k-in, at a load of 337.5 k-in separation of pour stop and concrete occurred.
- Deck ripped out around the puddle welds which attached deck to support members.
- No slip between deck and concrete occurred until after ultimate load.
- Concrete and deck were rotating about the inside edge of the top flange of the outer support member.

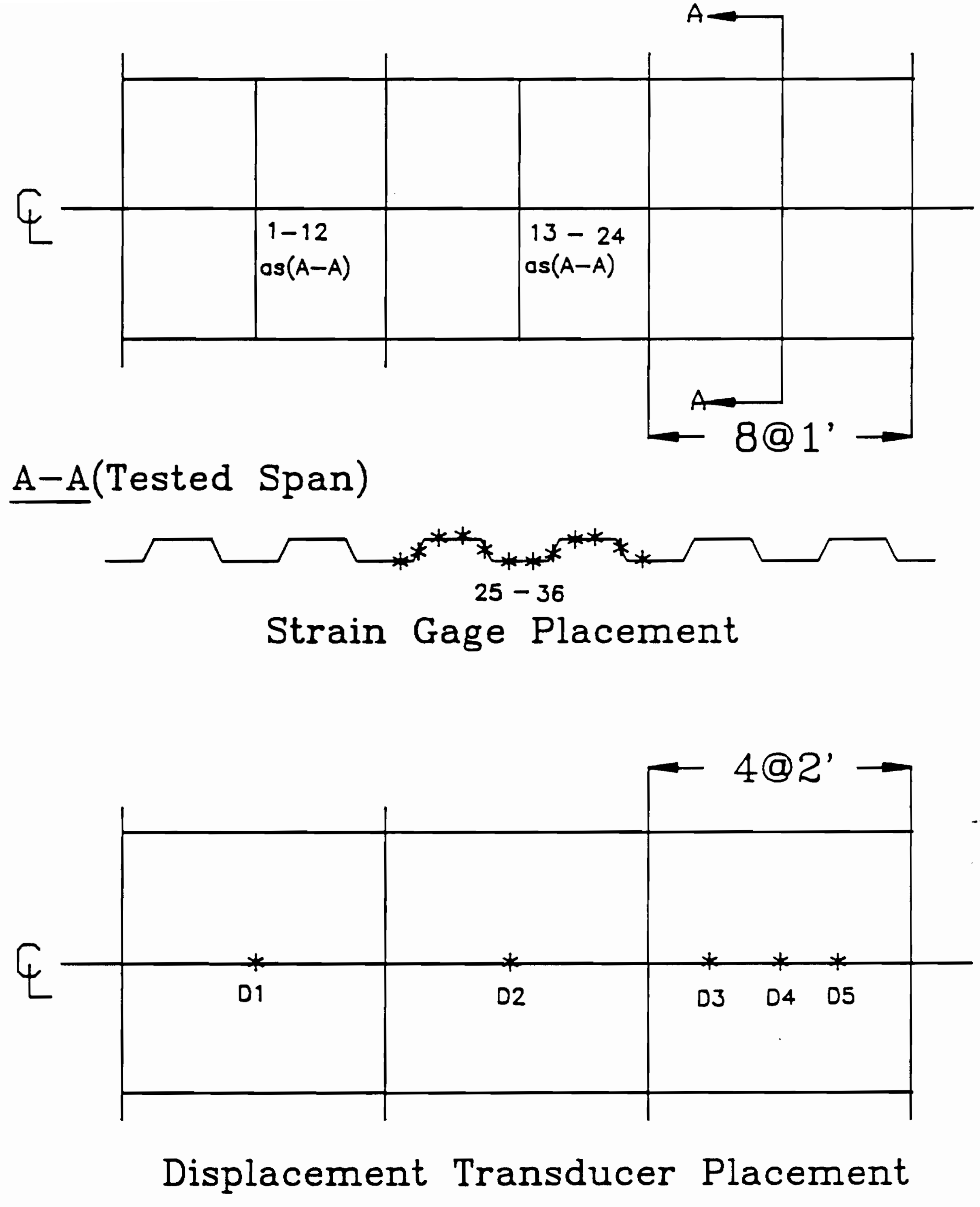


**Figure A7 SDI 2-2 Strain Gage, Displacement Transducer**

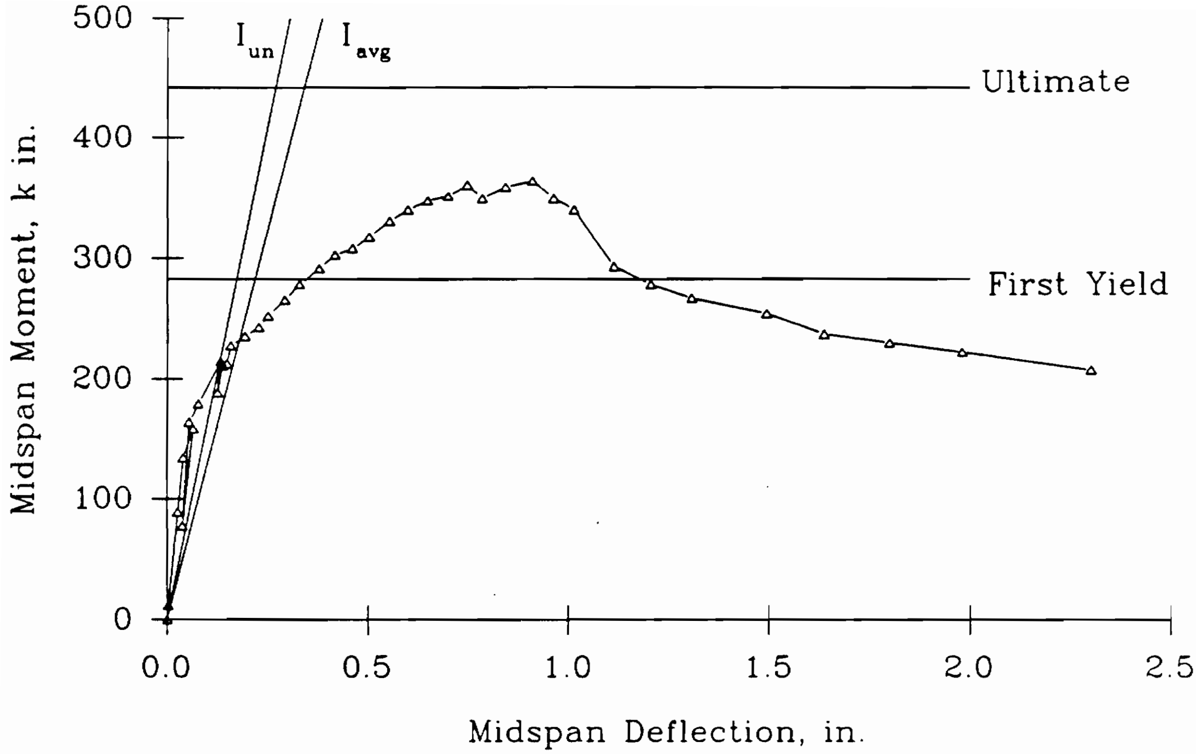


a) Midspan Moment vs. Midspan Deflection

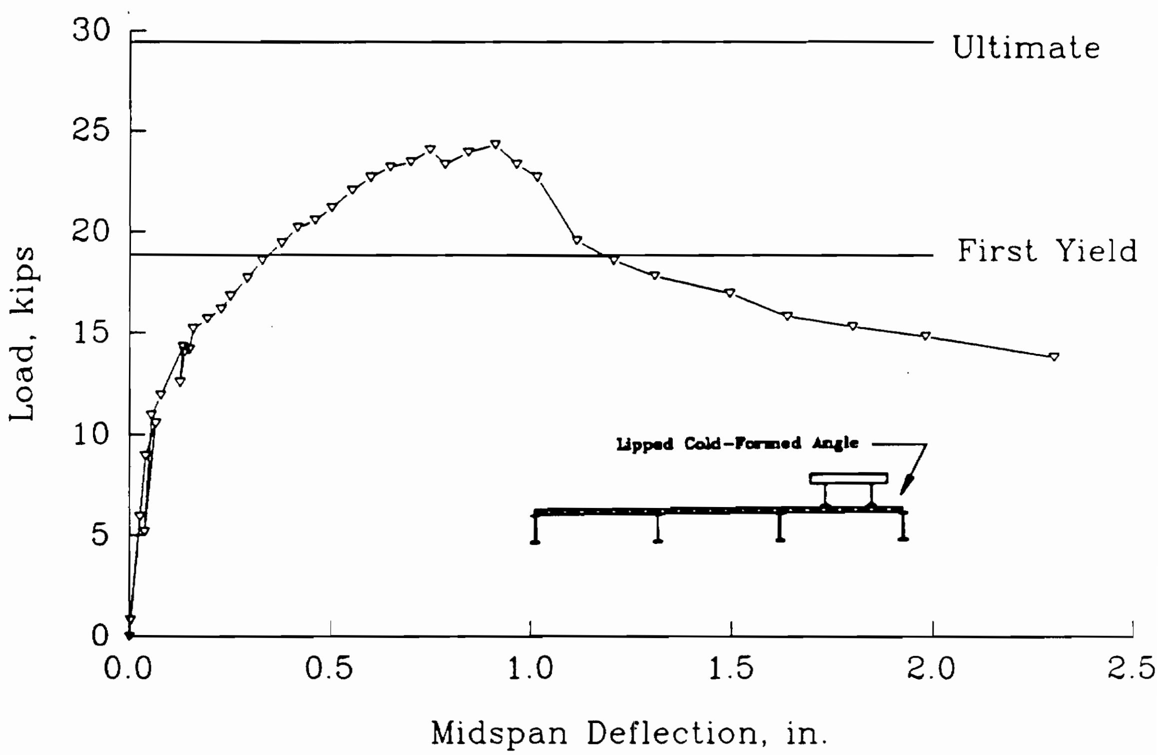


b) Load vs. Midspan Deflection

**Figure A8 SDI 2-2 Moment (Load) vs. Deflection Plot**

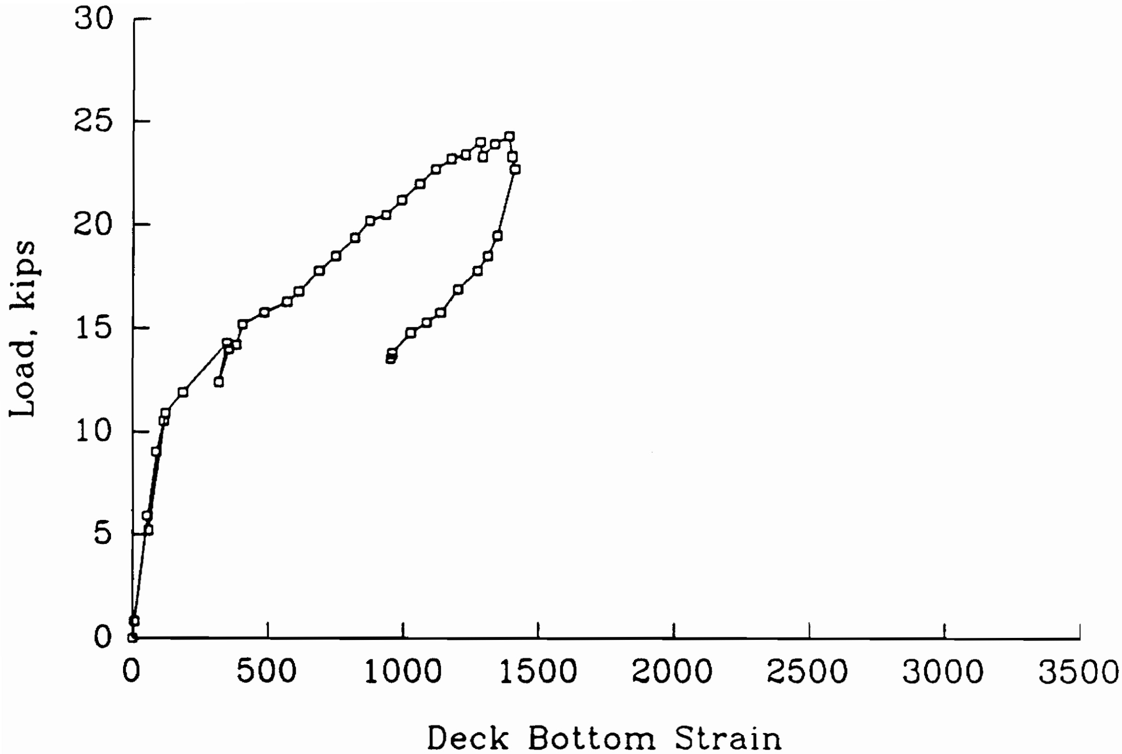


Load vs. Midspan Deck Bottom Strain

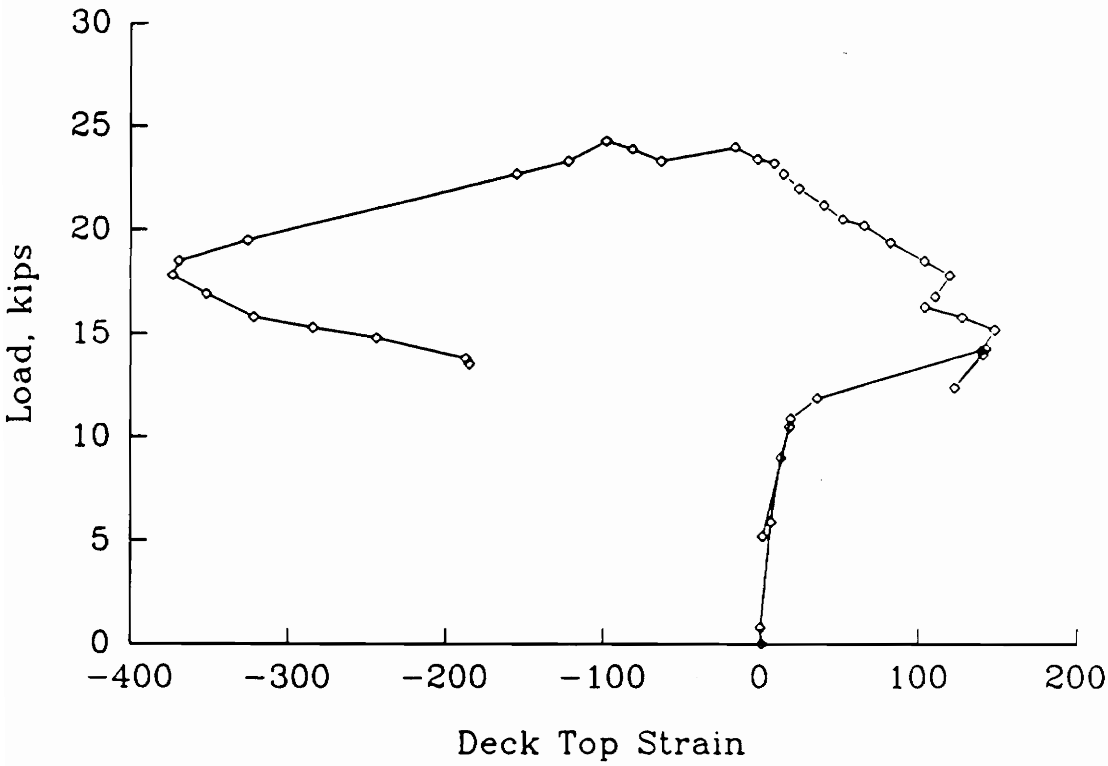


Load vs. Midspan Deck Top Strain

**Figure A9 SDI 2-2 Load vs. Strain Plots**

| | |
|---|---|
| Test Number: | SDI 3-1 |
| Date: | 20 March 1990 |
| Test Type: | Center Span |

---

<u>Measured Dimensions</u>

General

| | |
|---|---|
| Width: | 3 panel, each panel 2'-1", total 6'-1" |
| Span(s): | 8 ft/ 8 ft/ 8ft |
| Shear Span: | 30 in. |
| Midspan Strain: (concrete placement) | 282 micro strain |
| End Details: | Adjacent Slab / Adjacent Slab |
| Deck attachment: | puddle welds each flute |

Deck

| | |
|---|---|
| Type: | 20 gage, 2 in. depth |
| Measured Yield Stress: | 90 ksi |
| Measured Ultimate Stress: | 94 ksi |
| Modulus: | 29,500 ksi |
| Type I embossments | |
| Depth: | 0.094 in. |
| Horizontal Spacing, s: | 1.417 in. |
| Length: | 1.145 in. |

Concrete

| | |
|---|---|
| Type: | A4 |
| Test Strength: | 4400 psi |
| Depth: | 5 in, from bottom of deck, 3 in cover |
| Effective Depth: | 4 in. |

---

<u>Instrumentation</u>

| | |
|---|---|
| Strain Gages: | 22 (shown on diagram) |
| Displacement Transducers | D1-D5 (shown on diagram) |

---

<u>Test Results</u>

| | |
|---|---|
| Maximum Load: | 53.5 kips @2.004 in midspan deflection |
| Maximum Moment: | 802.5 k-in. |
| Maximum Deflection: | 2.111 in. (test stopped) |

Comments

- Cracking over the supports occurred at a moment of 162 k-in.
- Cracking under the spreader beams occurred at 260 k-in.
- Cracking between spreader beams occurred at a moment of 717 k-in.
- Deck was ripping out around the puddle welds that connected the deck to the support members
- No slip of the deck and concrete occurred until after ultimate.

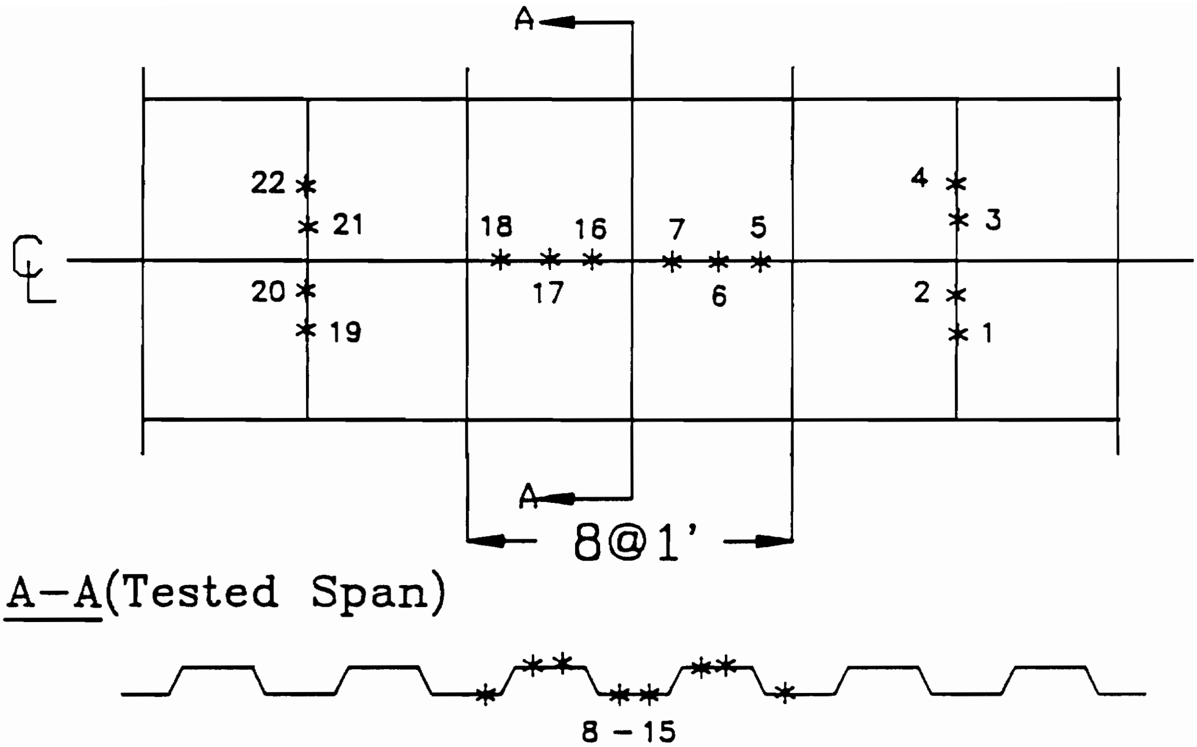


Strain Gage Placement

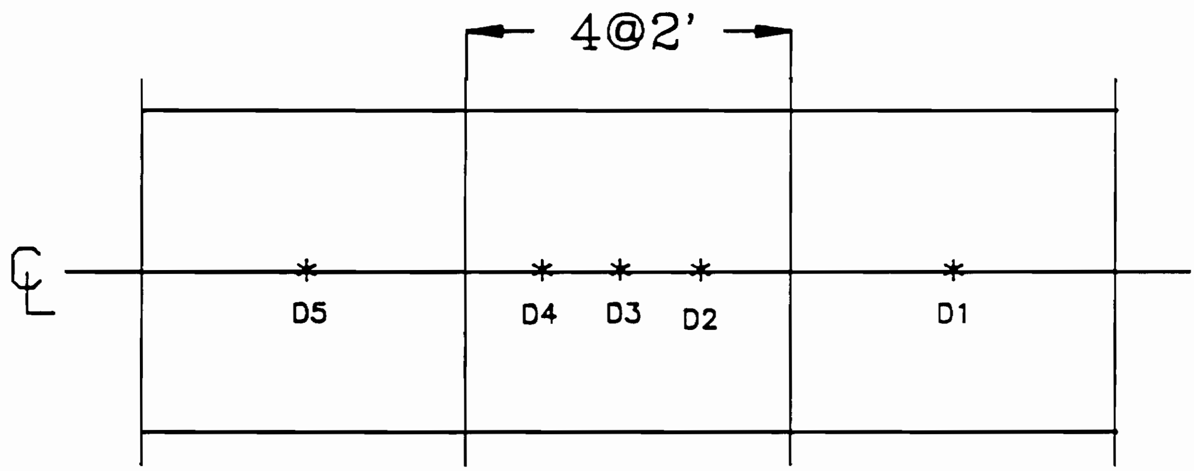


Displacement Transducer Placement

**Figure A10 SDI 3-1 Strain Gage, Displacement Transducer**

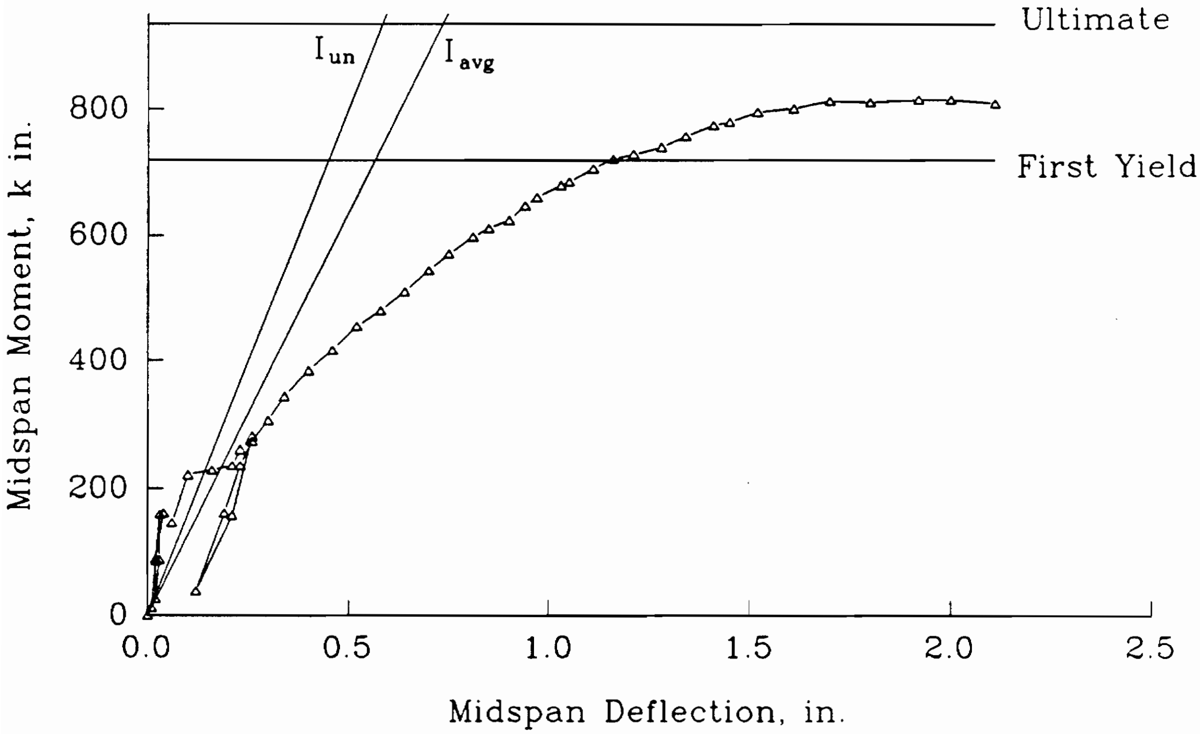


a) Midspan Moment vs. Midspan Deflection

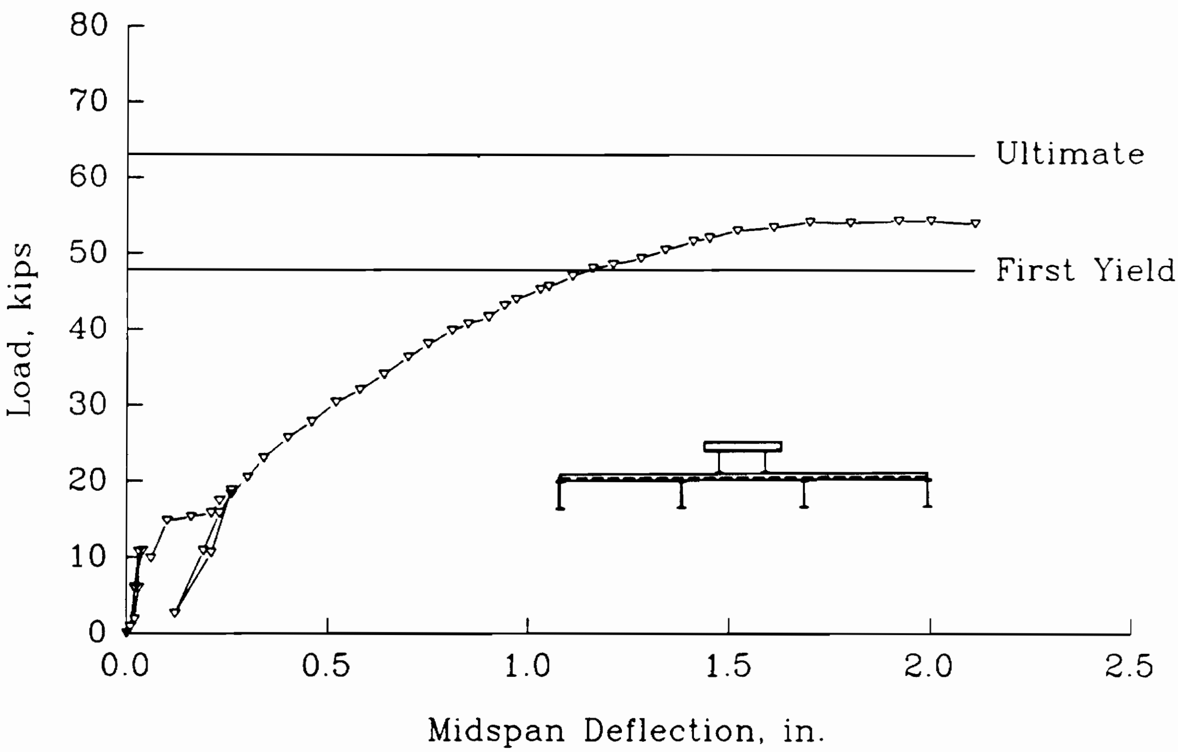


b) Load vs. Midspan Deflection

**Figure A11 SDI 3-1 Moment (Load) vs. Deflection Plot**

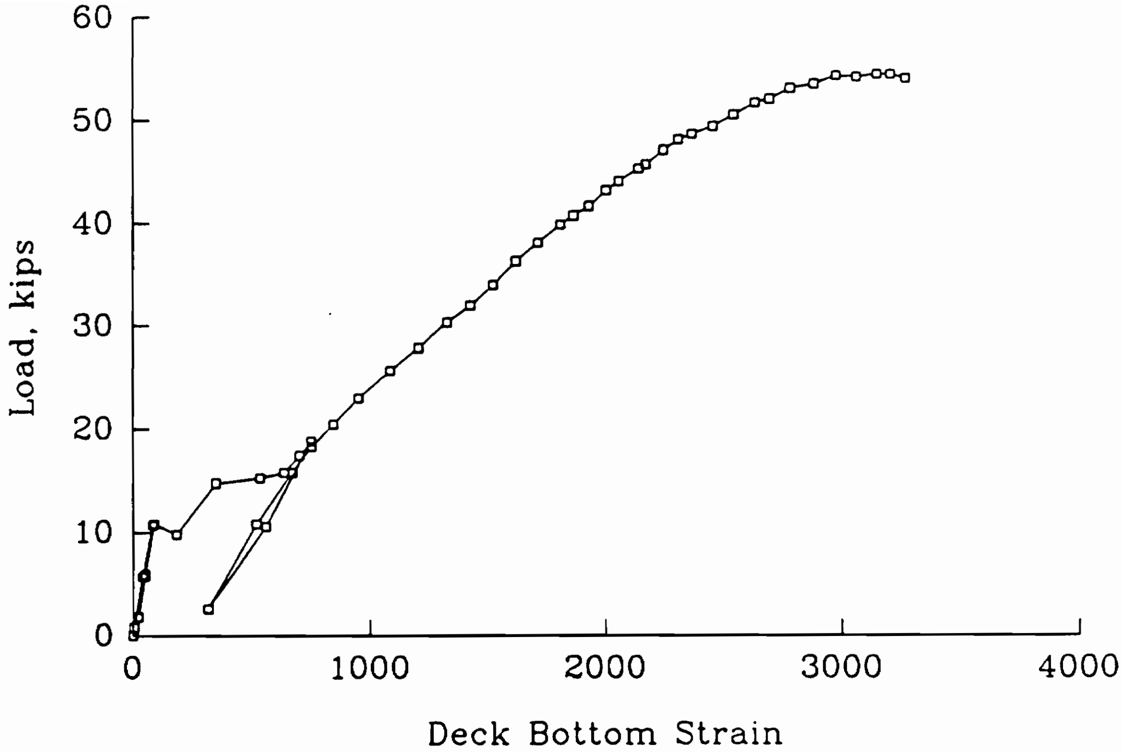


Load vs. Midspan Deck Bottom Strain

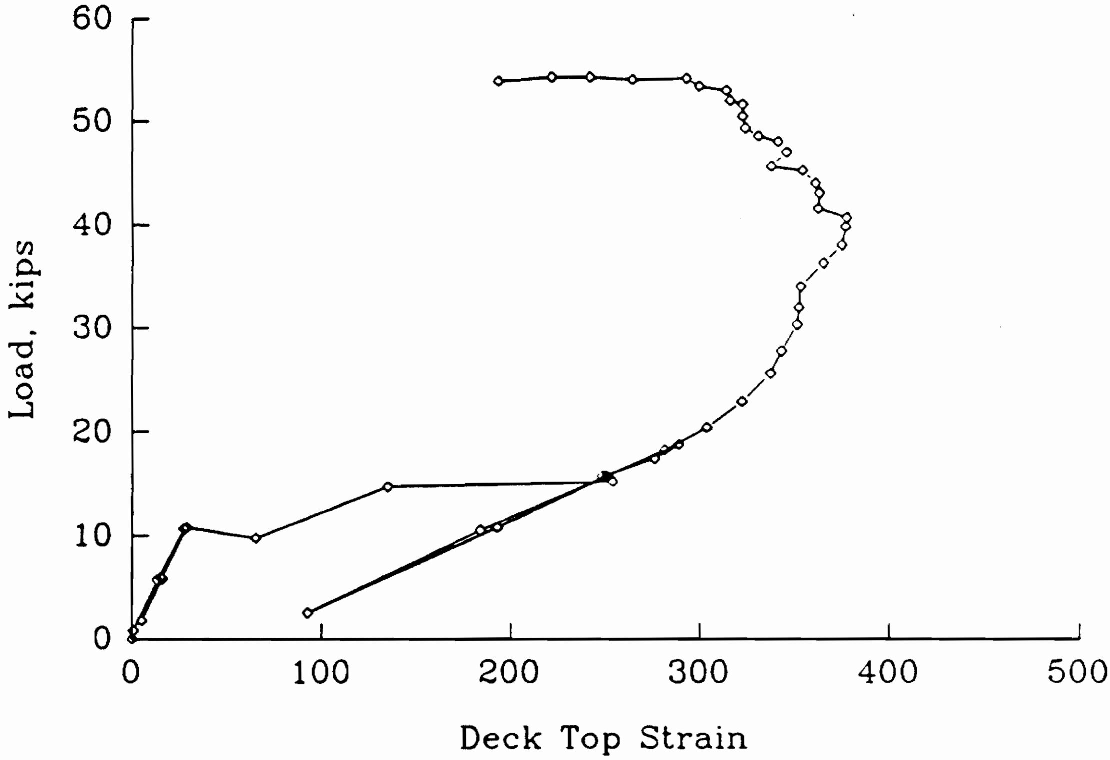


Load vs. Midspan Deck Top Strain

**Figure A12 SDI 3-1 Load vs. Strain Plots**

| | |
|---|---|
| Test Number: | SDI 4-1 |
| Date: | 23 April 1990 |
| Test Type: | End Span, Cold-Formed Angle w/ lips and studs |

Measured Dimensions

General

| | |
|---|---|
| Width: | 2 panel, each panel 3'-0", total 6'-0" |
| Span(s): | 8 ft/ 8 ft/ 8ft |
| Shear Span: | 30 in. |
| Midspan Strain: (concrete placement) | 260 micro strain |
| End Details: | Adjacent Slab / Cold-Formed Angle w/ studs |
| Deck attachment: | Puddle welds each flute<br>3/4 inch shear studs each flute |

Deck

| | |
|---|---|
| Type: | 20 gage, 2 in. depth |
| Measured Yield Stress: | 40 ksi |
| Measured Ultimate Stress: | 54 ksi |
| Modulus: | 29,500 ksi |
| Type II embossments | |
| Depth: 0.050 in. | |

Concrete

| | |
|---|---|
| Type: | A4 |
| Test Strength: | 4575 psi |
| Depth: | 5 in, from bottom of deck, 3 in cover |
| Effective Depth: | 4 in. |

Instrumentation

| | |
|---|---|
| Strain Gages: | 30 (shown on diagram) |
| Displacement Transducers | D1-D5 (shown on diagram) |

Test Results

| | |
|---|---|
| Maximum Load: | 29.6 kips<br>@1.298 in midspan deflection |
| Maximum Moment: | 444.0 k-in. |
| Maximum Deflection: | 2.024 in. (test stopped) |

Test Number: SDI 4-1

Comments

- Cracking over supports occurred at 58.5 k-in.
- Cracking under the spreader beam closest o the cold-formed angle detail occurred at 231 k-in.
- Cracking over the shear studs occurred after ultimate
- No recorded slip between deck and concrete

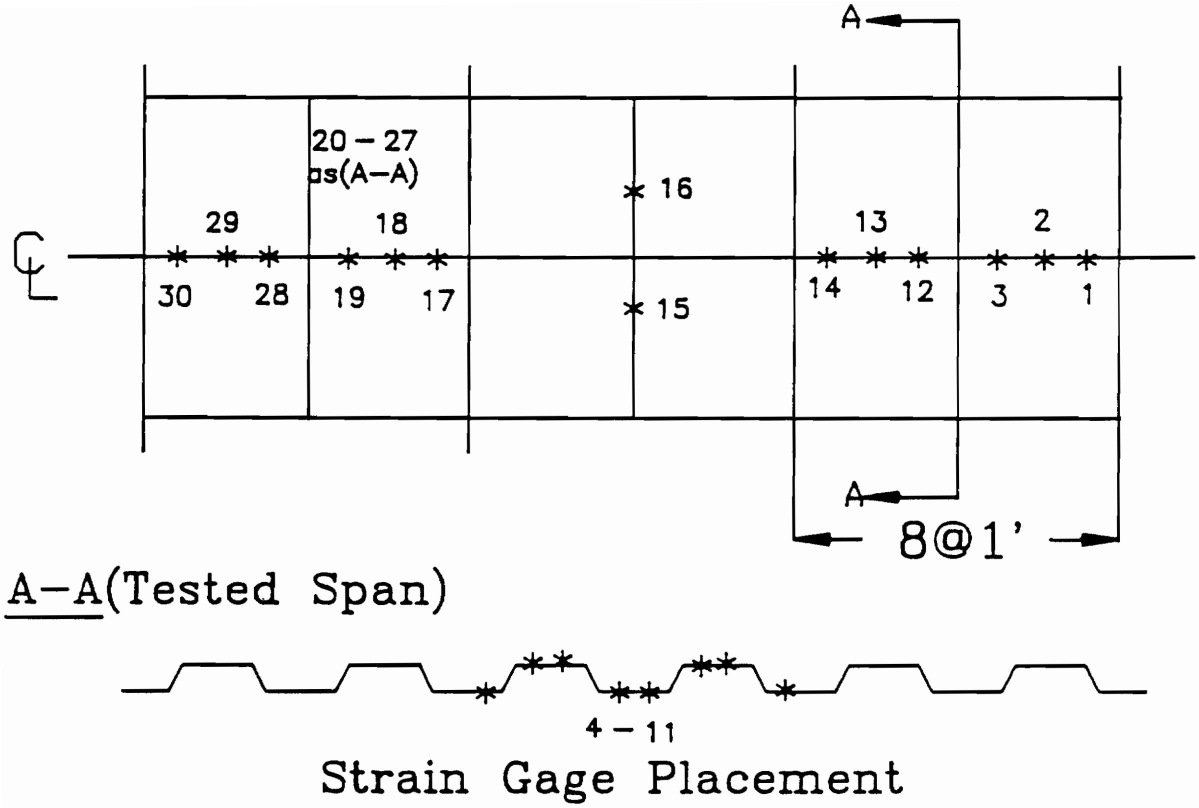


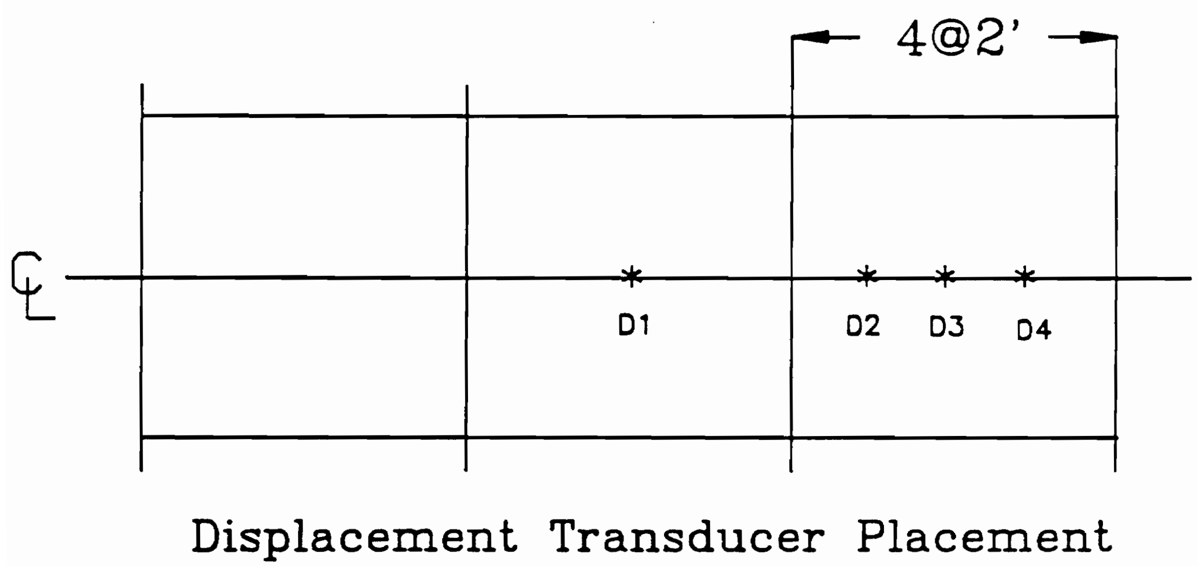


**Figure A13 SDI 4-1 Strain Gage, Displacement Transducer**

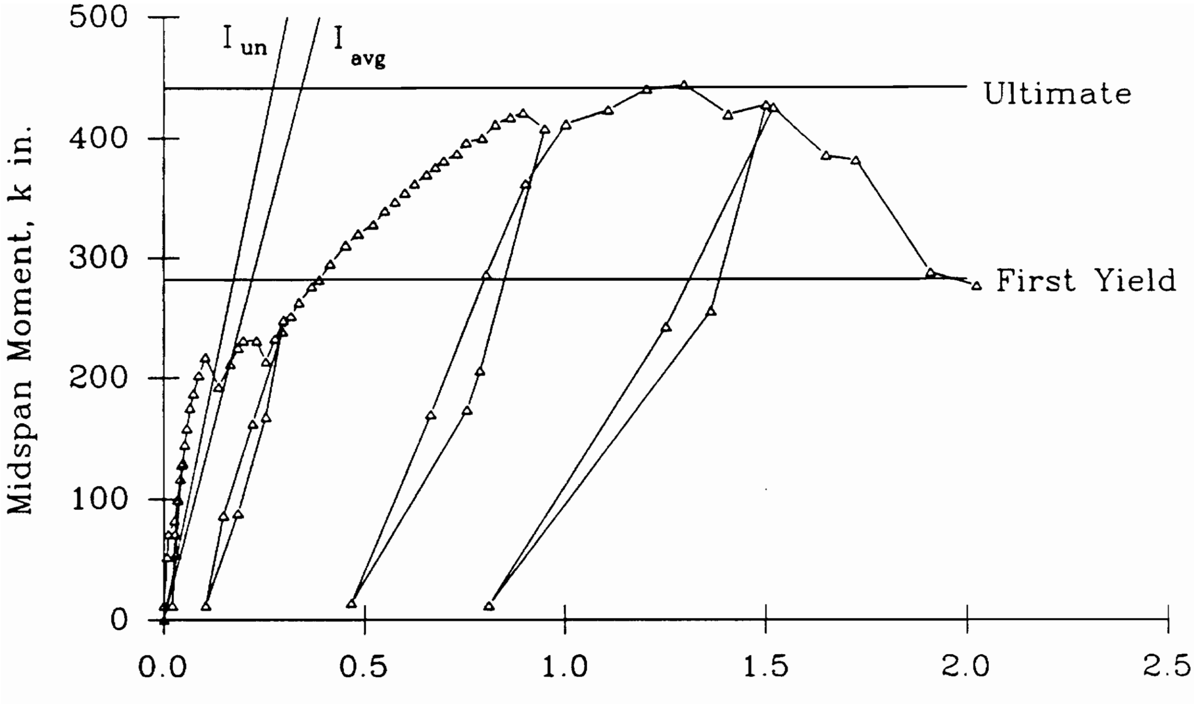


a) Midspan Moment vs. Midspan Deflection

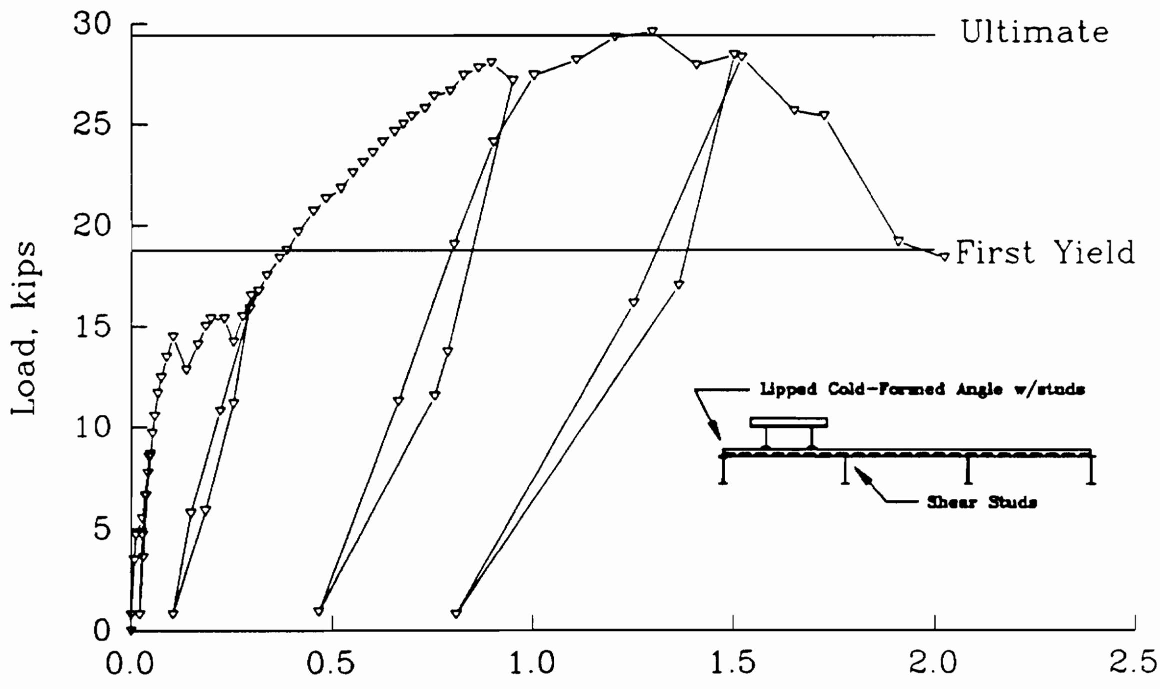


b) Load vs. Midspan Deflection

**Figure A14 SDI 4-1 Moment (Load) vs. Deflection Plot**

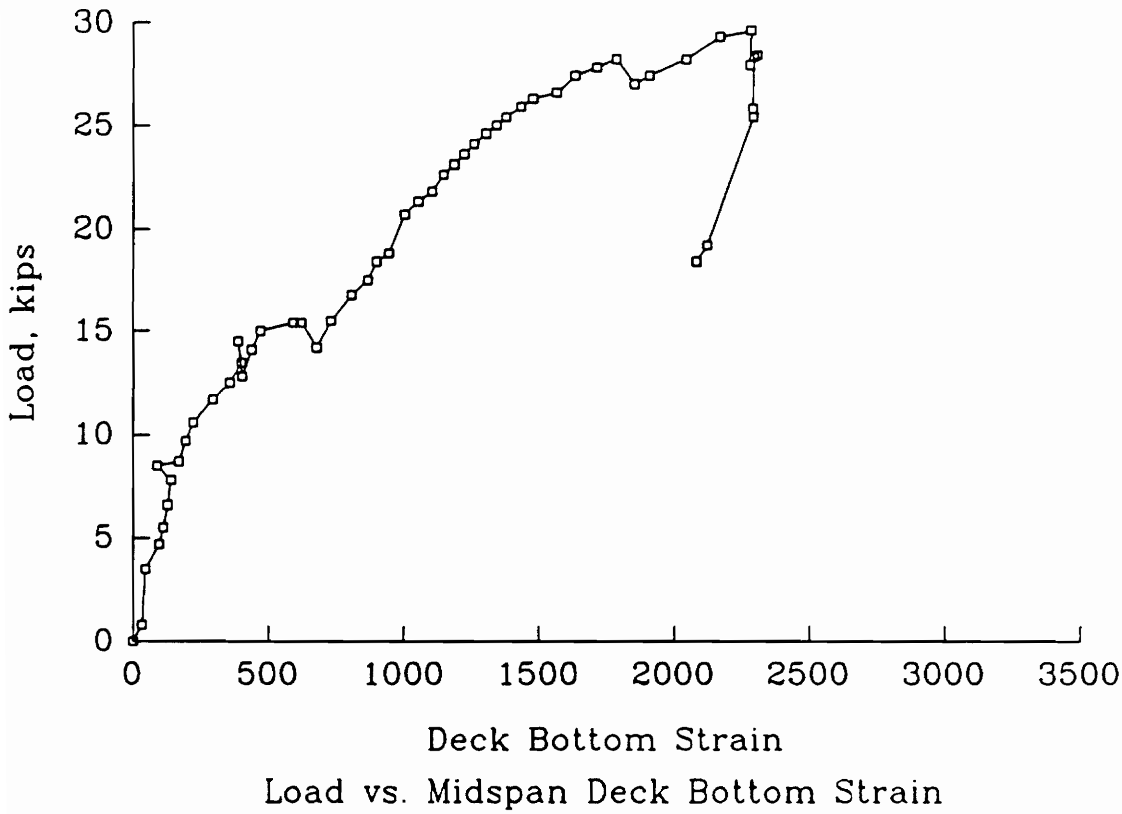


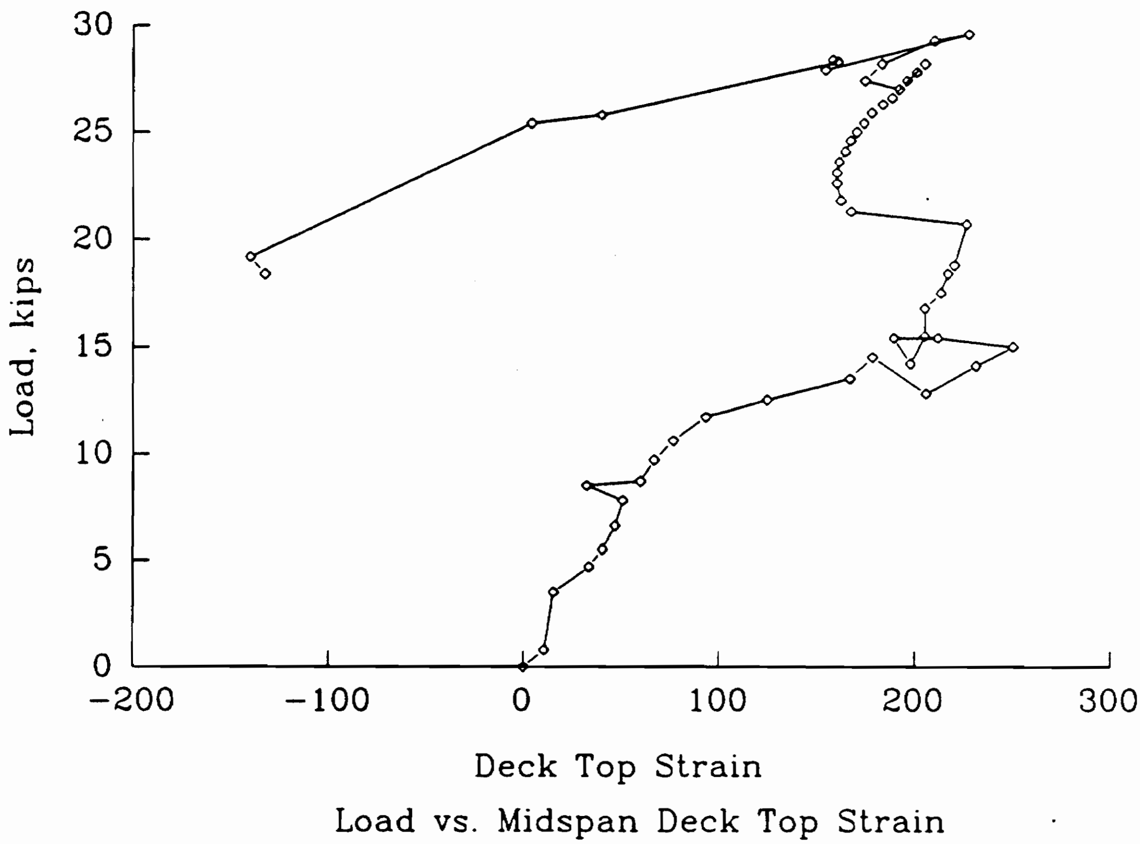


**Figure A15 SDI 4-1 Load vs. Strain Plots**

| | |
|---|---|
| Test Number: | SDI 4-2 |
| Date: | 26 April 1990 |
| Test Type: | End Span, Cold-Formed Angle w/ lips |

Measured Dimensions

General

| | |
|---|---|
| Width: | 2 panel, each panel 3'-0", total 6'-0" |
| Span(s): | 8 ft/ 8 ft/ 8ft |
| Shear Span: | 30 in. |
| Midspan Strain: (concrete placement) | 268 micro strain |
| End Details: | Adjacent Slab / Cold-Formed Angle |
| Deck attachment: | Puddle welds each flute |

Deck

| | |
|---|---|
| Type: | 20 gage, 2 in. depth |
| Measured Yield Stress: | 40 ksi |
| Measured Ultimate Stress: | 54 ksi |
| Modulus: | 29,500 ksi |
| Type II embossments Depth: 0.050 in. | |

Concrete

| | |
|---|---|
| Type: | A4 |
| Test Strength: | 4575 psi |
| Depth: | 5 in, from bottom of deck, 3 in cover |
| Effective Depth: | 4 in. |

Instrumentation

| | |
|---|---|
| Strain Gages: | 30 (shown on diagram) |
| Displacement Transducers | D1-D5 (shown on diagram) |

Test Results

| | |
|---|---|
| Maximum Load: | 20.3 kips @1.210 in midspan deflection |
| Maximum Moment: | 304.5 k-in. |
| Maximum Deflection: | 2.120 in. (test stopped) |

Test Number: SDI 4-2

Comments

- Immediately upon applying load, end slip was recorded.
- Cracking over the support occurred at a moment of 178.5 k-in.
- Cracking under the spreader beams occurred at 244.5 k-in.
- Post test inspection revealed that approximately 50% of the puddle welds did not fuse properly with the base metal

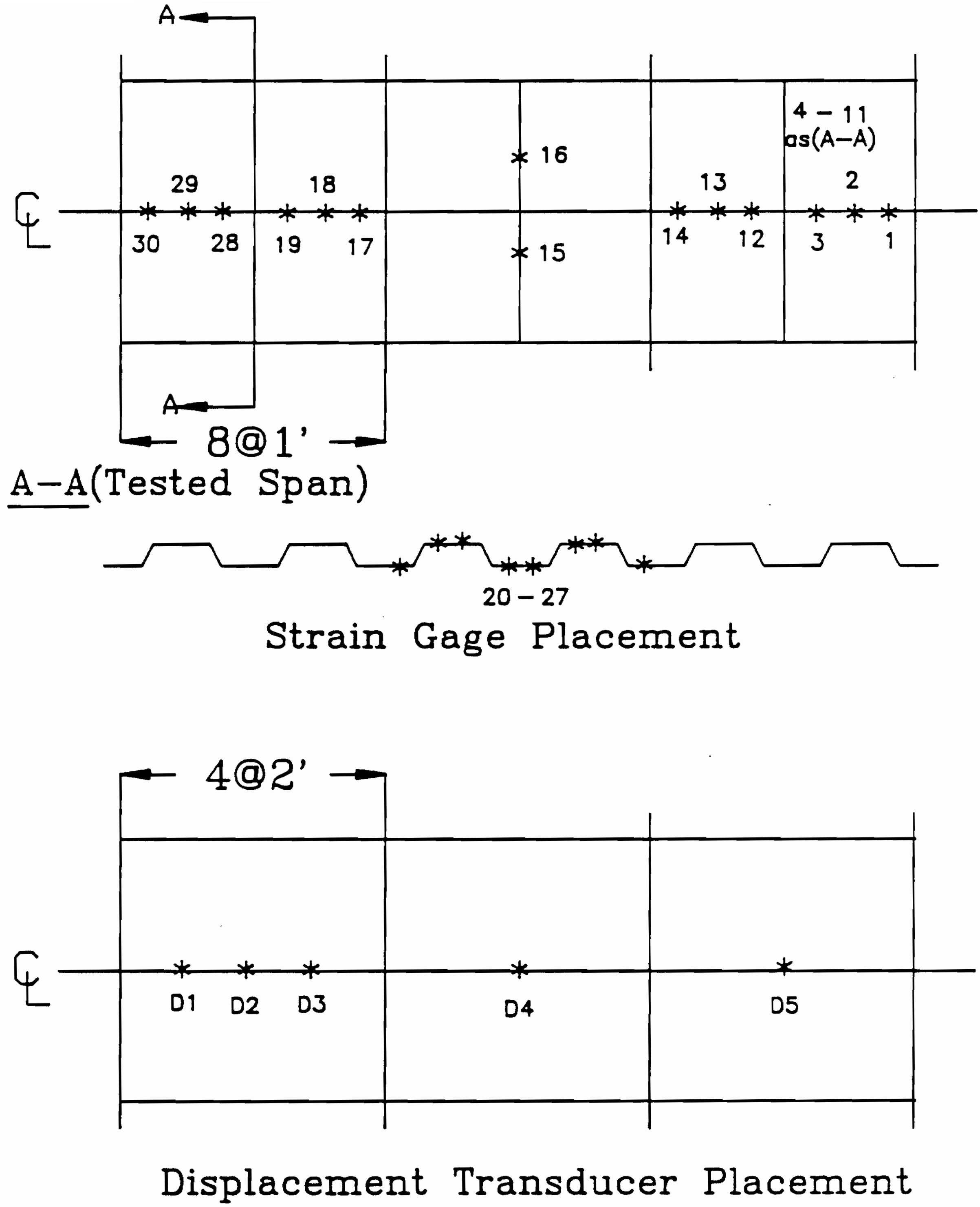


**Figure A16 SDI 4-2 Strain Gage, Displacement Transducer**

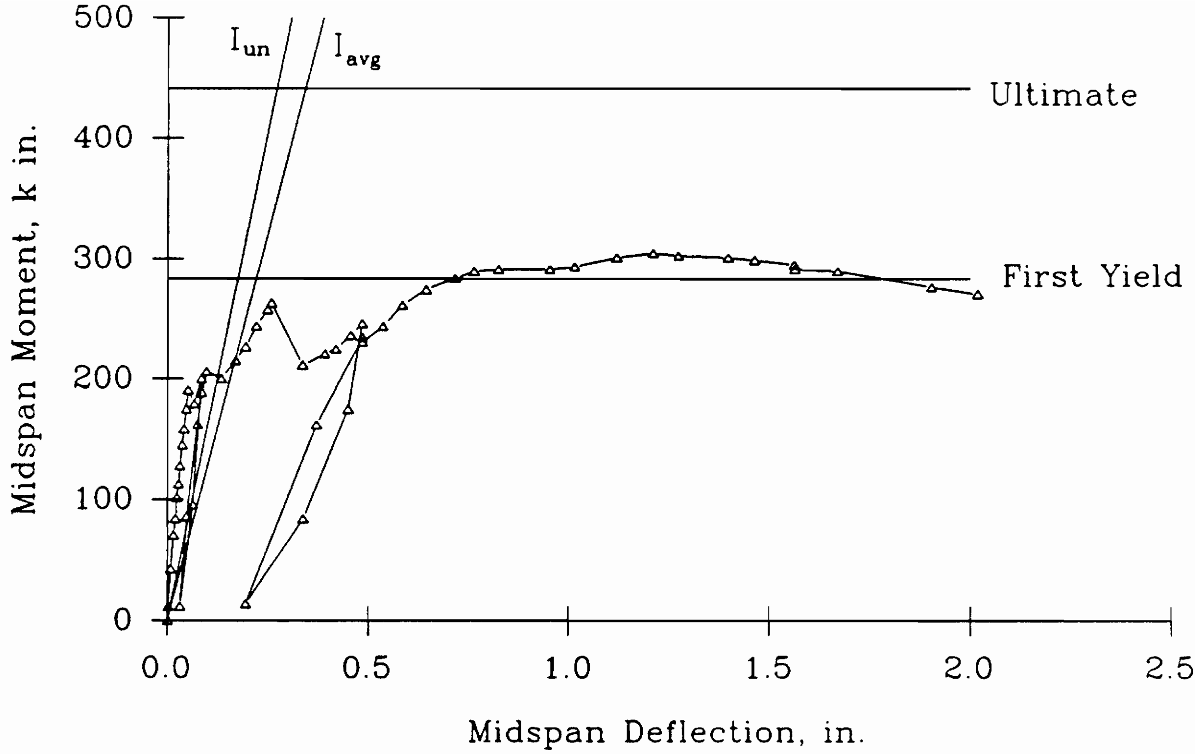


b) Midspan Moment vs. Midspan Deflection

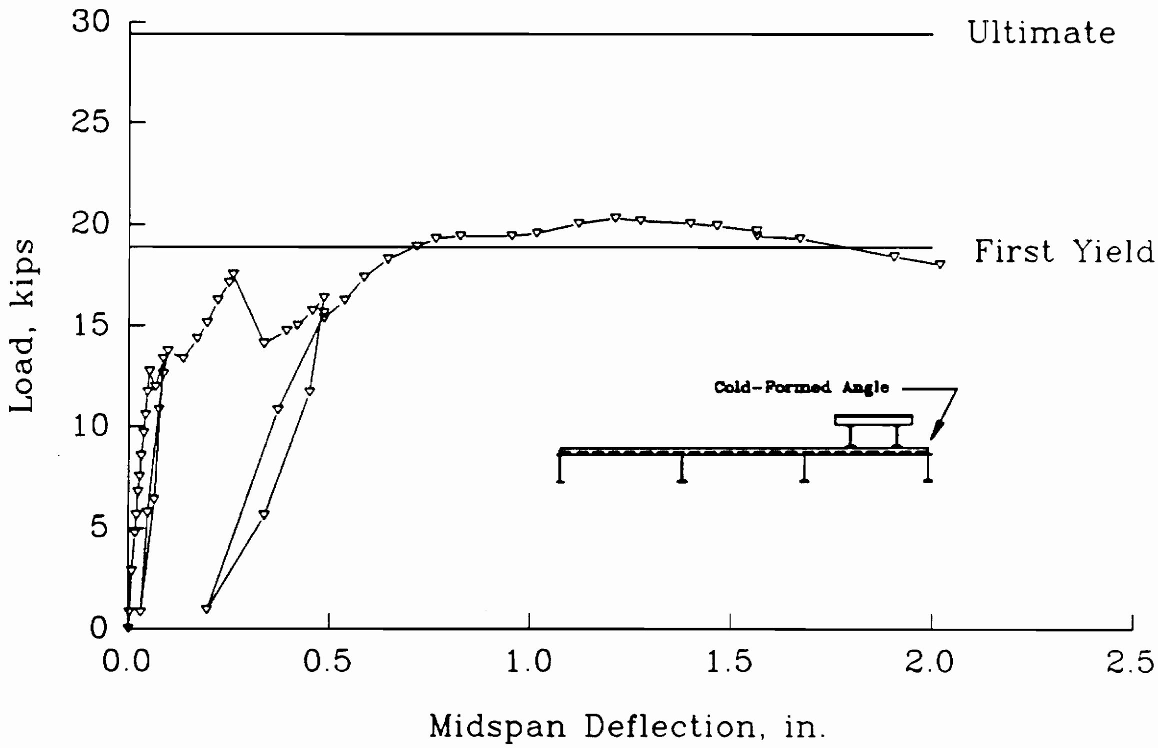


a) Load vs. Midspan Deflection

**Figure A17 SDI 4-2 Moment (Load) vs. Deflection Plot**

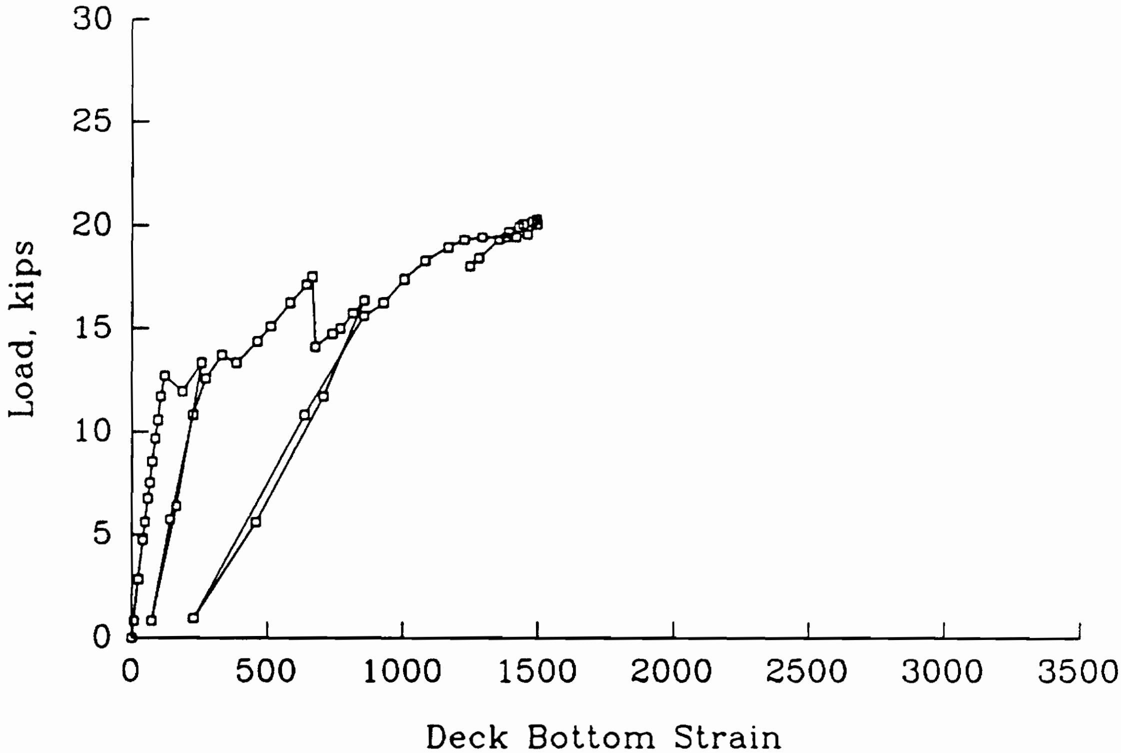


Load vs. Midspan Deck Bottom Strain

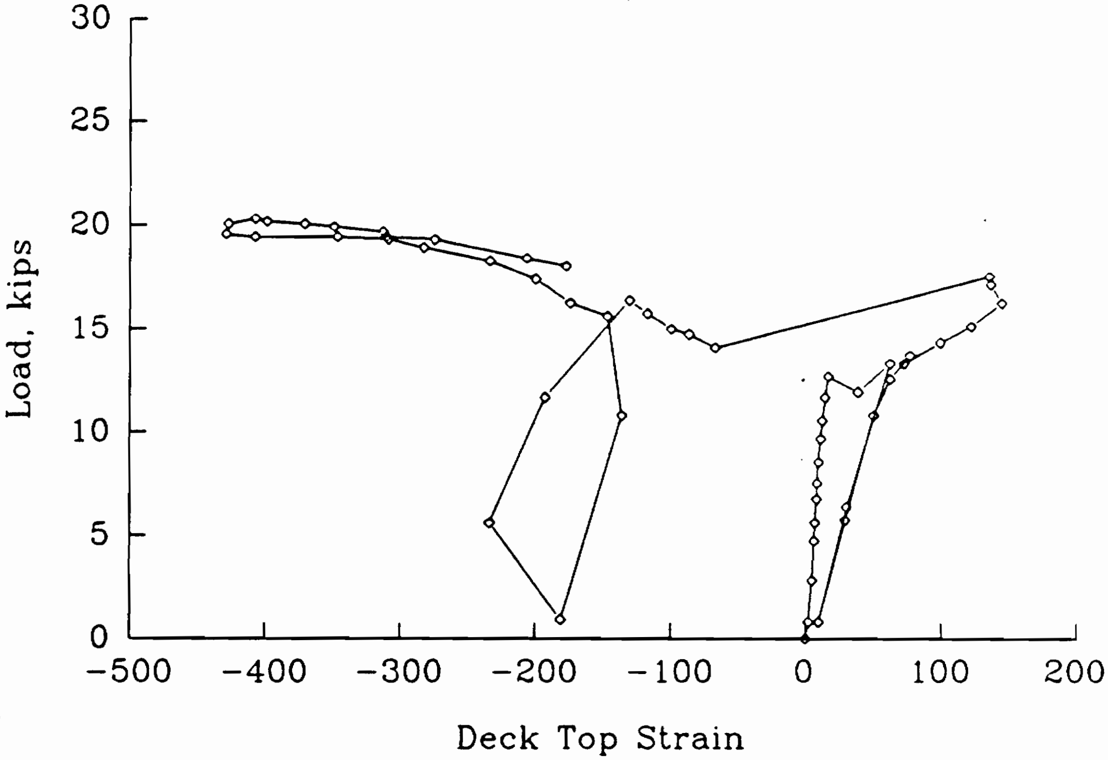


Load vs. Midspan Deck Top Strain

**Figure A18 SDI 4-2 Load vs. Strain Plots**

| | |
|---|---|
| Test Number: | SDI 5-1 |
| Date: | 20 June 1990 |
| Test Type: | End Span, Cold-Formed Angle w/ lips |

<u>Measured Dimensions</u>

General

| | |
|---|---|
| Width: | 2 panel, each panel 3'-0", total 6'-0" |
| Span(s): | 8 ft/ 8 ft/ 8ft |
| Shear Span: | 30 in. |
| Midspan Strain: (concrete placement) | 230 micro strain |
| End Details: | Adjacent Slab / Cold-Formed Angle w/lips |
| Deck attachment: | Puddle welds each flute |

Deck

| | |
|---|---|
| Type: | 20 gage, 2 in. depth |
| Measured Yield Stress: | 40 ksi |
| Measured Ultimate Stress: | 54 ksi |
| Modulus: | 29,500 ksi |
| Type II embossments | |
| Depth: 0.050 in. | |

Concrete

| | |
|---|---|
| Type: | A4 |
| Test Strength: | 3300 psi |
| Depth: | 5 in, from bottom of deck, 3 in cover |
| Effective Depth: | 4 in. |

<u>Instrumentation</u>

| | |
|---|---|
| Strain Gages: | 8 (shown on diagram) |
| Displacement Transducers | D1-D3 (shown on diagram) |

<u>Test Results</u>

| | |
|---|---|
| Maximum Load: | 19.7 kips @0.200 in midspan deflection |
| Maximum Moment: | 295.5 k-in. |
| Maximum Deflection: | 1.970 in. (test stopped) |

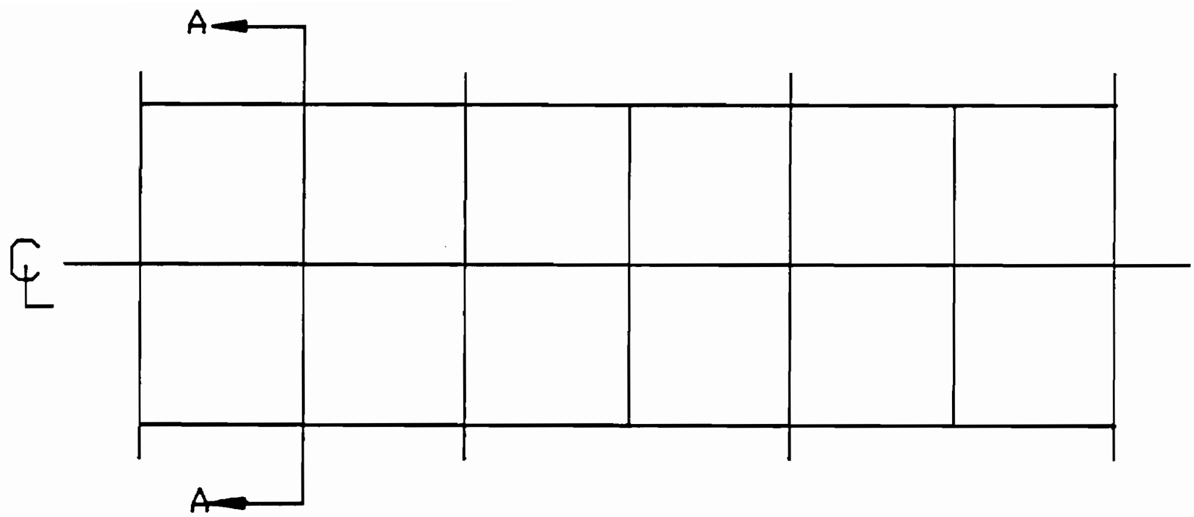


A–A(Tested Span)

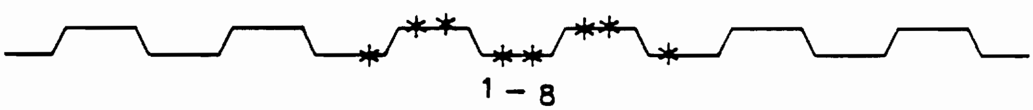


Strain Gage Placement

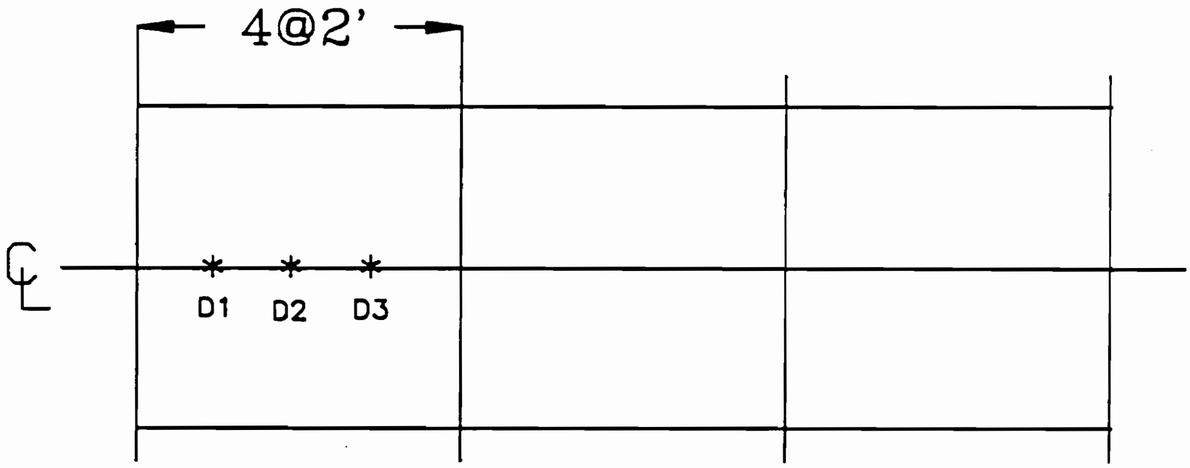


Displacement Transducer Placement

**Figure A19 SDI 5-1 Strain Gage, Displacement Transducer**

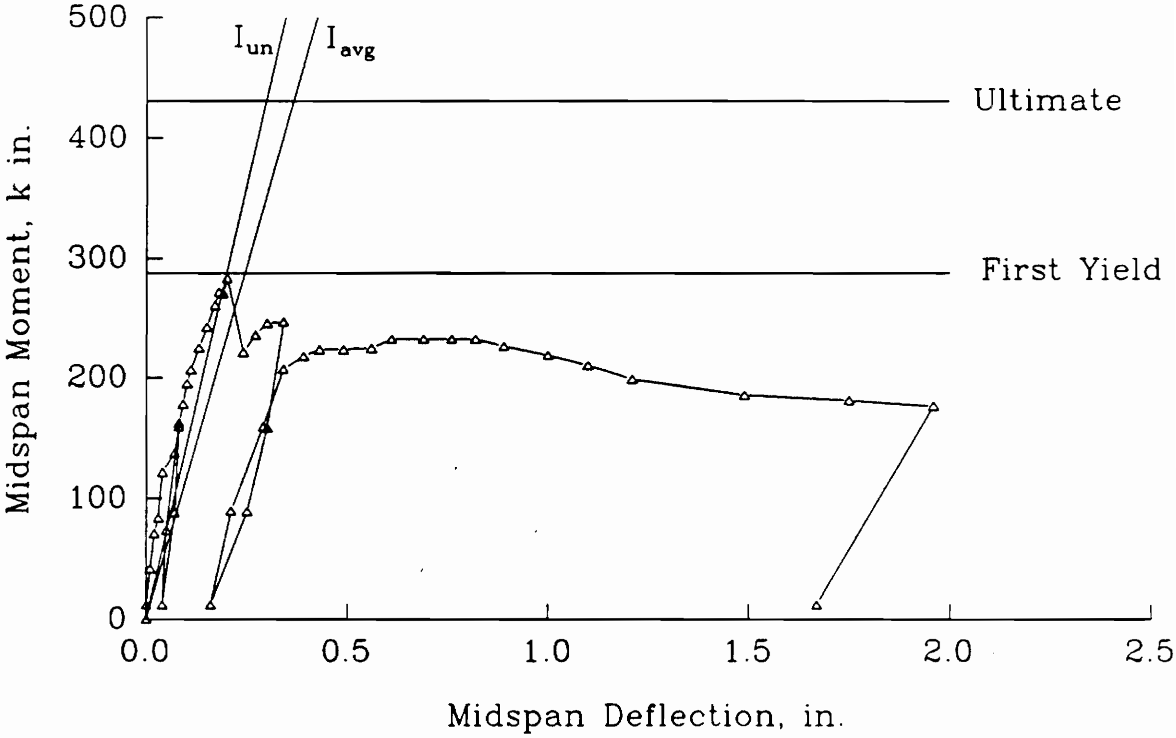


a) Midspan Moment vs. Midspan Deflection

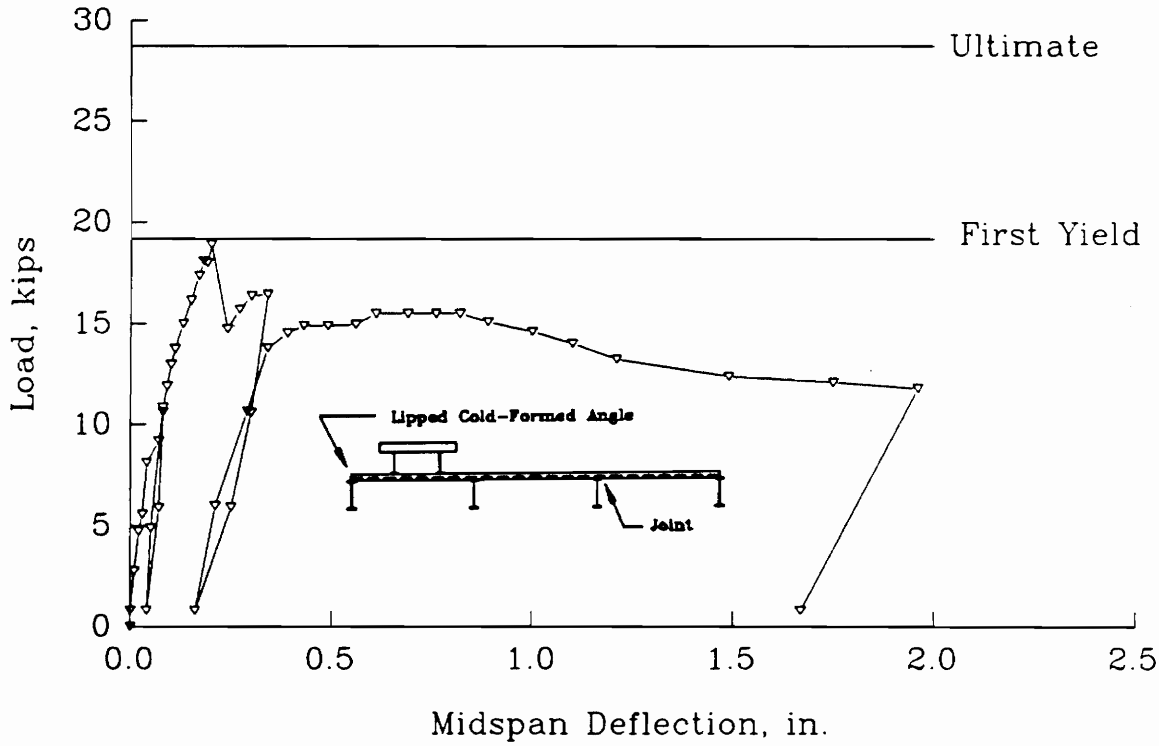


b) Load vs. Midspan Deflection

**Figure A20 SDI 5-1 Moment (Load) vs. Deflection Plot**

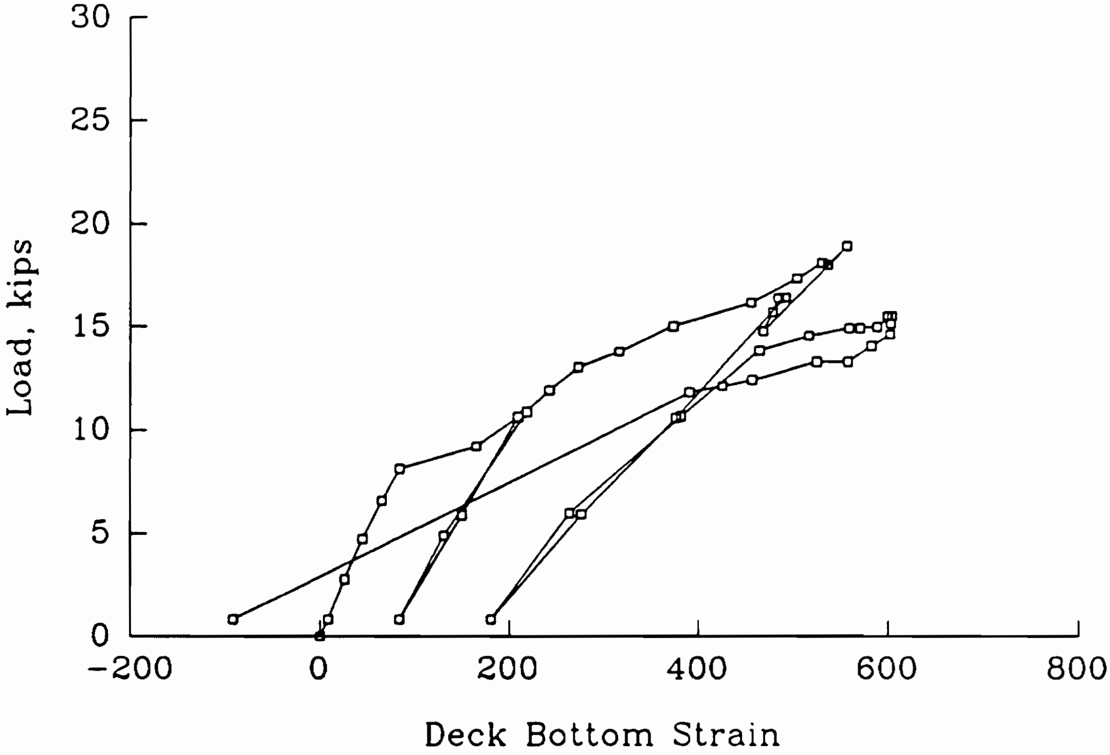


Load vs. Midspan Deck Bottom Strain

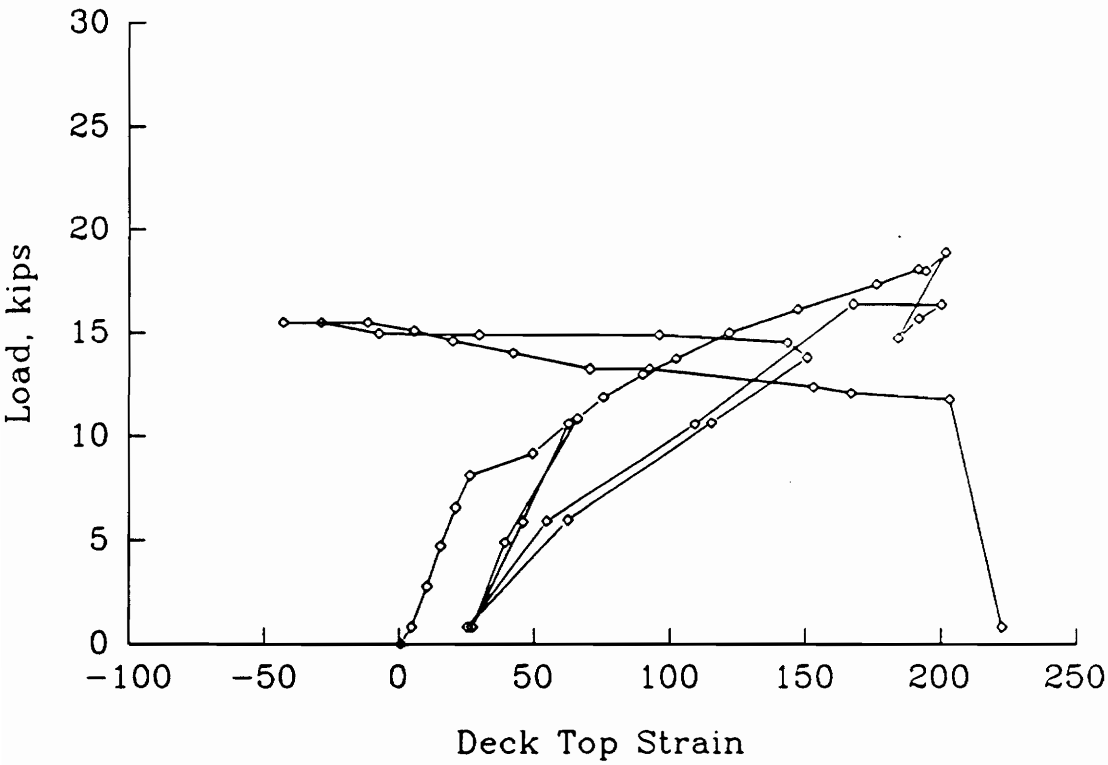


Load vs. Midspan Deck Top Strain

**Figure A21 SDI 5-1 Load vs. Strain Plots**

| | |
|---|---|
| Test Number: | SDI 5-2 |
| Date: | 20 June 1990 |
| Test Type: | End Span (joint), Cold-Formed Angle w/ lips |

Measured Dimensions

General

| | |
|---|---|
| Width: | 2 panel, each panel 3'-0", total 6'-0" |
| Span(s): | 8 ft/ 8 ft/ 8ft |
| Shear Span: | 30 in. |
| Midspan Strain: (concrete placement) | 380 micro strain |
| End Details: | Adjacent Slab (joint) / Cold-Formed Angle |
| Deck attachment: | Puddle welds each flute |

Deck

| | |
|---|---|
| Type: | 20 gage, 2 in. depth |
| Measured Yield Stress: | 40 ksi |
| Measured Ultimate Stress: | 54 ksi |
| Modulus: | 29,500 ksi |
| Type II embossments | |
| Depth: 0.050 in. | |

Concrete

| | |
|---|---|
| Type: | A4 |
| Test Strength: | 3300 psi |
| Depth: | 5 in, from bottom of deck, 3 in cover |
| Effective Depth: | 4 in. |

Instrumentation

| | |
|---|---|
| Strain Gages: | 8 (shown on diagram) |
| Displacement Transducers | D1-D3 (shown on diagram) |

Test Results

| | |
|---|---|
| Maximum Load: | 20.4 kips @0.220 in midspan deflection |
| Maximum Moment: | 306.00 k-in. |
| Maximum Deflection: | 2.020 in. (test stopped) |

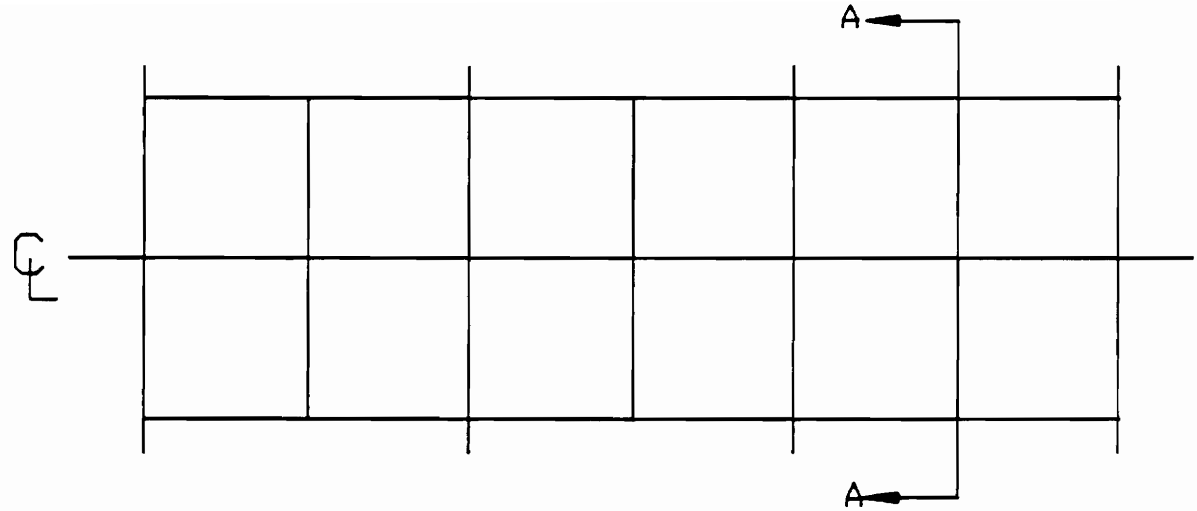


A–A(Tested Span)

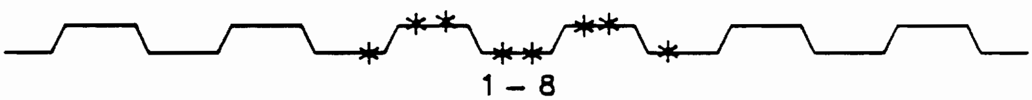


Strain Gage Placement

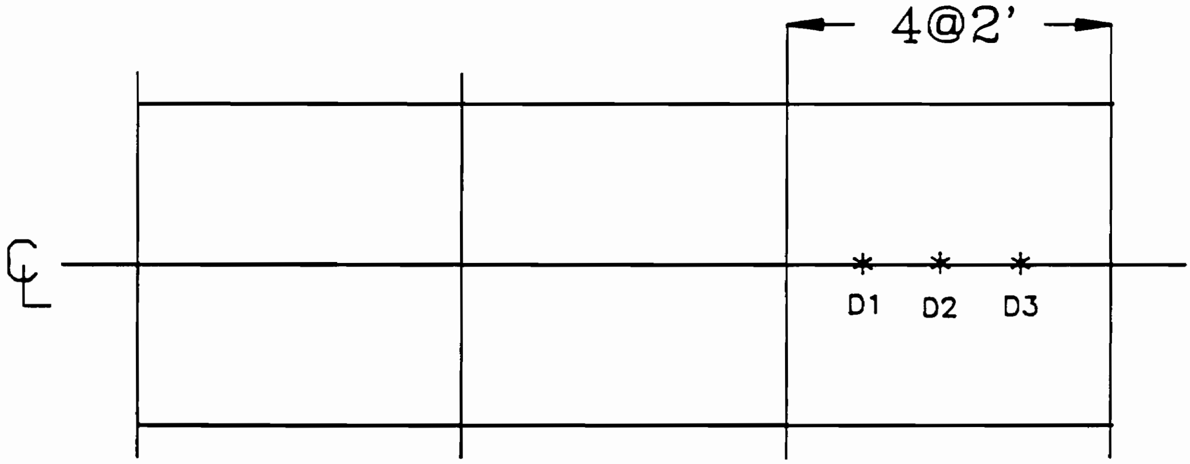


Displacement Transducer Placement

**Figure A22 SDI 5-2 Strain Gage, Displacement Transducer**

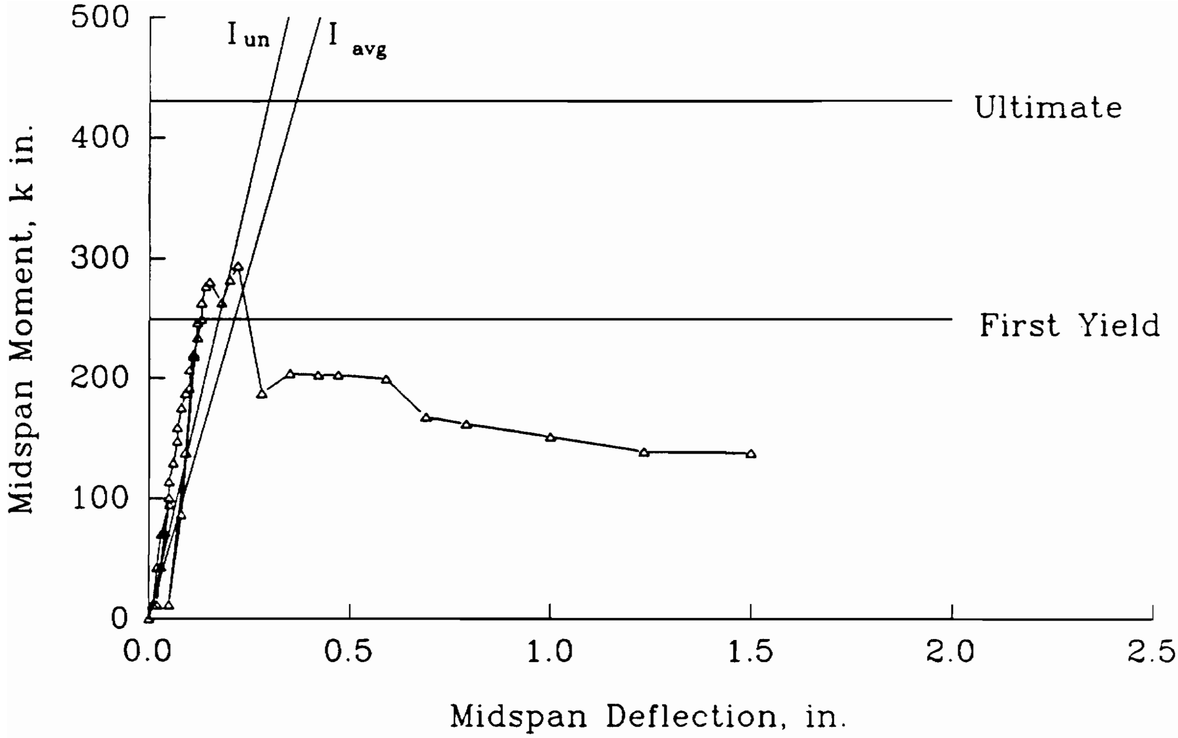


a) Midspan Moment vs. Midspan Deflection

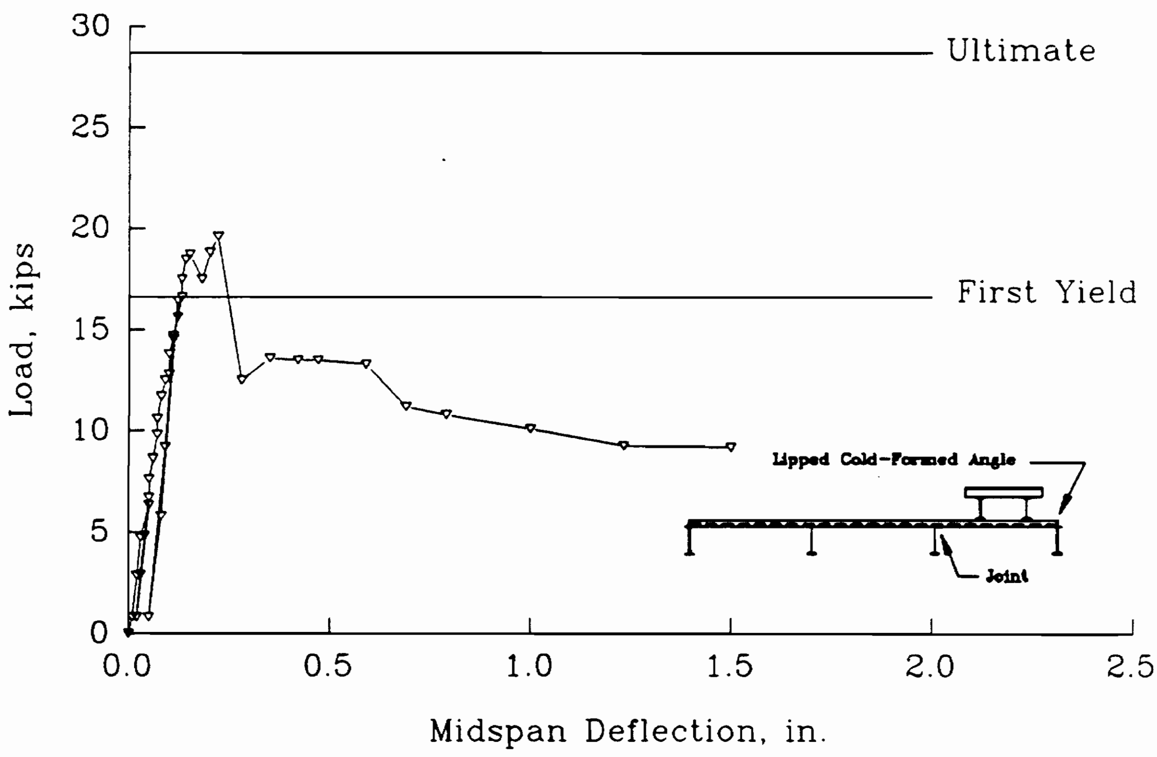


b) Load vs. Midspan Deflection

**Figure A23 SDI 5-2 Moment (Load) vs. Deflection Plot**

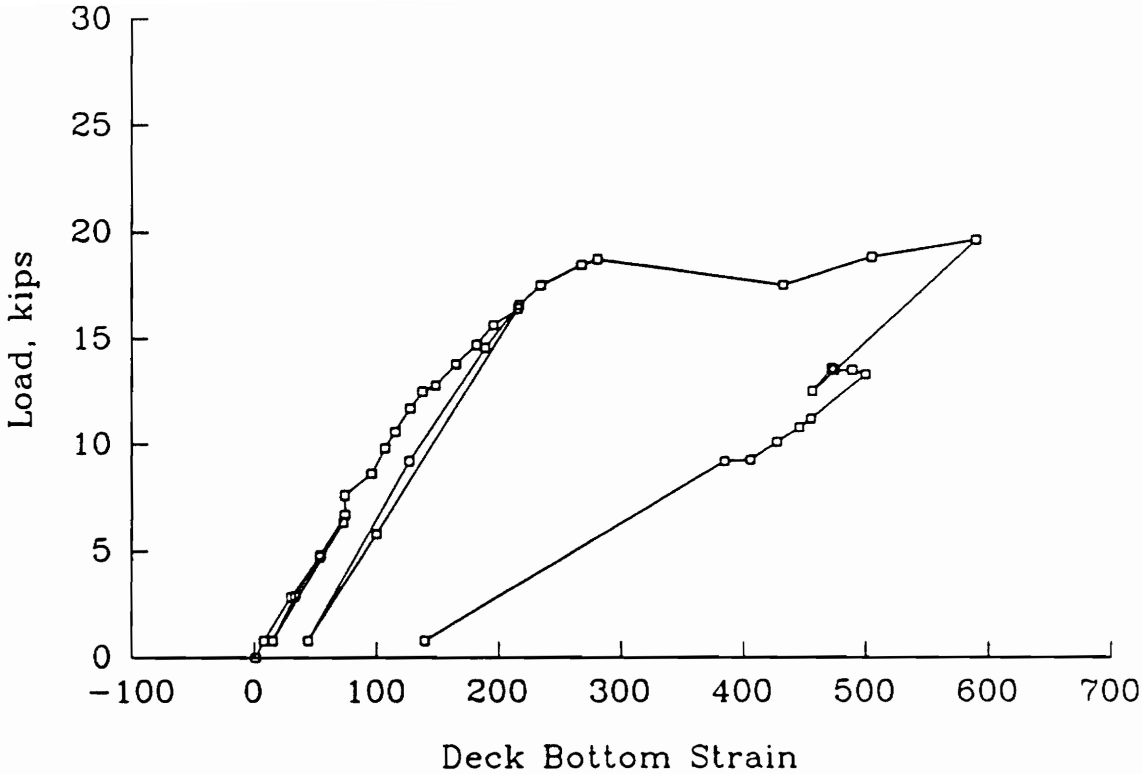


Load vs. Midspan Deck Bottom Strain

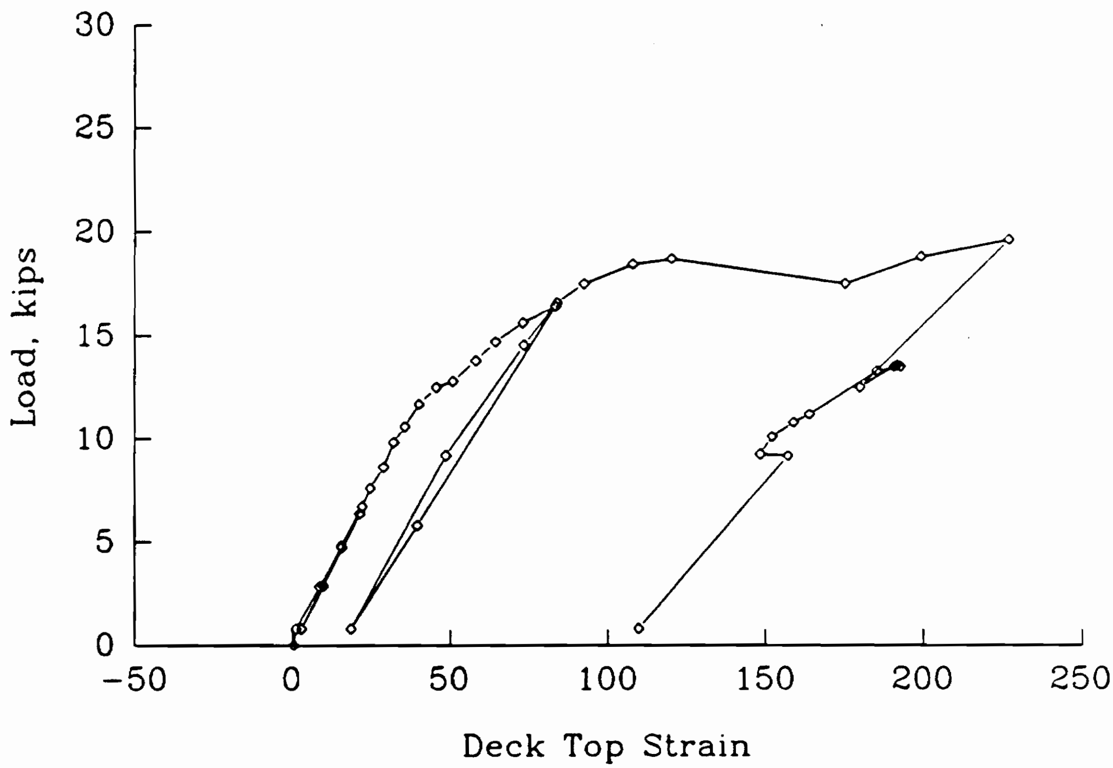


Load vs. Midspan Deck Top Strain

**Figure A24 SDI 5-2 Load vs. Strain Plots**

| | |
|---|---|
| Test Number: | SDI 6-1 (ASCE Standard) |
| Date: | 19 June 1990 |
| Test Type: | Single Span, Single Panel, Shear Bond |

Measured Dimensions

General

| | |
|---|---|
| Width: | 1 panel 3'-0" |
| Span(s): | 8 ft |
| Shear Span: | 30 in. |
| Midspan Strain: (concrete placement) | 323 micro strain |
| End Details: | None |
| Deck attachment: | None |

Deck

| | |
|---|---|
| Type: | 20 gage, 2 in. depth |
| Measured Yield Stress: | 40 ksi |
| Measured Ultimate Stress: | 54 ksi |
| Modulus: | 29,500 ksi |

Type II embossments

Depth: 0.050 in.

Concrete

| | |
|---|---|
| Type: | A4 |
| Test Strength: | 3300 psi |
| Depth: | 5 in, from bottom of deck, 3 in cover |
| Effective Depth: | 4 in. |

Instrumentation

| | |
|---|---|
| Strain Gages: | 2 (shown on diagram) |
| Displacement Transducers | D1-D3 (shown on diagram) |

Test Results

| | |
|---|---|
| Maximum Load: | 11.41 kips @0.244 in midspan deflection |
| Maximum Moment: | 171.15 k-in. |
| Maximum Deflection: | 1.052 in. (test stopped) |

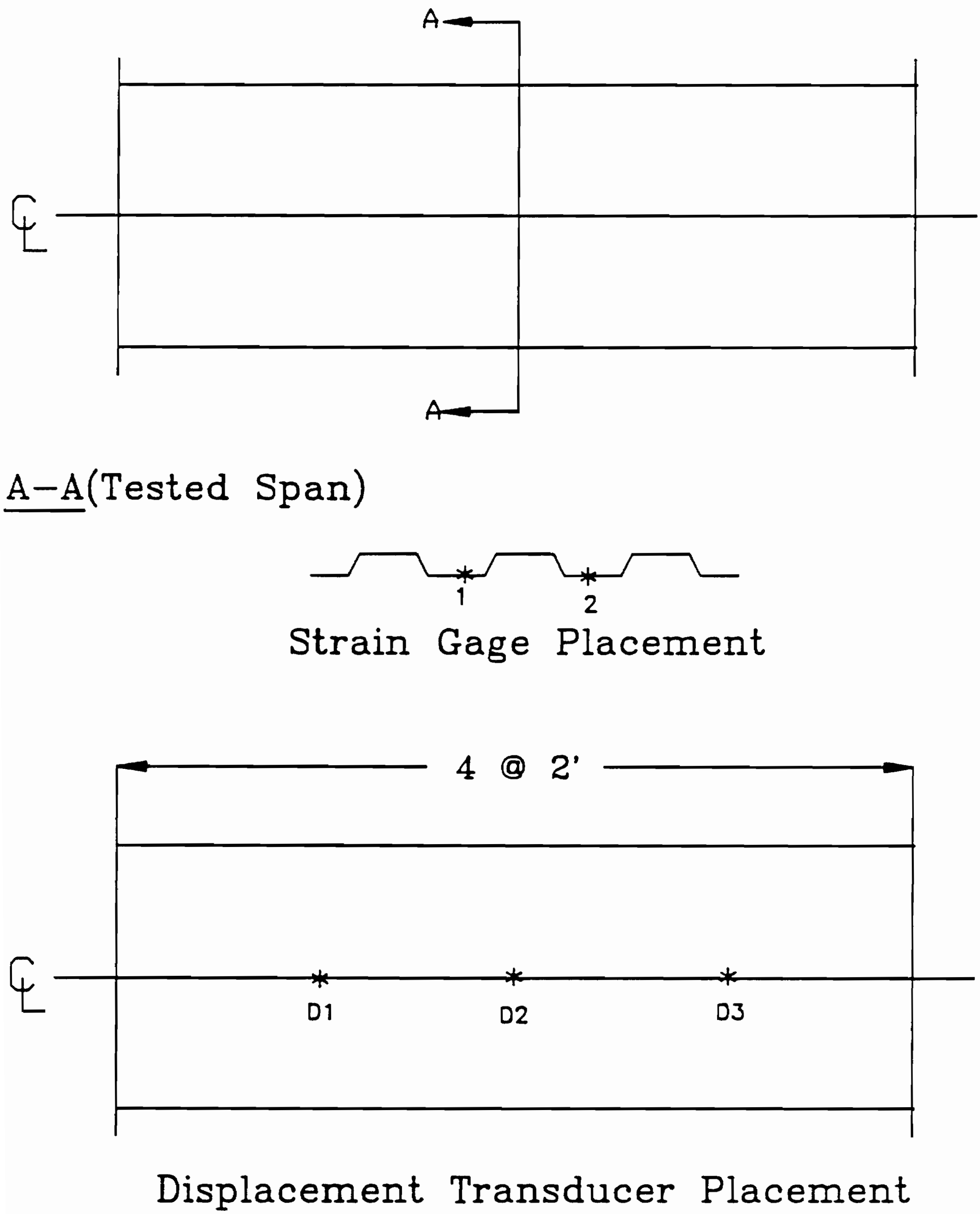


**Figure A25 ASCE Std. Strain Gage, Displacement Transducer**

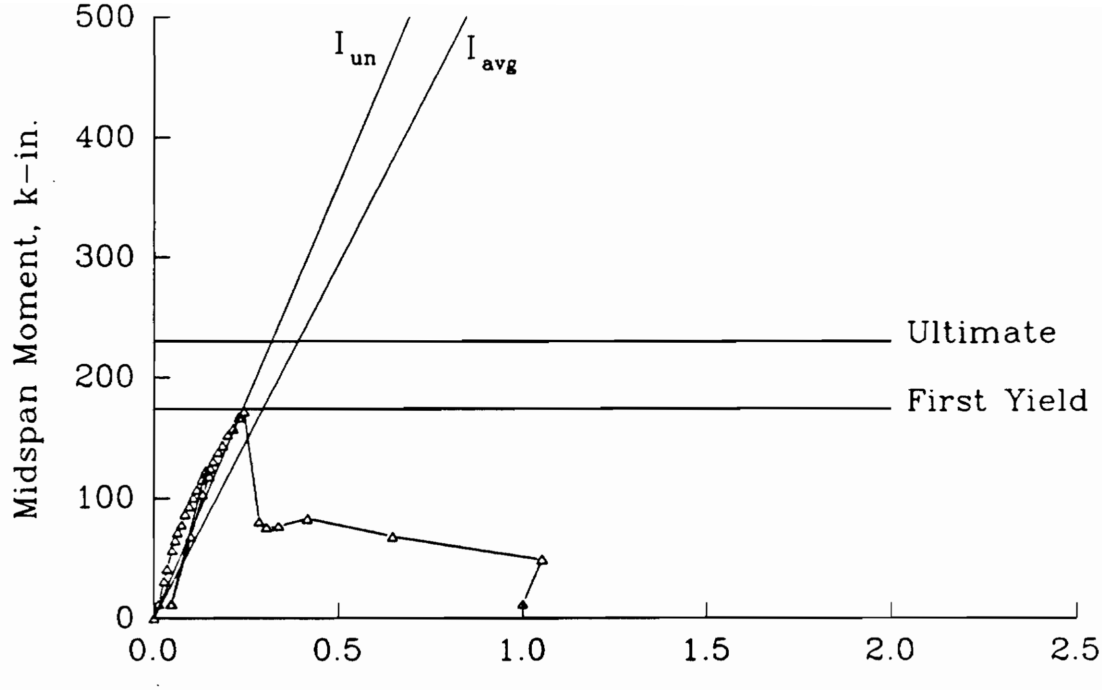


Midspan Moment vs. Midspan Deflection

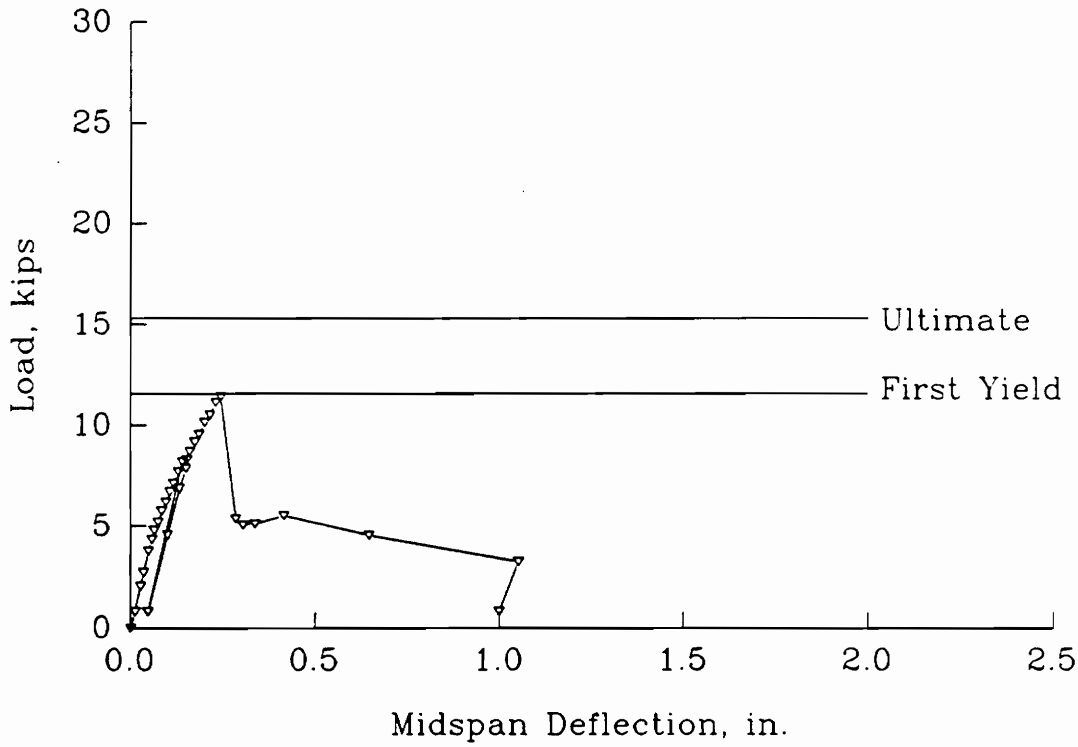


Load vs. Midspan Deflection

**Figure A26 ASCE Std. Moment (Load) vs. Deflection**

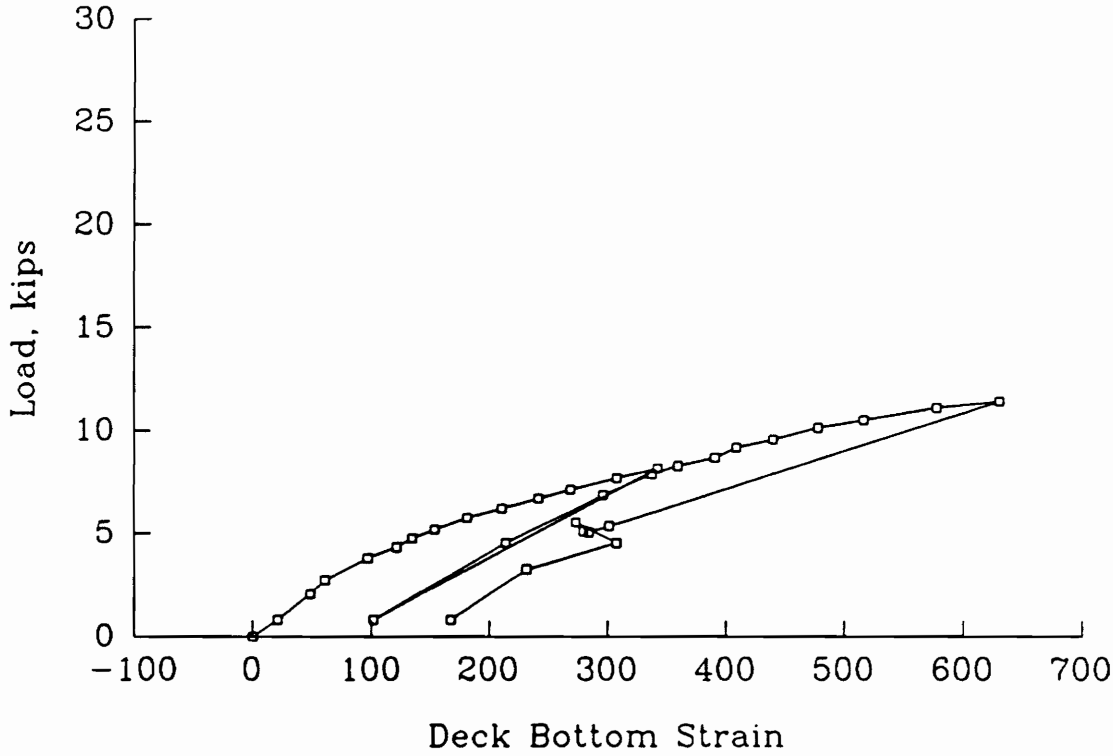


Load vs. Midspan Deck Bottom Strain

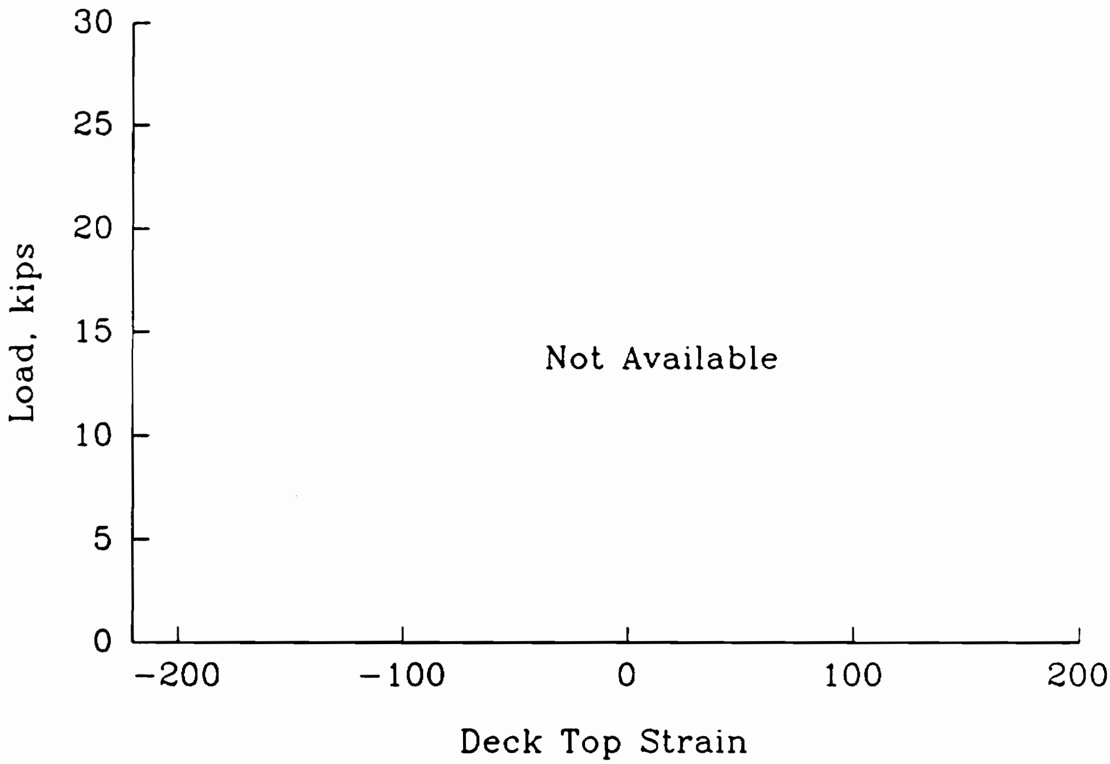


Load vs. Midspan Deck Top Strain

**Figure A27 SDI 6-1 Load vs. Strain Plots**

# APPENDIX B
# SAMPLE CALCULATIONS

## Theoretical Calculations for SDI-1-1

**Note:** See Chapter 4 *Strength and Stiffness Formulations* for equations

### Given:

$f_y$, = 40 ksi
$f'_c$ = 4.33 ksi
$E_s$ = 29,500 ksi (assumed)
$E_c$ = 3750.76 ksi (calculated)
$A_s$ = 0.521 in$^2$ / ft (calculated)
$I_{sf}$ = 0.409 in$^4$ / ft (catalog)
$\beta$ = 0.80 *(ACI-89 10.2.7.3)*

span, l = 96 in (8 ft)
shear span, l' = 30 in
width = 72 in (6 ft)
Cell Spacing, $C_s$ = 12 in
Avg. Rib Width = 6 in

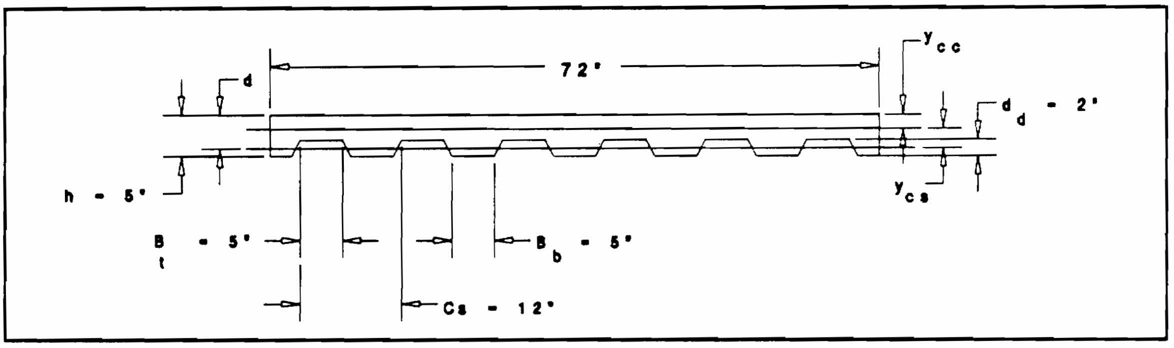


### Preliminary Calculations:

$n = E_s / E_c = 7.87$

$\rho = A_s / bd = 0.010854$ (steel ratio)

$\rho_{min} = 200 / f_y = 0.005$ *(ACI-89 10.5.1)*

$$\rho_b = \frac{\beta_1 \, 0.85 f'_c}{f_y} \; \frac{87{,}000}{87{,}000 + f_y}$$

$= 0.050425$

**Notice,** $\rho_{min} < \rho < \rho_b$ $\therefore$ O.K with *ACI-89* and slab is under-reinforced (ductile failure).

## Neutral Axis Location:

Assume $y_{cc} < t_c$ (Neutral axis above top of deck).

from *ASCE Standard Specifications for the Design and Construction of Composite Slabs and Commentary*,

$$y_{cc} = d \{ [ 2\rho n + (\rho n)^2 ]^{1/2} - \rho n \}$$

$$= 1.35 \text{ in (from top of slab)}$$

**Notice,** $y_{cc} < t_c$ $\therefore$ assumption was correct.

now,

$$y_{cs} = d - y_{cc}$$

$$= 2.65 \text{ in (neutral axis to center of steel deck)}$$

## Moments of Inertia:

from *ASCE Standard Specifications for the Design and Construction of Composite Slabs and Commentary*

Cracked:

$$I_c = (b/3)y_{cc}^3 + nA_s y_{cs}^2 + nI_{sf}$$

$$= 41.86 \text{ in}^4 / \text{ft}$$

$$= 251.13 \text{ in}^4$$

Uncracked:

$$I_u = (bt_c^3)/12 + bt_c(y_{cc} - 0.5t_c) + nI_{sf} + nA_s y_{cs}^2 + \ldots$$

$$((W_r bd_d)/C_s)(d_d^2/12) + (h - y_{cc} - 0.5d_d)^2$$

$$= 70.85 \text{ in}^4 / \text{ft}$$

$$= 425.07 \text{ in}^4$$

## Theoretical Calculations for SDI-1-1 ...continued

### Stiffness:

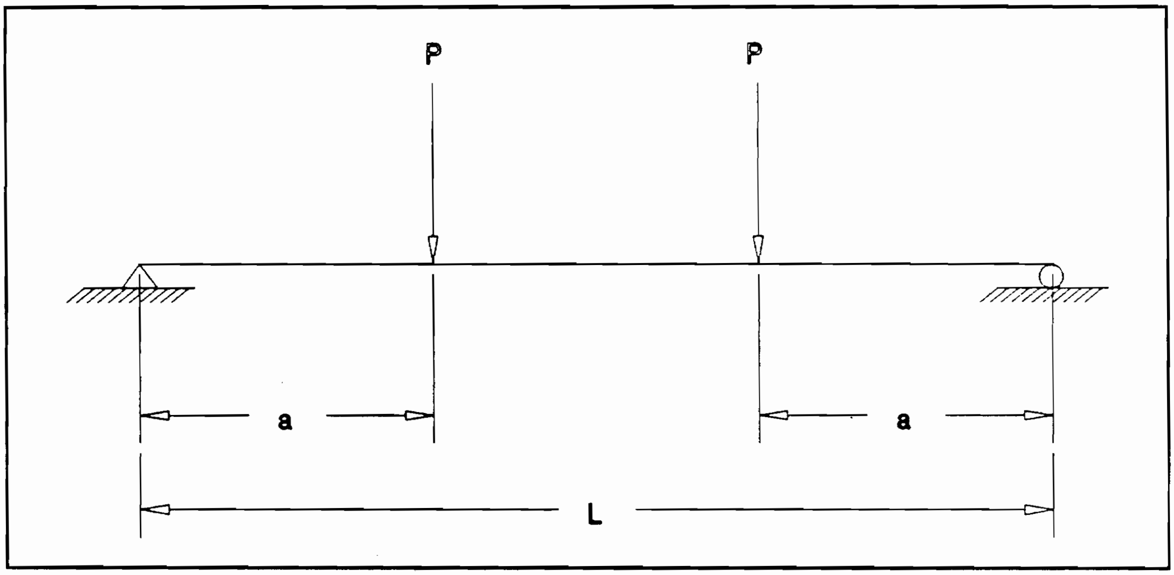


from the *AISI Manual of Steel Construction* 9th *Edition*

$\Delta_{cent} = \{Pa / (24\ EI)\}\ (3L^2 - 4a^2)$

$\Delta_{cent} = 8.01436\ (P / I)$   where $I = I_u$ or $I_c$

substituting yields,

$\Delta_{cent,cracked} = 0.03191\ P$

$\Delta_{cent,uncracked} = 0.01885\ P$

**Notice,** These are the two stiffness lines used for comparison.

# Theoretical Calculations for SDI-1-1 ...continued

## First Yield Calculations:

from *Draft Standard for the Structural Design of Composite Slabs*

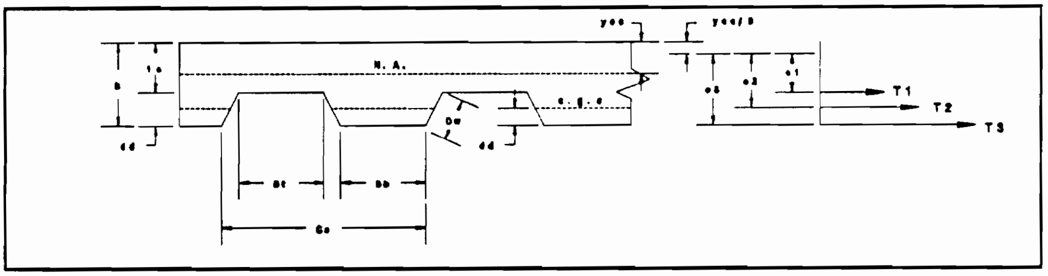

Now, corrections to $f_y$ must be made to account for initial deck strains due to concrete placement. This can be accounted for by Hooke's Law and the measured strains. $f_y$ can thus be reduced as follows:

$$\begin{aligned} \sigma &= E\epsilon \\ &= 29{,}500 \text{ ksi } (120\ \mu) \\ &= 3.54 \text{ ksi} \quad \text{reduction in } f_y \end{aligned}$$

now,

$$\begin{aligned} f_y &= 40 - 3.54 \\ &= 36.5 \text{ ksi} \end{aligned}$$

we can now proceed with calculation of first yield moment,

$$\begin{aligned} e_3 &= h - (y_{cc} / 3) \\ &= 5 - (1.35 / 3) \\ &= 4.55 \text{ in} \end{aligned}$$

$$\begin{aligned} e_2 &= e_3 - (d_d / 2) \\ &= 4.55 - (2 / 2) \\ &= 3.55 \text{ in} \end{aligned}$$

$$\begin{aligned} e_1 &= e_3 - d_d \\ &= 3.55 - 2 \\ &= 2.55 \text{ in} \end{aligned}$$

## Theoretical Calculations for SDI-1-1 ...continued

### First Yield Calculations: ...continued

$$T_1 = f_y (B_t\ t) [(h - y_{cc} - d_d) / (h - y_{cc})]$$

$$= 36.5 (5 (0.0358)) [(5 - 1.35 - 2) / (5 - 1.35)]$$
$$= 2.95 \text{ kips / ft}$$

$$T_2 = f_y (2D_w\ t) [(h - y_{cc} - d_d/2) / (h - y_{cc})]$$

$$= 36.5 ( 2(2^2 + 1^2)^{1/2}(0.0358)) [(5 - 1.35 - 2/2 ) / (5 - 1.35)]$$
$$= 4.24 \text{ kips / ft}$$

$$T_3 = f_y (B_b\ t)$$

$$= 36.5 ( 5 (0.0358))$$
$$= 6.53 \text{ kips / ft}$$

and now summing moments we get,

$$M_{et} = T_1 e_1 + T_2 e_2 + T_3 e_3$$

$$= 2.95(2.55) + 4.24(3.55) + 6.53(4.55)$$
$$= 52.29 \text{ kip·in / ft}$$
$$= 313.7 \text{ kip·in}$$

**Notice,** this is the first yield line used for comparison
(also note that this is Luttrell's method with K = 1.0)

## Theoretical Calculations for SDI-1-1 ...continued

### Ultimate Strength:

from *ACI-89*,

from above we already know that slab is under reinforced thus,

stress block height,

$$a = (A_s f_y) / (f_c' b)$$

$$= (0.521(40)) / (4.33\ (12))$$
$$= 0.401 \text{ in}$$

ultimate moment capacity

$$M_n = A_s f_y (d - a/2)$$

$$= 0.521(40)(4 - 0.401/2)$$
$$= 79.18 \text{ kip·in / ft}$$
$$= 475 \text{ kip·in}$$

**Notice,** this is ultimate load, it must now be corrected for self weight.

using the average depth of concrete (4 in) and a unit weight of 150 lbs / ft$^3$, we can calculate the moment induced by self weight
uniform load, w

$$w = (150 \text{ lbs / ft}^3)\ ((1 \text{ ft}) / (12 \text{ in}))^2\ (72 \text{ in})\ (4 \text{ in})$$
$$= 300 \text{ lbs / ft}$$
$$= 0.3 \text{ kips / ft}$$

now, center line moment due to self weight (assuming simple supports)

$$M_{conc} = (wL^2) / 8$$

$$= (0.3\ (8^2)) / 8$$
$$= 2.4 \text{ kip·ft}$$
$$= 28.8 \text{ kip·in}$$

thus, $M_u$ applied is

$$M_{u,applied} = 475 - 28.8$$
$$= 446.2 \text{ kip·in}$$

**Notice,** this is the ultimate line used for comparison

# VITA

Craig Steven Young was born in Richlands, Virginia on the $9^{th}$ of April 1965. He graduated from Highlight Academy of Education in 1983. He received the Associate of Science in Engineering degree from Southwest Virginia Community College in 1987, the Bachelor of Science in Civil Engineering at Virginia Polytechnic Institute and State University (VPI&SU) in 1989. During the stay at VPI&SU he worked for the Virginia Department of Transportation as Inspector/Field Engineer and for Structural Engineers Inc. as a Design Engineer/Computer Programmer. He entered the Virginia Polytechnic and State University Charles Edward Via Department of Structures Graduate Program, in pursuit of a Master of Science in Civil Engineering, in the Fall of 1989.